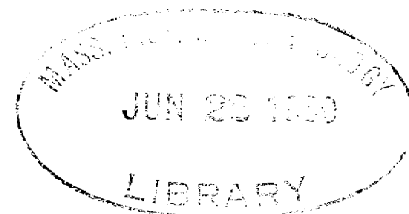


METAL OXIDE-OXYGEN ELECTRODES AND FUEL CELLS

by

Dominick A. Sama



S.B., Massachusetts Institute of Technology
(1954)

S.M., Massachusetts Institute of Technology
(1955)

SUBMITTED IN PARTIAL FULFILLMENT OF THE
REQUIREMENTS FOR THE DEGREE OF
DOCTOR OF SCIENCE

at the

MASSACHUSETTS INSTITUTE OF TECHNOLOGY
MARCH 1960

Signature of Author _____
Department of Chemical Engineering, March 25, 1960

Certified by _____ Thesis Supervisor

_____ Thesis Supervisor

Accepted by _____
Chairman, Departmental Committee on Graduate Students

METAL OXIDE-OXYGEN ELECTRODES AND FUEL CELLS

by

Dominick A. Sama

Submitted to the Department of Chemical Engineering on March 25, 1960, in partial fulfillment of the requirements for the degree, Doctor of Science in Chemical Engineering.

ABSTRACT

This study was undertaken to gain insight into the mechanism of operation, and the rate-determining step at partially submerged, air-depolarized metal electrodes.

It was found that at smooth, flat electrodes of copper, nickel, and silver in caustic cells, the rate of air depolarization was limited by the mass-transport rate of oxygen through the electrolyte to the electrode. When compared to the porous-type oxygen electrodes normally used in fuel cells, the results indicate that the operation of these oxygen electrodes might also be limited by the mass-transport rate of oxygen.

A wiped, rotating, partially submerged oxygen electrode, designed to eliminate the resistance to oxygen transport posed by the electrolyte, was used to measure the oxidation rate of the electrode surfaces. The data are compared with fuel cell rate requirements and are discussed in terms of oxidation theory.

At 32°C and an oxygen partial pressure of 0.844 atm, an oxidation rate equivalent to a current density of 26 ma/cm² was obtained with a smooth copper surface. In a porous electrode, where the true surface area is many times the apparent area, this oxidation rate is adequate to meet the rate requirements of a fuel cell. With nickel and silver the results were not so conclusive; however, they indicate that the oxidation rates of these metals might also satisfy fuel cell rate requirements.

These findings show the importance of reducing the mass-transfer resistance of the electrolyte in fuel cell electrodes.

The oxidation of copper was found to follow the logarithmic law

$$w = k_1 \log(k_2 t + 1)$$

where w is the oxide weight and t is exposure time. It was also found that k_1 in this equation was independent of oxygen partial pressure, while k_2 was proportional to the square root of the oxygen partial pressure.

These findings are consistent with a derivation of the logarithmic equation by Evans which assumes that the rate of oxidation is limited by the rate at which oxygen, in some form, travels through the oxide layer to the metal surface. The dependency of k_2 on the square root of the oxygen partial pressure indicates, in the light of the Evans theory, that oxygen in the monatomic form O , O^- , or $O^=$ is the species transported through the oxide layer.

The oxidation of silver appeared to fit the parabolic equation

$$w^2 = k_1 t$$

however, more accurate data are needed to definitely establish this conclusion.

Reliable oxidation-rate data were not obtained for nickel.

Thesis Supervisors: Harold C. Weber
Professor of Chemical Engineering

Herman P. Meissner
Professor of Chemical Engineering

ACKNOWLEDGMENT

The author wishes to express his sincere appreciation to Professors Harold C. Weber and Herman P. Meissner for the guidance and assistance which were so liberally given him throughout the course of this thesis.

Professors David C. White and Herbert H. Woodson of the Electrical Engineering Department were instrumental in obtaining financial assistance. Their interest and encouragement are gratefully acknowledged.

The assistance of the personnel and staff of the Electrical Engineering Department and the Electronic Systems Laboratory was indispensable, both during the investigation and in the preparation of this report.

The author is indebted to the Standard Oil Foundation and to the Aeronautical Accessories Laboratory, Wright Air Development Division, Wright-Patterson Air Force Base, for the financial support which made this thesis possible.

Department of Chemical Engineering
Massachusetts Institute of Technology
Cambridge 39, Massachusetts
March 25, 1960

Professor Philip Franklin
Secretary of the Faculty
Massachusetts Institute of Technology
Cambridge 39, Massachusetts

Dear Sir:

The thesis entitled "Metal Oxide-Oxygen Electrodes and Fuel Cells" is hereby submitted in partial fulfillment of the requirements for the degree of Doctor of Science in Chemical Engineering.

Respectfully submitted,

Dominick A. Sama

TABLE OF CONTENTS

	<u>page</u>	
LIST OF FIGURES		vii
LIST OF TABLES		ix
CHAPTER I	SUMMARY	1
CHAPTER II	INTRODUCTION	11
A.	OBJECT OF INVESTIGATION	11
B.	DEFINITION AND DISCUSSION OF FUEL CELLS	11
C.	MASS TRANSFER PROCESSES IN FUEL CELLS	17
D.	REVIEW OF FUEL CELLS	20
1.	Hydrogen, Oxygen Fuel Cells	20
2.	Carbonaceous Fuels	23
3.	Redox Cells	24
E.	METABOLISM AND FUEL CELLS	26
F.	ISOLATION OF OXYGEN ELECTRODE	26
CHAPTER III	APPARATUS	29
A.	STATIONARY ELECTRODE	29
B.	ROTATING ELECTRODE	30
1.	Electrochemical System	32
a.	Oxygen Electrode	32
b.	Rubber Wiper	32
c.	Zinc Anodes	34
d.	Lucite Box	35
e.	Lift Pump	35
2.	Driving Mechanism	36
3.	Measurements	36
CHAPTER IV	RESULTS AND DISCUSSION OF RESULTS	39
A.	MECHANISM OF OXYGEN TRANSPORT TO AIR- DEPOLARIZED CATHODES	39
1.	Introduction	39
2.	Results	40
a.	Mechanism	40
b.	Rate Determining Step	45
c.	Drowning of Electrodes	49

TABLE OF CONTENTS (continued)

	<u>page</u>
B. RATE OF OXIDATION OF ELECTRODE SURFACES	51
1. Characteristics of Wiped, Rotating, Partially Submerged Oxygen Electrodes	51
a. Discussion	51
b. Results	53
2. Oxidation of Metals	55
a. Introduction	55
b. Results	61
i. Copper	61
ii. Silver	76
iii. Nickel	79
c. Comparison of Oxidation Rates with Oxygen Electrode Requirements	83
CHAPTER V CONCLUSIONS AND RECOMMENDATIONS	87
APPENDIX A DETAILS OF ROTATING ELECTRODES, AND OPERATING CHARACTERISTICS	89
APPENDIX B DISCUSSION OF GALVANIC CURRENTS	91
1. Steel-Wool Anode	92
2. Zinc Anode	93
APPENDIX C CONCENTRATION CELL EFFECT	95
APPENDIX D NOMENCLATURE	99
APPENDIX E LITERATURE CITATIONS	101
APPENDIX F BIBLIOGRAPHY ON FUEL CELLS	105
APPENDIX G BIOGRAPHICAL NOTE	129

LIST OF FIGURES

	<u>page</u>
1 Redox Cell	25
2 Cell with Air-Depolarized Cathode	29
3 Depth Gauge	30
4 Measurement of Exposed Height	30
5 Complete Apparatus	31
6 Electrochemical System	31
7 Rotating Electrode	33
8 Electrical Contact to Rotating Electrode	33
9 Wiper	34
10 Measurement of Cell Current	37
11 Possible Oxygen Transport Mechanisms	40
12 Horizontal and Vertical Cathodes	44
13 Vertical and Inclined Cathodes	44
14 Effect of Wiping on Current of Rotating Copper Electrode	54
15 Effect of Resistance on Current of Rotating Copper Electrode	54
16 Metal Oxidation Model	56
17 Data for Rotating Copper Electrode	62
18 Copper Oxide Thickness versus Exposure Time	65
19 Copper Oxide Thickness versus Exposure Time	65
20 Test of Parabolic Equation, Copper	67
21 Test of Parabolic Equation, Copper	67
22 Test of Logarithmic Equation, Copper	68
23 Test of Logarithmic Equation, Copper	71
24 Test of Logarithmic Equation, Copper	71
25 k_1 versus Partial Pressure O_2	74
26 k_1' versus Partial Pressure O_2	74
27 k_2 versus Square Root of Oxygen Partial Pressure	74
28 k_2' versus Square Root of Oxygen Partial Pressure	74
29 Data for Rotating Silver Electrode	76
30 Silver Oxide Thickness versus Exposure Time	78
31 Test of Parabolic Equation, Silver	78
32 Data for Rotating Nickel Electrode	81

LIST OF TABLES

1	Results, Partially Submerged Copper Electrode	<u>page</u>	41
2	Results, Inclined Partially Submerged Copper Electrode		45
3	Results, Partially Submerged Cu, Ni, and Ag Electrodes		46
4	Calculated Constants of Logarithmic Equation		69
5	Calculated Values of k_2 Based on Average Value of k_1		69
6	Calculated Values of k_2' Based on Average Value of k_1'		70
7	Data, Completely Submerged Cathodes with Steel-Wool Anode		92

CHAPTER I

SUMMARY

Fuel cells were discussed by Davy in 1801, and the first fuel cell was built by Grove in 1839; but, in spite of this long history and much effort, an economical fuel cell has yet to be built. Though both hydrogen and carbon-containing fuels have been used in fuel cells, the net rate of reaction has been much less than that required to produce current densities of 100 ma/cm^2 of electrode area, which has been proposed as a rough criterion for an economical low-pressure fuel cell. The lack of success appears, at least partly, due to the fact that some physical and chemical processes occurring in fuel cells are still not completely understood.

The purpose of this thesis was to try to gain insight into the mechanism of operation and into the rate-determining step at partially submerged, air-depolarized metal electrodes. The metals studied -- copper, nickel, and silver -- have all been used in the past, directly as oxygen electrodes or as activation agents for oxygen electrodes made of porous carbon.

The oxygen electrode, rather than a fuel electrode, was chosen for study here because, though the fuel used may vary widely, an oxygen electrode is necessary for the operation of any direct fuel cell. Also, it appears that the output of some of the more successful hydrogen-oxygen fuel cells is limited by the operation of the oxygen electrode. Finally, since some of the processes occurring at both the fuel and the oxygen electrode are in ways very similar, it is felt that a better understanding of the processes at the oxygen electrode is an important step toward understanding fuel cells as a whole.

Most fuel cell electrodes, in order to achieve higher apparent current densities, are constructed of porous materials; however, an extensive analysis of results is not possible with porous electrodes. This is due to the fact that the area and

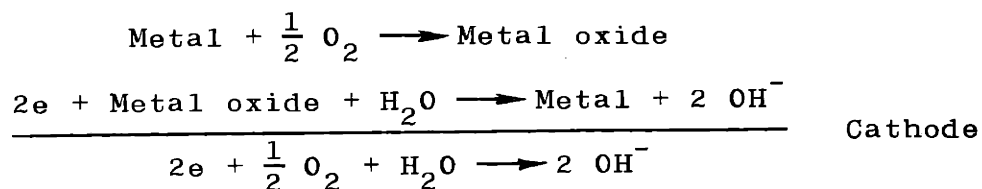
the geometry of the active portion of porous electrodes are not known. For this reason the electrodes used in this work were smooth metal surfaces.

Much work on fuel cells, in an effort to obtain higher rates, has been conducted at high temperatures. This has been especially true when carbon, or carbon-containing fuels, were used. However, it is a fact that animals metabolize foods at low temperatures and low pressure, at rates which are significant. This suggests that it might be possible to construct a fuel cell which operates at reasonable rates with alcohols, carbohydrates, or possibly even hydrocarbons, without resorting to high temperatures and pressures. For this reason the oxygen electrodes were studied at room temperature and atmospheric pressure.

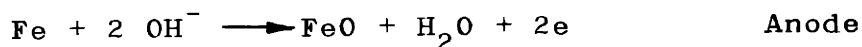
In order for a fuel cell oxygen electrode to function at any given rate, it is necessary to have a sufficient oxygen transport rate to the electrode. Since the solubility and diffusivity of oxygen in electrolytes are quite small, one might expect that the oxygen transport rate could limit the rate of operation of an oxygen electrode. However, most work on fuel cells has assumed that chemical reaction rates limited the operation of the cell; and the possibility that mass transport rates are controlling has been almost entirely neglected. Therefore, in this thesis, especial attention has been devoted to the relative importance of the transport rate and the chemical reaction rate in the reaction of oxygen at an oxygen electrode.

For the investigation of the mechanism and rate of operation of an oxygen electrode, it is necessary that the operation of the cell be limited by the electrode. This can be accomplished by having small internal and external resistances, and a small oxygen electrode area relative to the anode area. Under these conditions, the maximum current obtainable from the cell will be dependent on the rate of reactions at the oxygen electrode. This technique of "isolating" the oxygen electrode was employed in all the cells used in this thesis.

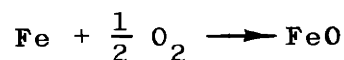
The first stage of the experimental work centered about the use of partially submerged copper, nickel, and silver cathodes, in conjunction with a steel-wool anode in a 20% KOH electrolyte. The area of the air-depolarized metal electrodes was far less than the steel-wool anode, as required to isolate the oxygen electrode. The overall electrode reactions may be represented as



and



so that the net cell reaction is



The partially submerged electrode is wetted by the electrolyte; and the latter creeps, as a thin film, a small distance up the face of the electrode. Thus, the electrode is made up of three distinct areas: that submerged in the bulk electrolyte; that covered by a thin film of electrolyte, i.e. the "wetted exposed" area; and the exposed portion which is not covered by electrolyte.

In order for electrochemical action to take place, electrolyte must be present; therefore, the electrochemical action can take place only at the submerged or wetted-exposed areas.

The current obtainable from a completely submerged electrode is quite small; however, when electrolyte is removed so that the electrode is only partially submerged, the current rises sharply. Thus, the oxygen depolarization at a partially submerged electrode occurs primarily at the wetted-exposed portion of the electrode. This reflects the fact that the oxygen transport to the electrode is much greater at the wetted-exposed portion than at the submerged portion of the electrode. Therefore, the mechanism of oxygen transport to the wetted-

exposed area is, in effect, the mechanism by which oxygen travels to the electrode.

Oxygen can arrive at the wetted-exposed area of the electrode by transport through the thin electrolyte film, or by direct contact at the air-electrode-electrolyte perimeter. It was found that the current was not dependent on the three-phase perimeter, but rather on the total area of the wetted-exposed portion. These results indicate that the mechanism of oxygen transport to partially submerged, air-depolarized electrodes is solution and transport through the thin electrolyte film that creeps up the face of the electrode.

It was found that the current obtainable from partially submerged copper, nickel, or silver electrodes was essentially the same when the electrolyte-electrode geometry of the wetted-exposed portion was the same. The fact that the current does not depend on the chemical nature of the electrode indicates that the rate-determining step is not a chemical reaction, but rather a mass transfer process, presumably the transport of oxygen through the thin electrolyte film. This was confirmed by the finding that the current decreased when the temperature was increased.

When porous fuel cell electrodes become completely permeated by electrolyte, the current which can be drawn from them drops off sharply. This is called "drowning" of the electrode. Consideration of the above findings indicates that the drowning of these electrodes is due to a large increase in the resistance to oxygen transport, and not to poisoning of the electrode. They also indicate that, in oxygen electrodes which are not drowned, the current may still be limited by the mass transport of oxygen through the electrolyte; and pose the questions: What kind of current densities can be obtained from an oxygen electrode when this oxygen transport resistance is eliminated, and how does this current density compare with fuel cell requirements? The wiped, rotating, partially submerged electrode was designed to try to answer these questions.

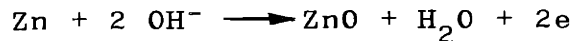
The cells used in this part of the experimental work consisted of the rotating cathode, a 20% KOH electrolyte, and a wound zinc-wire anode whose area was approximately 100 times the cathode area. The cell as a whole was designed to make the oxidation step at the rotating electrode limiting. Zinc was chosen as the anode partly because it results in a higher cell voltage and, correspondingly, a higher electrochemical reduction rate at the rotating electrode. The cell operated inside an airtight lucite box whose atmosphere was kept saturated, with respect to the electrolyte, by means of a small pump which continuously bubbled the enclosed air through an electrolyte bath. The total pressure inside the lucite box was one atmosphere. The variables studied were electrode metal, time of exposure of the surface, and oxygen partial pressure of the enclosed atmosphere. The metals used, as in the previous experiments, were copper, nickel, and silver. The exposure time was determined by measuring the exposed perimeter of the electrode and the R.P.M. An Orsat apparatus with an ammoniacal cuprous-chloride absorbent was used to determine the oxygen partial pressure.

The rotating electrode consists of a metal ring embedded in the rim of a lucite disc. The surface of the rotating electrode, as it emerges from the electrolyte bath, is wiped free of electrolyte by a gum-rubber wiper. This eliminates the resistance of the electrolyte to oxygen transport that limited the output of the stationary, partially submerged electrodes and allows oxygen free access to the electrode surface. The operation of the rotating electrode is divided into two separate steps: oxidation in the exposed portion and electrochemical reduction in the submerged portion; and this, in principle, permits them to be studied separately. The work done here with the rotating electrode concerned itself only with the rate of oxidation of the exposed portion.

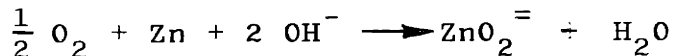
During the operation of the cell, the rotating electrode is not consumed. The metal surface is oxidized when exposed

to oxygen and is electrochemically reduced when it re-enters the electrolyte. This alternate oxidation and electrochemical reduction continues indefinitely so that the rotating electrode, in effect, is a means of removing oxygen from the atmosphere and of transferring this oxygen as hydroxyl ions into the electrolyte. The overall reaction occurring at the rotating electrode during the operation of the cell is the same as the stationary oxygen electrodes, used in the first part of the work.

At the anode, the zinc undergoes electrochemical oxidation to zinc oxide, which then dissolves in the electrolyte. This exposes fresh zinc surface which can react further. The reactions at the zinc anode are



so that the overall cell reaction is



The effect of the rubber wiper in decreasing the resistance to oxygen transport is shown in Fig. 14. The currents measured represent the sum of two currents: that due to depolarization by oxygen and that due to other electrochemical reactions. The latter current, due to the presence of two dissimilar metals in an electrolyte, has been arbitrarily termed the "galvanic" current. The presence of an electrolyte film on the unwiped, rotating electrode cuts the oxygen transport to the electrode surface to an almost negligible quantity, so that the current obtained from the unwiped electrode is essentially entirely galvanic. The current at the wiped electrode is much higher and is primarily due to depolarization by oxygen.

Figure 15 is a plot of the current produced by a cell using a wiped, copper electrode rotating at a constant R.P.M. as a function of the external resistance. It is seen that the current increases with decreasing resistance until the external resistance is about 3 ohms. Further lowering of the resistance results in no change in the current and is an indication that

the rates of the electrochemical reactions are not limiting the cell current. It was also found that doubling the zinc-anode area did not result in a current change. These results lead to the conclusion that the maximum current is limited by the oxidation step in the exposed portion of the rotating electrode.

This conclusion was tested by adding an electrolyte "mask," as shown in Fig. 6, to the wiped, rotating, partially submerged electrode. The addition of the mask serves to decrease the exposed area of the electrode to oxygen, and increase its submerged area in the electrolyte. When the mask was added and the exposed area decreased, the current was also found to decrease. This confirms the previous conclusion that the maximum cell current was limited by the oxidation step, occurring in the exposed portion of the electrode.

Using a rotating copper electrode and an external resistance of 0.352 ohms, a current density of 26 ma/cm² exposed area was obtained at 32°C under an oxygen partial pressure of 0.844 atm. This current density needs only to be raised by a factor of four to satisfy the proposed criterion, 100 ma/cm², of an economical fuel cell. When differences in surface roughness and in oxide thickness between the rotating electrode and a porous electrode are considered, it is seen that such a factor is easily attainable. Therefore, the conclusion is that, as far as oxidation rate is concerned, a porous electrode containing, or made of, copper can be expected to provide current densities of 100 ma/cm². Using nickel and silver surfaces, the results are not so clear-cut; however, though they are not conclusive, they indicate that this may be true for these metals too.

The results of the above work show the importance of reducing the mass-transfer resistance of the electrolyte in fuel cell electrodes.

The primary purpose of the rotating electrode was to provide information about the magnitudes of metal-oxidation rates; however, it can also be used to investigate the actual mechanism of oxidation. The electrode surfaces, inherently,

must be contaminated by electrolyte; and this presents a problem of applicability of results. In spite of this, the oxidation-rate data obtained with the rotating electrode, especially in the case of copper, lead to very interesting conclusions when viewed in the light of metal-oxidation theory.

The data, see Fig. 17, obtained for the rotating copper electrode were compared with the common metal-oxidation rate "laws". It was found that the data could not be expressed by either the linear-rate law

$$w = k_1 t + k_2$$

or the parabolic-rate law

$$w^2 = k_1 t + k_2$$

where w is the oxide weight and t is exposure time.

If electrolyte resistance to oxygen transport were still limiting, the oxidation would be directly proportional to the exposure time and the oxygen partial pressure. Noncorrespondence to the linear equation suggests that the electrolyte resistance to oxygen transport has indeed been made negligible by the wiper, and this is supported by the fact that the current was not proportional to the oxygen partial pressure.

The copper-oxidation data were found to follow the logarithmic law

$$w = k_1 \log (k_2 t + 1)$$

which is often found to hold for low-temperature oxidation of metals. In addition, it was found that k_1 in this equation was independent of oxygen partial pressure, while k_2 was proportional to the square root of the partial pressure. The logarithmic law has been derived from theoretical considerations by a number of workers, and the results were compared with the predictions afforded by different derivations. The partial-pressure effects were found to be compatible with a theory proposed by Evans.^{49*}

*Superscript numerals refer to numbered items in Appendix E.

Evans proposed that the rate of oxidation is limited by the mass-transport rate of oxygen in some form through "leaky" points in the oxide film. These leaky points (pores, dislocations, or discontinuities) are assumed to decrease as oxidation progresses due to the fact that the oxide is less dense than the metal and expands, thereby closing up leaks. In the derivation, k_1 comes from a quantity that represents the number of leaky points at a given oxide weight, and is not a function of oxygen partial pressure. The second constant, k_2 , represents the rate at which oxygen moves through a leak, and is clearly dependent on the oxygen partial pressure.

In his derivation Evans does not specify the form of oxygen which is transported along the leaks; but, if oxygen in the diatomic form is the species transported, k_2 would be directly proportional to the oxygen partial pressure. The finding that k_2 is proportional to the square root of the oxygen partial pressure, if the Evans model is correct, indicates that a monatomic oxygen species, O , O^- , or O^{\equiv} , is the form transported along the leaks.

With silver the results were not so conclusive. The effect of oxygen partial pressure on the oxidation rate was less than for copper; and it suggests, therefore, that the oxidation mechanism is different. The oxidation data appeared to fit the parabolic equation

$$w^2 = k_1 t$$

however, more accurate data are needed to definitely establish this conclusion.

The presence of large and varying currents, due to side reactions, made it impossible to obtain accurate oxidation data for nickel; therefore, no analysis could be made. It did appear, however, that the oxidation rate, as with copper, was a strong function of the oxygen partial pressure.

The wiped, partially submerged, rotating electrode presents an interesting method of conducting low-temperature oxidation studies. It is suggested that it be used for further work with

silver and nickel, as well as for other metals, and activated carbon surfaces.

CHAPTER II

INTRODUCTION

A. OBJECT OF INVESTIGATION

The object of this thesis was to investigate the relative importance of mass-transfer and chemical-reaction rates at oxygen electrodes in low-temperature, low-pressure, liquid-electrolyte fuel cells. Some of the processes occurring at both the fuel and oxygen electrodes are quite similar physically, and it is felt that a better understanding of these processes at either electrode will help the understanding of fuel cells as a whole.

The decision to study the oxygen electrode was based on a number of factors. First, though there are many fuels which can be used in the cell, they must all be used in conjunction with an oxygen electrode. The oxygen electrode and its problems are, thereby, encountered in all direct fuel cells. In addition, in some of the more successful hydrogen-oxygen fuel cells, the output appears to be limited by the oxygen electrode.

The most successful oxygen electrodes are made of porous metals, or metal-activated porous carbons; and, for this reason, it was decided to use metals as oxygen electrodes. The use of a porous electrode in a fuel cell is very advantageous since it provides a large surface area; however, in a study of mechanism such a construction makes the interpretation of results difficult. Therefore, only flat surfaces were used.

The metals used were copper, silver, and nickel--all of which have been used as electrodes in fuel cells or as activation agents in porous carbon electrodes.

B. DEFINITION AND DISCUSSION OF FUEL CELLS

A fuel cell is a device which oxidizes fuels electrochemically such that chemical energy is converted directly to electrical energy without the intermediate conversion to heat.

As a result, it is not subject to the Carnot efficiency and theoretically can operate at 100% efficiency. The only difference between a fuel cell and an ordinary battery is that the former consumes fuel and oxygen, while the latter does not.

The simplest way to visualize the operation of a fuel cell is to consider it as the reverse of electrolysis. If platinum electrodes are inserted in slightly acidified water and a current passed through them, hydrogen will be evolved at the cathode and oxygen at the anode. The electrical energy used to decompose the water is converted to chemical energy. If the reverse experiment is carried out (e.g., two platinum electrodes are inserted in acidified water, one surrounded by oxygen and the other by hydrogen), we find a potential difference between the electrodes; and a small current can be continuously drawn from the cell. The hydrogen and oxygen surrounding the platinum electrodes are consumed in the ratio 2 to 1, and water is formed. The chemical energy of the H_2, O_2 system is converted directly to electrical energy without the intermediate generation of heat; and we have a fuel cell.

Such a cell was actually built by Grove in 1839¹ and was the first demonstration that a fuel cell was possible. The trouble with the Grove cell is that the rate of energy formation is very slow, and an enormous cell is required to give even moderate current drains. In the hundred odd years since the construction of this cell, the slow rate of energy production has remained the stumbling block in the development of economical fuel cells.

It is not the heat of reaction of the fuel which is converted to electrical energy in the fuel cell, but rather the change in free energy. However, in many cases the change in free energy is about equal to the heat of reaction; and this has led to some confusion.

$$\Delta F = \Delta H - T\Delta S \quad \text{or} \quad -\Delta F = -\Delta H + T\Delta S \quad (1)$$

where

ΔF = maximum isothermal reversible work done on the system ($-\Delta F$ = work done by the system)

ΔH = change in enthalpy ($-\Delta H$ = heat of reaction)
 $T\Delta S$ = minimum heat transfer necessary to maintain
 constant temperature

From this equation it is clear that, when heat is transferred into the system, ΔS is positive and $-\Delta F$ is greater than $-\Delta H$. That is, the maximum reversible isothermal work is greater than the heat of reaction. When heat is transferred out of the system, ΔS is negative and $-\Delta F$ is less than $-\Delta H$. When T or ΔS are small, such that $T\Delta S$ is negligible compared to ΔH , the maximum reversible isothermal work is equal to the heat of reaction.

For the isothermal oxidation of carbon or hydrogen at room temperature, the latter is true. The maximum reversible isothermal work is about equal to the heat of reaction. If the oxidation is carried out by the normal combustion process, only a fraction (the Carnot efficiency) of the chemical energy can be converted into work. Present power plants can be constructed to operate at about 40% efficiency; but, if the oxidation is carried out electrochemically in an ideal fuel cell, the conversion to work is complete.

The work obtained from an electrical cell is the product of the number of electrons transferred and the voltage of the cell. If the electrical cell is considered to be a reversible isothermal system as above,

$$E \times n_e \times f = -\Delta F \quad \text{or} \quad E = \frac{-\Delta F}{n_e \times f} \quad (2)$$

where

ΔF = free energy change in joules/gm mole

f = number of coulombs in a gm equivalent = 96,500

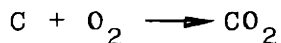
n_e = number of electrons transferred per molecule

E = theoretical maximum cell voltage obtainable
 from the given chemical reaction

The voltage of a cell when no current is flowing (i.e., the open-cell voltage) is the highest experimentally obtainable. For a reversible cell, the open-cell voltage is equal to the theoretical maximum voltage. Knowledge of the

theoretical maximum voltage is important since the operating voltage divided by the theoretical maximum voltage is the efficiency of the cell.

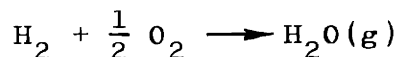
For the reaction



$$\Delta F = -94,260 \text{ cal/gm mole at } 25^\circ\text{C}$$

$$E = \frac{-(-94,260 \text{ cal/gm mole})(4.185 \text{ joules/cal})}{4(96,500)} = 1.02 \text{ volts}$$

For the reaction



$$\Delta F = -54,600 \text{ cal/gm mole}$$

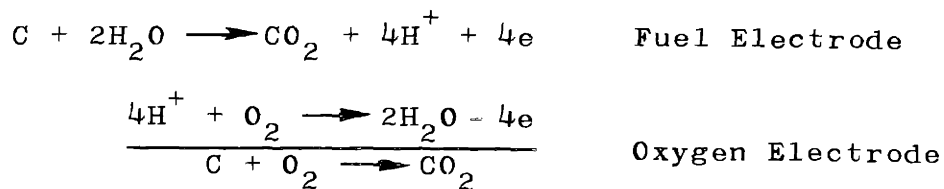
and

$$E = 1.19 \text{ volts}$$

These theoretical maximum voltages are functions of temperature since ΔF is a function of temperature, but the effect of temperature may not be strong. The theoretical voltage of the C, O_2 cell remains nearly constant, being 1.01 v at 1500°C ; while the H_2, O_2 cell drops to 0.77 v at 1500°C .

In order for a fuel to be oxidized electrochemically in a fuel cell, it is necessary to have electrons generated at one of the electrodes and consumed at the other electrode. In order for a reaction to generate or consume electrons, ions must be involved in the reaction. This is, in general, the difference between combustion and electrochemical combustion. In the former, the reaction is between atoms or molecules; while, in the latter, at least one ionic species is present.

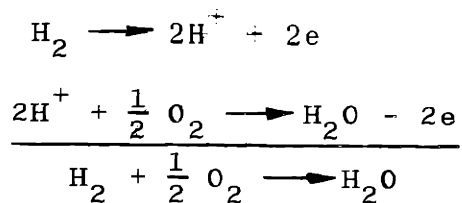
Another requirement of a fuel cell, since the electrodes are separated, is the provision of some means of mass transfer of oxygen to the fuel electrode, or of fuel to the oxygen electrode. The ionic species involved in the electrode reactions may also be the means of mass transfer, but this is not necessary. For example, we can envision the oxidation of carbon in a fuel cell as occurring, according to the following equations:



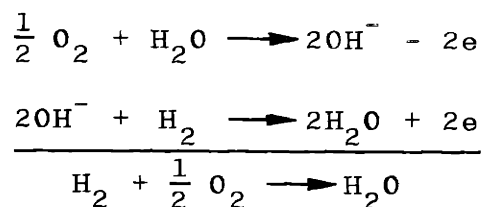
In this case hydrogen ions are the ionic species and "carry the current" in the electrolyte, while the mass transfer is accomplished by water going from the oxygen electrode to the fuel electrode.

It is seen from the above equations that, though ions are involved at the electrodes, the fuel and the oxygen are not ionized, nor are they parts of the ions. It is a common misconception to believe that either or both the fuel or the oxygen must be ionized or be parts of the ionic species, entering into the electrode reactions.

For fuel cell systems in which the ion transference also provides mass transference, it is necessary for either the oxygen or the fuel to be part of the ion. This can be seen in the following sets of equations:



or

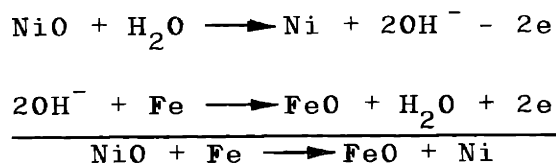


The first set of reactions are those which occur during the reverse of electrolysis in a slightly acidified electrolyte. The ion involved in the reactions is a fuel-containing one, the hydrogen ion. The ion involved in the second set of reactions is an oxygen-containing ion, the hydroxyl ion.

For a continuously operating fuel cell, the electrodes, if they are not the actual reactants, and the electrolyte must

not change in composition with time. Storage batteries of the metal oxide-caustic-metal type operate with no change in electrolyte composition, and hence may be used as a starting point.

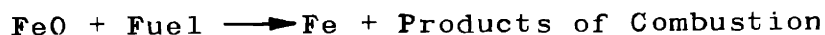
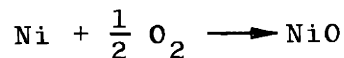
An example of a caustic storage battery is the familiar Edison storage battery, consisting of a nickel oxide cathode, a 20 per cent KOH electrolyte, and an iron anode. During discharge the nickel oxide is reduced to nickel, the iron is oxidized to iron oxide, and the electrolyte remains unchanged.



Thus, if the nickel electrode can be kept oxidized by air and the iron electrode reduced by fuel, the cell will always be charged; and we have, in effect, a fuel cell.

It is important to note that in this fuel cell the open-circuit voltage does not depend on the fuel used. The maximum efficiency of this fuel cell is the open-circuit voltage of the nickel oxide-iron cell divided by the maximum theoretical voltage of the fuel-oxygen system.

The reason for this loss of efficiency is the presence of free-energy changes in the activation steps at the electrodes.



These reactions do not involve ions and, therefore, cannot contribute to the work output of the cell.

In order to obtain higher efficiencies, electrodes which have lower free-energy changes in the activation steps must be used. By using carbon activated with metals, open-circuit voltages equal to the fuel-oxygen system have been achieved; i.e., the free-energy changes in the activation steps are negligible.

Keeping in mind the fact that any number of electrode systems may be used, we return to the consideration of the Edison storage battery as a generalized fuel cell.

In order to understand how this general fuel cell operates, it is necessary to examine the physical and chemical steps involved. Broadly, we have the following eight separate steps:

- (1) Mass transfer of oxygen to the nickel cathode.
- (2) Rate of reaction of oxygen with the nickel cathode.
- (3) Rate of reaction of nickel oxide with the electrolyte to form oxygen-containing ions.
- (4) Mass transfer of oxygen-containing ions from the nickel cathode to the iron anode.
- (5) Rate of reaction of the oxygen-containing ions with the iron anode.
- (6) Mass transfer of fuel to the iron anode.
- (7) Rate of reaction of the fuel with iron oxide.
- (8) Mass transfer of products of combustion from the iron anode.

Any one of these steps, if it is slow compared with the others, will limit the operation of the cell.

Current densities obtainable from caustic cells are high; therefore, one would think that steps 3, 4, and 5 are rapid and not rate controlling. Most of the emphasis in past work on fuel cells has centered on finding the right activators to catalyze the rates of reaction of oxygen with the oxygen electrode and fuel with the fuel electrode (steps 2 and 7). The possibility that the mass-transfer processes (steps 1, 6, and 8) may control the rates of fuel cell reactions has been all but neglected.

C. MASS-TRANSFER PROCESSES IN FUEL CELLS

The actual mass-transfer processes by which oxygen or fuel enter into reaction at the electrodes of a fuel cell have not been determined; however, some important conclusions may be arrived at from an overall consideration of the operation of a fuel cell electrode. The discussion will deal only with the oxygen electrode; but it is, in general, equally valid for the fuel electrode (if the fuel is a gas).

Adams² has suggested a current density of 100 ma/cm^2 as the criterion for an economical fuel cell. This can, in turn, be converted to the oxygen consumption required of an economic fuel cell.

$$\begin{aligned}
0.1 \text{ amp/cm}^2 &= 0.1 \text{ Coulombs/sec cm}^2 \times 6.02 \\
&\times 10^{23} \text{ molecules O}_2/\text{gm mole} \\
&\times \frac{1}{96,500} \text{ gm equiv/coulomb} \times \frac{1}{4} \text{ gm mole/gm equiv} \\
&= 1.56 \times 10^{17} \text{ molecules O}_2/\text{sec cm}^2
\end{aligned}$$

Next, one can calculate the rate at which oxygen molecules strike a surface from the formula

$$N \text{ collisions/cm}^2 \text{ sec} = 0.23 C \sqrt{\frac{3RT}{M}} \quad (3)$$

where

$$C = \text{the number of molecules of O}_2 \text{ in a cm}^3$$

$$R = 8.314 \times 10^7 \text{ ergs/deg K gm mole}$$

$$M = 32$$

$$T = 293^\circ \text{ K}$$

Assuming that air at atmospheric pressure is the source of oxygen, so that the oxygen partial pressure is about 0.21 atm, we find that $C = 5.25 \times 10^{18}$; and the rate at which oxygen molecules strike the surface is $N = 5.78 \times 10^{22}$ molecules/sec cm^2 . This is a factor of about 370,000 times greater than what is required to maintain a current density of 100 ma/ cm^2 . This picture, however, assumes that none of the oxygen molecules react with the wall.

If the oxygen atoms hitting the surface are adsorbed, the oxygen partial pressure will decrease near the surface; and a stagnant gas layer with an oxygen partial pressure gradient will form. The rate at which oxygen molecules reach the surface will be dependent on the thickness of the stagnant layer and the diffusivity of gaseous oxygen through it.

An estimate of the thickness of the stagnant layer necessary to limit oxygen diffusion to 1.56×10^{17} molecules O_2/cm^2 sec can be obtained from the equation for diffusion of a gas through a stagnant layer:³

$$N_A = \frac{D_V P}{RT\Delta Z} \ln \frac{P_{B1}}{P_{B2}} \quad (4)$$

where D_V = Diffusivity of the diffusing gas
 P = Total pressure
 P_B = Partial pressure of the inert gas
in the stagnant film
 ΔZ = Stagnant-film thickness
 N_A = Moles of gas A diffusing per unit time,
per unit area

Reid and Sherwood⁴ give a value of $D_V P = 0.175 \text{ atm cm}^2/\text{sec}$ for the diffusion of oxygen through air at 273°K . Assuming $p_B = 1 \text{ atm}$ at the copper surface, and neglecting the change of diffusivity with temperature, we get

$$\Delta Z = \frac{0.175 \text{ atm cm}^2/\text{sec} (\ln \frac{1}{0.79}) (6.02 \times 10^{23} \text{ molecules O}_2/\text{gm mole})}{82 \text{ atm cm}^3/^\circ\text{K gm mole} (293^\circ\text{K}) (1.56 \times 10^{17} \text{ molecules O}_2/\text{cm}^2 \text{ sec})}$$

$$\Delta Z = 6.6 \text{ cm}$$

Thus, a stagnant gas layer as thick as 6.6 cm would still allow enough oxygen diffusion to maintain a current density of 100 ma/cm^2 ; and, hence, this part of the mass-transfer process presents no problem.

In order for an electrochemical reaction to occur at an oxygen electrode, it is necessary for both electrolyte and oxygen to be in contact with the electrode; and the presence of the electrolyte may present a serious resistance to mass transfer.

For example, suppose that the electrode is covered by electrolyte. The oxygen must first dissolve in the electrolyte, and then be carried by convection and diffusion to the electrode surface. Noting that the solubility and diffusivity of oxygen in strong electrolytes are very small, one might expect a very low mass-transfer rate.

Solubility and diffusivity data could not be found in the literature for oxygen in 20% KOH; however, they are reported for 20% NaOH, and they should be of about the same order of magnitude. The solubility of oxygen in 20% NaOH is 2.77×10^{-5} gm moles per liter under 0.21 atm O_2 pressure, and the diffusivity is about $1 \times 10^{-6} \text{ cm}^2/\text{sec}$.

Assuming the oxygen has to diffuse a distance of only 0.001 cm, that the air electrolyte interface is saturated, and that there is no dissolved oxygen at the electrode interface, the mass-transfer rate in 20 per cent NaOH can be estimated:

$$N = \frac{D_L (C_1 - C_0) A}{Z} \quad (5)$$

Let

$$A = 1 \text{ cm}^2$$

$$C_1 = 2.77 \times 10^{-5} \text{ gm moles } O_2/\text{liter} \times \frac{1 \text{ liter}}{1000 \text{ cm}^3} \times 6.02 \times 10^{23} \text{ molecules } O_2/\text{gm mole } O_2 = 1.67 \times 10^{16} \text{ molecules } O_2/\text{cm}^3$$

$$C_0 = 0$$

$$D_L = 1 \times 10^{-6} \text{ cm}^2/\text{sec}$$

$$Z = 0.001 \text{ cm}$$

$$N = \frac{(1 \times 10^{-6})(1.67 \times 10^{16} - 0)}{.001} = 1.67 \times 10^{13} \text{ molecules } O_2/\text{sec}$$

which corresponds to a current density of about 0.01 ma/cm², or about 10,000 times less than required. Thus, it is evident that, if the process by which oxygen is transported from the gas phase to the electrode surface is by diffusion through the electrolyte, then the resistance to mass transfer is very large and might very well be controlling.

D. REVIEW OF FUEL CELLS

1. Hydrogen, Oxygen Fuel Cells

Fuel cells have a long history, dating back to 1801 when Sir Humphry Davy suggested that it should be possible to construct electrical cells which consumed fuel and oxygen.

The Grove cell, the first fuel cell, was improved by Mond and Langer in 1889,⁵ who obtained current densities of 6.5 milliamperes per cm² of electrode surface at an operating voltage of 0.73 v. This was achieved with electrodes of perforated platinum foil coated with platinum black. The theoretical maximum voltage of an H₂,O₂ cell is 1.19 v; thus, an operating

voltage of 0.73 v represents an efficiency of over 61 per cent. However, it is seen that the current density of this cell is much smaller than the 100 ma/cm^2 suggested by Adams.

The diffusion gas electrodes of Schmid (1923)⁶ permitted currents of up to 25 ma/cm^2 at hydrogen electrodes and led to the development of the most successful H_2, O_2 fuel cells to date.

Schmid used an activated, hollow, porous carbon electrode into which the hydrogen was led. The electrode was submerged in a caustic electrolyte, and the hydrogen diffused to the electrode-electrolyte interface. The carbon was activated by electrodepositing platinum in its pores, and the electrolyte was kept from entering the pores of the electrode by keeping the hydrogen gas at a slightly higher pressure than the electrolyte. If the electrolyte entered and filled all the pores of the electrode, the electrode became "drowned" and did not function properly. Though present-day fuel cell electrodes are constructed to prevent drowning, the actual mechanism of drowning is still not clear.

The oxygen electrode, the other member of the H_2, O_2 fuel cell, had not yet reached such a state of development; so, the H_2, O_2 cell had to wait for an improved oxygen electrode. In 1947 the oxygen electrode of a commercial "heavy duty" air-depolarized caustic battery had a rated current density of only 7.2 ma/cm^2 .⁷

O. K. Davtyan⁸ caused a renewed interest in fuel cells when in 1947 he reported current densities of 20 to 35 ma/cm^2 for a H_2, O_2 fuel cell. Davtyan had two fuel cells: a low-temperature (room temperature) liquid electrolyte cell and a high-temperature solid electrolyte cell.

The Davtyan low-temperature cell uses porous carbon electrodes containing 10 per cent finely divided nickel or silver and a 35 per cent KOH electrolyte. The electrodes are coated with a thin layer of wax to prevent wetting by the electrolyte and subsequent drowning. The operating voltage is 0.75 to 0.80 v at current densities of 25 to 35 ma/cm^2 , representing an efficiency of about 65 per cent.

The high-temperature solid electrolyte cell operates at about 700°C with air and either H_2 or CO . The anode is $\text{Fe}/\text{Fe}_2\text{O}_3$ with 20 per cent clay, and the cathode is $\text{Fe}_2\text{O}_3/\text{Fe}_3\text{O}_4$ with 20 per cent clay. A mixture of Na_2CO_3 , soda glass, CeO_2 , WO_3 , and clay is used as the electrolyte. A voltage of 0.75 to 0.785 v was obtained at a current density of 20 to 30 ma/cm^2 . One of the principal problems in the operation of this cell is cracking of the electrolyte, due to thermal stresses, which allows the hot combustible to come in contact with the hot air and results in an explosion.

In 1951 Kordesch and Marko^{9,10,11} prepared oxygen electrodes, similar to the Schmid gas diffusion electrode, in which current densities of 30 ma/cm^2 were attained. The porous carbon electrodes were activated with metals and metal oxides by adding solutions of the metal nitrates to the electrodes and then decomposing the nitrates by heating. Electrodes activated in the above manner are also effective as hydrogen electrodes and form the basis of the National Carbon H_2, O_2 fuel cell.

The National Carbon fuel cell also uses a concentrated KOH electrolyte and operates best at about 55°C .¹² At atmospheric pressure the operating voltage is 0.8 v, and the current density is 10 to 20 ma/cm^2 ; but with increased pressure it is capable of current densities of 200 ma/cm^2 .

Another important H_2, O_2 cell is the high-pressure Bacon cell^{13,14} which uses porous nickel electrodes. In these electrodes drowning is prevented by using a surface layer of finer porosity and by keeping the hydrogen and oxygen at slightly higher pressures than the electrolyte. At 200 to 240°C and 800 psi, Bacon obtained current densities of over 1000 ma/cm^2 at a voltage of 0.6 v. The principal difficulty of this cell was deterioration of the oxygen electrode, but Bacon has recently reported considerable improvement in the durability of the oxygen electrode.¹⁵ This was accomplished by adding lithium to the nickel oxide lattice of the surface of the electrode. With a 600-psi-pressure H_2, O_2 fuel cell, operating at 679 ma/cm^2 and 0.585 v, Bacon has achieved power outputs of 8.5 kw/ft^3 .

The weight-to-energy ratio of such a cell is dependent mainly on the weight of the steel cylinders used to store the gases, and is about 21 lbs/kw hour.

2. Carbonaceous Fuels

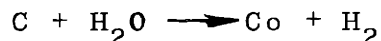
Most of our naturally occurring fuels can be traced back to plant life and, as a result, are mainly carbon-containing compounds. These fuels are essentially storers of energy originally obtained from the sun and trapped by the process of photosynthesis. The use of these fuels is more economical than those like hydrogen, which in general is not found in the natural state.

A great deal of work has been directed towards the use of carbon or coal in fuel cells, but the success obtained with carbon fuel cells has not been great and is very small indeed when compared with the hydrogen fuel cells.

The principal problem seems to be that carbon is not as reactive as other fuels; and, as a result, high temperatures have been used. At high temperatures aqueous electrolytes require the use of exceedingly high pressures, making the equipment bulky and prohibitively expensive. Fused electrolytes or solid electrolytes are, unfortunately, not as good as aqueous electrolytes. In addition, at high temperatures the electrolyte itself may react with the electrodes.

Two general types of carbon fuel cells have been proposed: direct and indirect cells. An example of a direct carbon fuel cell is the Bauer, Preis¹⁶ cell in which the anode is carbon; the electrolyte is solid and made of CeO_2 , WO_3 , and clay; and the cathode is Fe_3O_4 . In order for the conductivity of the electrolyte to be sufficiently high, the operating temperature was raised to above 1000°C . At a temperature of 1100°C the voltage was 0.55 v with current densities of only 3.8 ma/cm^2 .

In an indirect fuel cell, carbon is used to produce an intermediate substance which is reacted in the fuel cell. For example, by passing steam over hot coke, water gas can be produced.



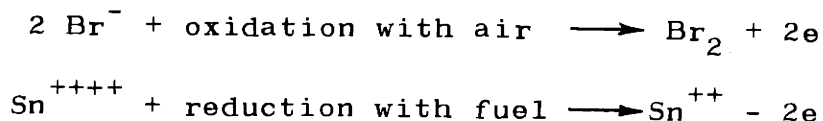
Since it can operate on a CO, H_2 mixture, the Davtayan high-temperature solid electrolyte cell previously described can be used as an indirect-type carbon fuel cell.

Gorin^{17,18,19} obtained a series of patents covering the operation of such an indirect cell in which the solid electrolyte was a soda glass with monazite sand, WO_3 , and sodium silicate. This cell is unique because the heat liberated by the fuel cell is used in the gasification of the carbon, thus increasing the total over-all efficiency of the system. Gorin claimed over-all efficiencies of 70 to 80 per cent; but, though the patents were obtained in 1951 and 1952, nothing further has been reported about this fuel cell.

With the exception of carbon monoxide, very little work has been reported on the use of carbon-compound fuels in fuel cells; however, the recent announcement by the Allis Chalmers Manufacturing Company²⁰ of the development of a fuel cell tractor, operating on propane and oxygen, is certainly a very important step towards an economical fuel cell. The Allis Chalmers fuel cell apparently operates at low temperature and pressure with a liquid electrolyte, and drives a 20-horsepower motor. The operating efficiency is said to be about 60%.

3. Redox Cells

An entirely different type of fuel cell was developed by Posner²¹ which makes use of the high rates of reaction of ionic oxidation-reduction reactions. This so-called "redox" cell uses two electrolytes, called anolyte and catholyte, which are separated by a semi-permeable membrane, and inert electrodes. In the cell the anolyte becomes reduced and the catholyte oxidized. The anolyte and catholyte are continuously removed and regenerated by treatment with air and fuel, respectively, outside the cell. For example, using a bromine solution as the anolyte and the stannous ion as the catholyte, the cell can be represented as in Fig. 1. The regeneration reactions, carried on outside the cell, are:



The advantage of such a system lies in the fact that the oxidation of the fuel, the adsorption of the oxygen, and the

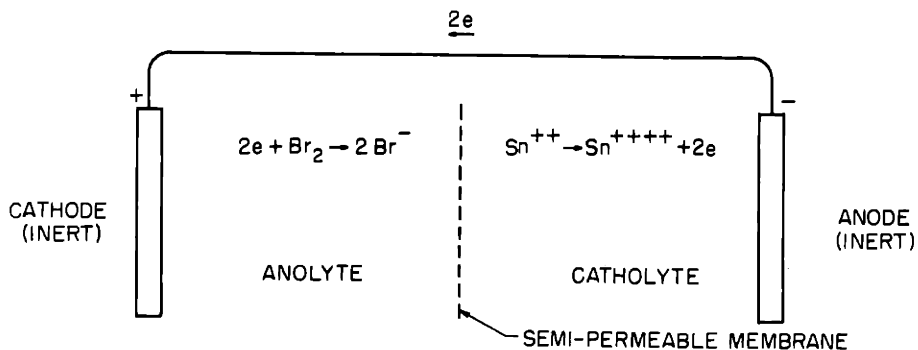


Fig. 1 Redox Cell

actual operation of the cell may be carried out under different conditions of temperature and pressure such that output is optimized for each process.

Since ionic oxidation-reduction reactions proceed rapidly, the use of such a method is attractive. However, an anolyte-catholyte system having a satisfactorily high potential has not yet been found; and oxidation of the fuel by the catholyte still needs to be improved.

A large number of fuel cells, too numerous to report here, have been proposed since the Grove cell. More information can be found from the many reviews of fuel cells which have appeared in the literature.^{2, 22-29}

In addition, a bibliography on fuel cells is presented in the appendix of this thesis. This bibliography was compiled by Mr. A. M. Adams of the Central Electricity Research Laboratories, Leatherhead, England, and is reproduced through the courtesy of the Director, Dr. J. S. Forrest. The bibliography covers work done prior to 1950 and is so well cross-indexed that it becomes an invaluable aid to anyone interested in the subject of fuel cells.

E. METABOLISM AND FUEL CELLS

One of the properties of all living things is that they have the ability to move; i.e., they produce mechanical energy from other forms of energy. In addition, particularly in the case of electric eels, animals are known to convert the chemical energy of food into electrical energy.

Metabolism studies have shown that the conversion of chemical energy to mechanical energy in animals and muscle movement is at least 20 per cent.³⁰ Such an efficiency would require a heat engine whose upper operating temperature is 100°C, which is too high to exist in living cells. Thus, the chemical energy of food must be converted to mechanical energy without an intermediate conversion to heat.

Since the useful energy derived by animals from food appears primarily as mechanical energy and not as electrical energy, animals are not fuel cells in the strict sense of the word. However, the fuel-cell problem is mainly one of rate; and animal metabolism is a process which occurs at a significant rate. Of course, enzymes, nature's catalysts, are quite complex agents; but, nevertheless, it is possible to oxidize carbon compounds at appreciable rates without resorting to the high temperatures and pressures used in some fuel cells. This shows that it is possible to construct a low-temperature, low-pressure fuel cell with fuels such as alcohols, carbohydrates, and possibly even hydrocarbons. These considerations helped lead to the decision to study a low-temperature, low-pressure oxygen electrode.

In addition, one should note that the above discussion also suggests the study of the direct conversion of chemical energy to mechanical energy. This is an energy-conversion process that certainly deserves more attention than has been given it heretofore.

F. ISOLATION OF OXYGEN ELECTRODE

The oxygen electrode was chosen to be studied in this thesis; but, since there are two electrodes in an electrical

cell, one must in general also reckon with the second member. By proper construction of the cell, however, one may make the rate of reaction at one of the electrodes limiting so that the current is really a measure of the rate of reaction at this electrode; and so, in a sense, it is "isolated" from the second electrode.

The current of a cell may be limited by any one of four factors: the external resistance, the internal resistance, and the rates of reaction at either electrode. For example, if either the external or internal resistances were infinite, the current would be zero, irrespective of at what rate the reactions at the electrodes could proceed. By using a strong electrolyte, close electrode spacing, and a low external resistance, the current will depend on the rates of reaction at the electrodes.

In order for the current to be limited by the reaction at one electrode, the product of the rate of reaction and the area of that electrode must be much less than for the second electrode. Assuming, for sake of argument, that the rates of reaction are approximately the same, then if the area of one electrode is very much smaller than the second electrode, the current will be limited by, and be a measure of, the rate of reaction at the first electrode. Thus, in order to study the rate of reaction of oxygen at an oxygen electrode, the area of the oxygen electrode must be very small in comparison to the area of the second electrode. This principle has been maintained in all cells used to investigate the oxygen electrode in this thesis.

In these cells, since we are primarily interested in the rate of reaction, the question of reversibility or of open-circuit voltage does not exist. As a matter of fact, the nature of the second electrode is unimportant once it is established that it does not influence the current of the cell.

CHAPTER III

APPARATUS

The experimental work in this thesis was divided into two parts: work with a stationary submerged oxygen electrode, and that with a rotating submerged oxygen electrode.

A. STATIONARY ELECTRODE

The stationary electrode was used to study the mechanism of oxygen transport to air-depolarized metal electrodes, and the apparatus is shown in Fig. 2.

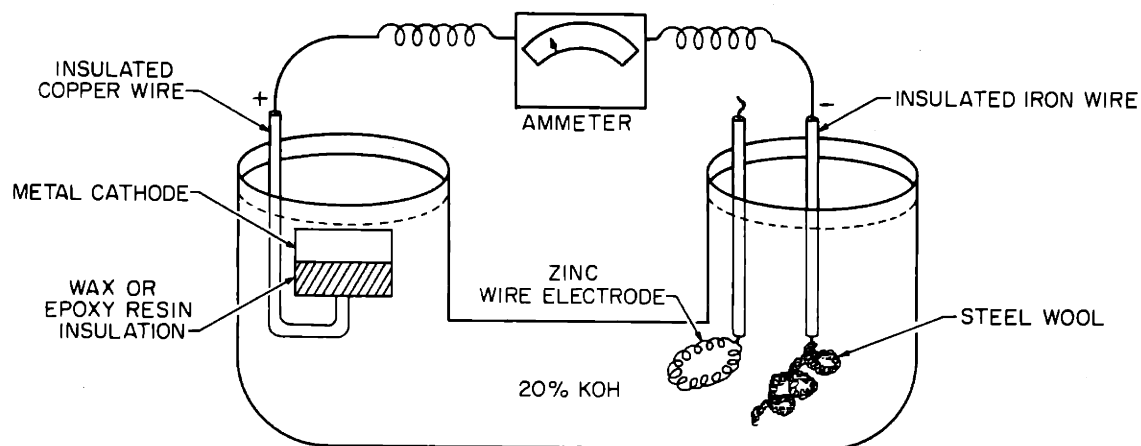


Fig. 2 Cell with Air-Depolarized Cathode

The contact between the copper wire and the metal electrode was mechanical, and insulated with wax or epoxy resin. The anode was a piece of steel wool whose surface area was much larger than the area of the metal electrode. The zinc electrode was made of 0.10 or 0.12" diameter zinc wire.

In order for the steel-wool electrode to function properly, it must not contain any entrained oxygen. The entrained oxygen is removed by connecting the steel-wool electrode to a zinc electrode for about a minute. Hydrogen is evolved at the steel wool, and this sweeps it clean of any entrained oxygen.

The experiment starts with the oxygen electrode completely submerged. The current is observed; and the depth of the top edge of the cathode, with respect to the top of the U-tube, is measured with a depth gauge.

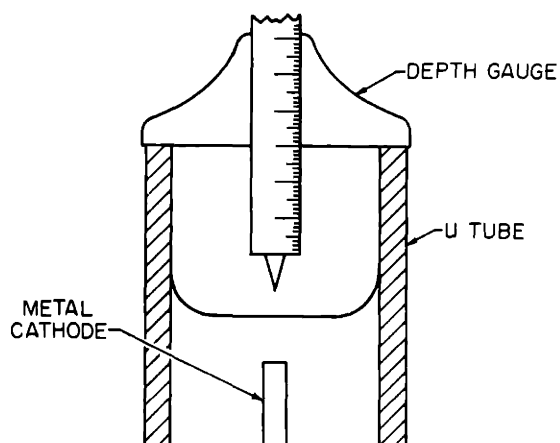


Fig. 3 Depth Gauge

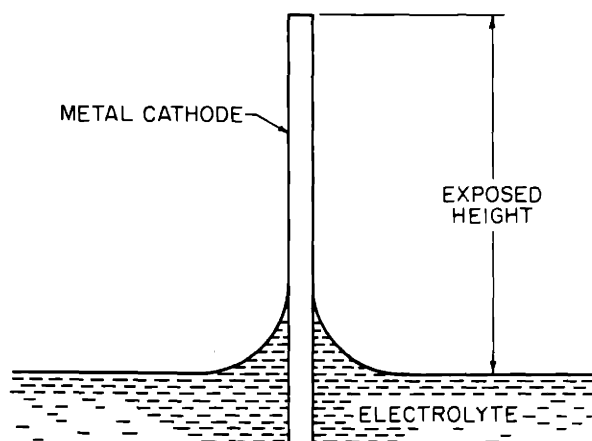


Fig. 4 Measurement of Exposed Height

with respect to the top of the U-tube, is measured with a depth gauge. The depth gauge is equipped with a needle point and is shown in Fig. 3.

Electrolyte is then removed with a pipet from the steel-wool leg of the U-tube, so that the electrolyte level is lowered a few 64^{ths} of an inch at a time. The current and the position of the electrolyte are measured after each electrolyte withdrawal. The needle point of the depth gauge permits the accurate location of the electrolyte level.

The electrolyte position is measured from the main portion of the surface, not near the menisci. The exposed height of the electrode is taken as the height of the top of the electrode above the

electrolyte position, and is shown schematically in Fig. 4.

B. ROTATING ELECTRODE

The complete apparatus used to measure the oxidation rate of metal surfaces is shown in Fig. 5. The equipment can be divided into three parts: the electrochemical system, the driving mechanism, and the measuring instruments.

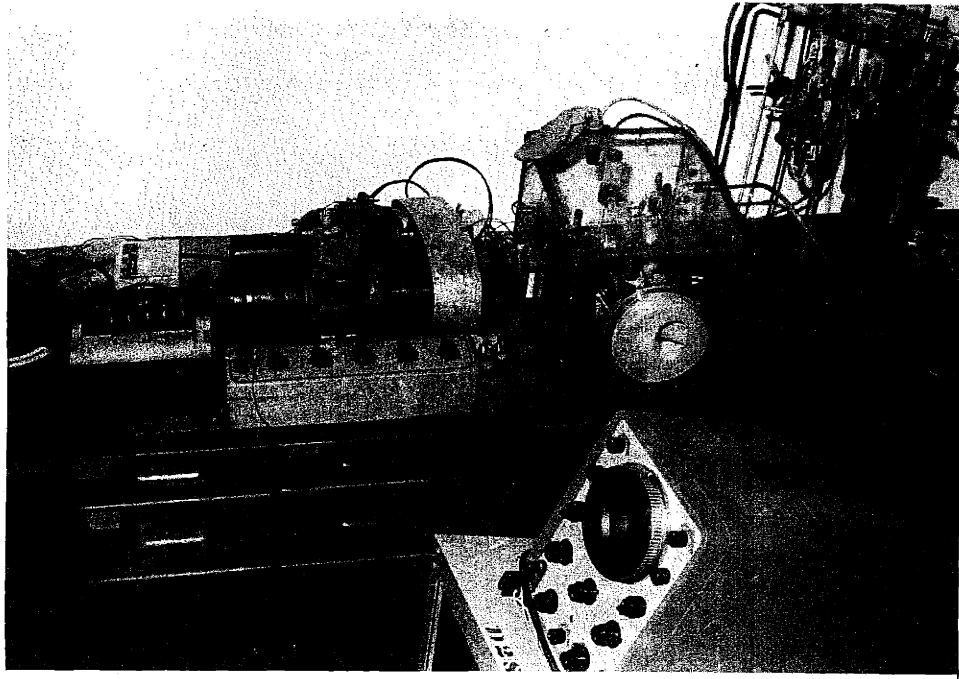


Fig. 5 Complete Apparatus

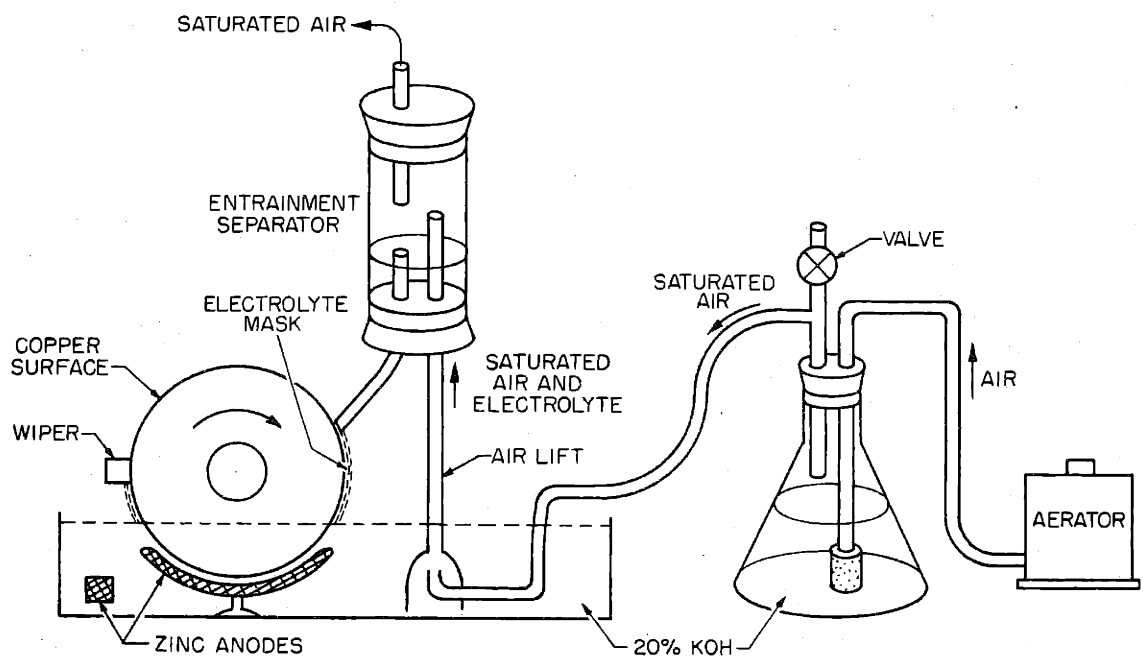


Fig. 6 Electrochemical System

1. Electrochemical System

The electrochemical system is that contained in the lucite box; and, as seen in Fig. 6, it is made up of a number of components: the rotating electrode, rubber wiper, zinc anodes, an air saturator, and a lift pump.

a. Oxygen Electrode. The rotating oxygen electrode is designed to expose a continuous source of oxide-free metal surface to an oxygen atmosphere. It essentially consists of a copper ring embedded in the rim of a lucite disc. The diameter of the disc is 7.84 cm, and the edge is machined so that it is flat and smooth. Three such electrodes were made, one of which was silver plated and another nickel plated. Figure 7 is a photograph of a rotating oxygen electrode.

The two rods connected to the lucite disc are made of brass, and the smaller of the rods is electrically connected to the copper ring by means of a wire which passes through the lucite disc. The large rod attaches to the driving shaft, and is electrically insulated from the copper ring to isolate any spurious currents which may originate in the motor.

Electrical contact with the electrode is made by means of a spring-loaded brass contact which fits into a recess at the center of the small rod, as shown in Fig. 8. A lucite sleeve with silicone grease is provided to prevent spattered electrolyte from reaching and corroding the contact area.

The electrode surface was cleaned with No. 400A silicon-carbide paper just prior to making a run.

b. Rubber Wiper. If the rotating electrode is to measure the rate of oxidation of a metal surface, it is imperative that an adequate amount of oxygen has access to the surface. The presence of an electrolyte film on the metal surface would greatly limit the transport rate of oxygen; so, it becomes necessary to find a means of removing it. This was done by wiping with a specially designed gum-rubber wiper, as shown in Fig. 9.

The complete removal of the electrolyte film by means of a wiper is difficult; however, it is possible by proper positioning of the rubber wiper (a trial-and-error process) to

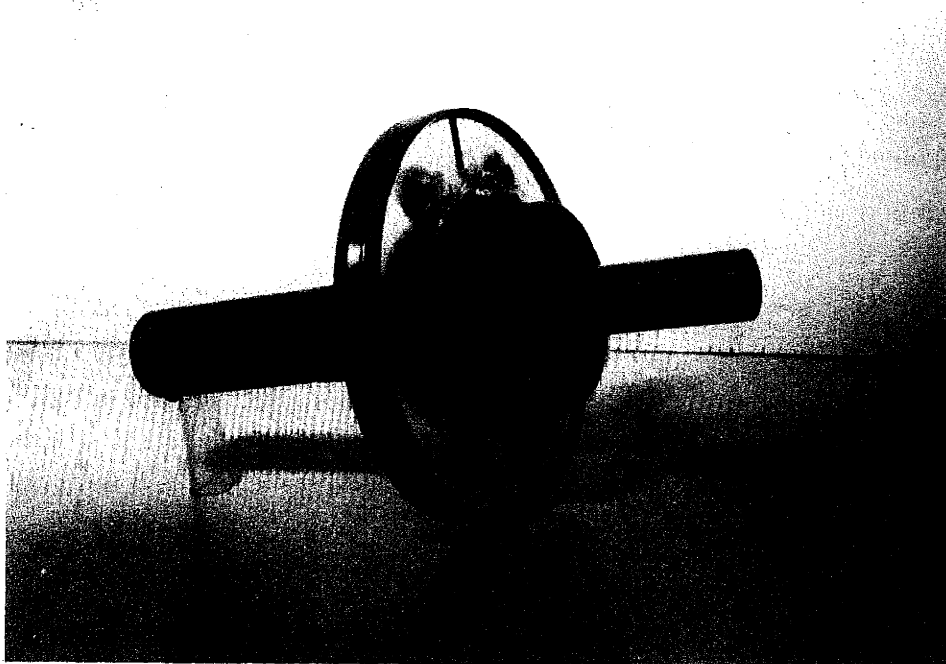


Fig. 7 Rotating Electrode

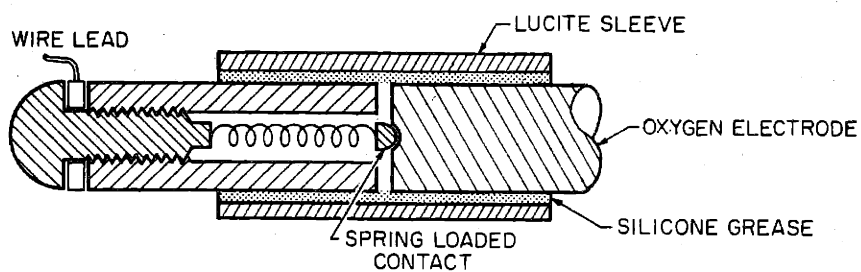


Fig. 8 Electrical Contact to Rotating Electrode

obtain a metal surface free of electrolyte film. Once a position which gives good wiping is obtained, it is fairly easy to return to; and, hence, the wiping action can be stopped or started repeatedly.

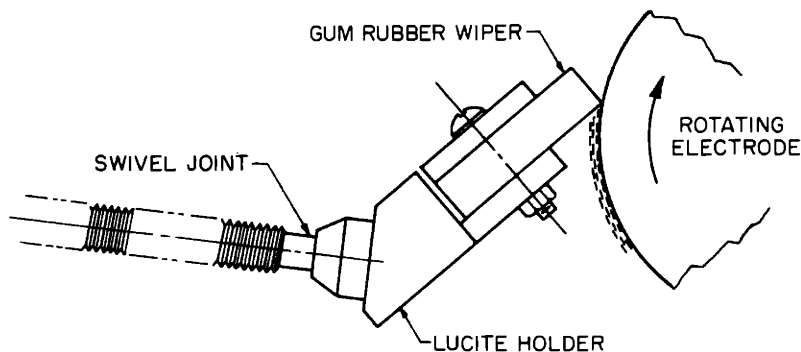


Fig. 9 Wiper

A sensitive test for wiping consists of placing another wiper on the wiped rotating metal surface. The wiping action is deemed successful when no electrolyte accumulates at the second rubber wiper. One could argue that the second wiper is only wiping as good as the first; and, hence, even with poor wiping at the first wiper, no electrolyte should accumulate on the second wiper. However, one must note that there is an essential difference between the two wipers. The first wiper operates with a large accumulation of electrolyte on one side of it; whereas, the second wiper does not. For this reason, the second wiper should always wipe better; thus, when nothing accumulates at the second wiper, the electrolyte film must have been removed by the first wiper.

The easiest and quickest method of determining the presence or absence of an electrolyte film is by sighting the surface at a glancing angle. An electrolyte film is easily visible this way.

c. Zinc Anodes. The anodes used with the rotating electrode were made from 100- or 150-foot lengths of 0.012" diameter zinc wire, wrapped around lucite frames. The surface area of such an electrode is 300 to 400 cm². The total surface area of

the rotating oxygen electrode is about 9 cm^2 ; and, since only a portion of the electrode is being used for electrochemical action, it is seen that the area of the zinc electrode is approximately 100 times greater than the oxygen electrode.

The zinc electrode was rocker shaped and held in place about $1/4$ " away from the metal surface of the rotating electrode by means of a suction cup, as shown in Fig. 6.

A second zinc anode, which could be switched into or out of the circuit, was also present. This provides a convenient means of doubling or halving the anode area.

d. Lucite Box. It was found that humidity affected the current obtainable from the cell*; and so, it became necessary to provide a controlled atmosphere above the oxygen electrode. This was done by enclosing the cell in a lucite box and keeping the contents saturated, with respect to the 20% KOH electrolyte.

The air was kept saturated, with respect to the electrolyte, by circulating it through a gas sparger immersed in electrolyte. The air was circulated by an ordinary aquarium aerator, as shown in Fig. 6.

The airtight lucite box also made it possible to vary the partial pressure of oxygen in the system. The oxygen partial pressure was varied by admitting O_2 or N_2 from gas cylinders.

A rubber glove was mounted on the front lucite panel in order to permit manipulations within the lucite box during a run. The glove, a thin-walled surgeon's glove, tended to collapse due to the increased pressure within the box when one tried to insert his hand in the glove. This problem was solved by connecting a normally deflated balloon to the lucite box. In this way the pressure inside the box remained constant, and it was possible to use the rubber glove without any difficulty.

e. Lift Pump. The final part of the electrochemical system is the lift pump. The purpose of the pump is to vary the ratio of the exposed to the submerged areas of the rotating oxygen electrode. This is done by adding a layer of electrolyte to a portion of the wiped electrode surface. See Fig. 6.

*The effect of humidity on the output of the cell is described in detail in the appendix.

The presence of the electrolyte "mask" essentially eliminates transport of oxygen to this portion of the electrode surface. Thus, the ratio of exposed to submerged areas can be changed by adding or removing the electrolyte mask.

The advantage of the air lift is that it is simple and has no moving parts. It is made of glass; hence, there is no problem of corrosion or of contamination of the electrolyte. In addition, it operates on the air leaving the saturating flask, and needs no separate source of power. The operation of the air lift can be halted by opening the valve above the air saturator. This diverts the air stream, and permits the continued operation of the air saturator.

2. Driving Mechanism

The rotating oxygen electrode was driven by a Graham Variable Speed Transmission with a directly connected 1/12-horsepower motor. The transmission operates by means of a traction ring and tapered rollers, and the output R.P.M. can be varied continuously from zero to maximum R.P.M. by means of a control gear. The particular model employed, 15M, had a maximum R.P.M. of 1100.

A 16-to-one gear reducer was used to increase the torque to the rotating electrode. In addition to increasing the torque, this permitted closer R.P.M. control within the now narrower R.P.M. range of 0 to 68.7.

The output shaft of the gear box enters the lucite box through a flange in the wall so that the driving mechanism is outside the box and the rotating electrode inside the box. This protects the driving mechanism from possible contact with the corrosive electrolyte. Also, the heat generated by the motor, transmission, and the gear box is dissipated to the atmosphere and does not serve to increase the temperature at the oxygen electrode.

3. Measurements

The R.P.M. was measured by an R.P.M. meter consisting of a d-c generator and a voltmeter which measured its output. The

generator was attached, by means of gears and a link belt, directly to the output of the Graham drive. The voltmeter had two scales, giving R.P.M. readings of 0 to 750 and 0 to 1500. This arrangement was found to give, except at very low R.P.M.'s, stable and accurate readings.

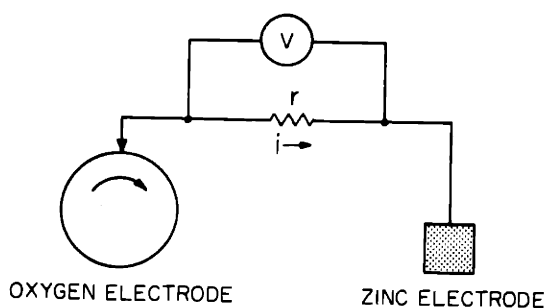


Fig. 10 Measurement of Cell Current

The current of the electrochemical cell was determined by measuring the voltage across a known resistance in

the circuit. This is shown schematically in Fig. 10.

The known resistance was provided by a Heath Kit Decade Resistance Box which was previously calibrated, using a d-c resistance bridge. Two extra resistances were added to the resistance box in order to extend the resistance range to below 1 ohm.

The voltage was measured by means of an oscilloscope, or a voltmeter. The oscilloscope was found to be convenient when the external resistance was varied over a wide range. The voltages which varied from millivolts to about a volt could be easily accommodated on the oscilloscope by varying the sensitivity. The oscilloscope used was a Hewlett Packard Model No. 130A, which has a maximum sensitivity of 1 mv per cm and a calibrated sensitivity selector.

For most of the experimental work, the external resistance was kept constant; and the voltage across it did not vary over such a wide range. In this case an ordinary millivoltmeter was more convenient to use. The meter employed was a Siemens-Halske voltmeter, which had a voltage range of 0 to 18 mv and an internal resistance of 423 ohms. The meter was adapted to read 0 to 36 mv and 0 to 72 mv, by adding resistances of 423 and 1269 ohms, respectively, in series with the internal resistance of the meter. These resistances were added or removed by

means of switches so that the range of the voltmeter could be changed whenever necessary.

The final measuring instrument was the Orsat gas analyser. The measurement of the oxygen partial pressure, and indeed the entire apparatus itself, is simplified by the fact that the oxygen concentration is essentially constant throughout a run.

If the oxygen electrode operated continuously at a current of as high as 100 ma, the oxygen consumption would be about 20 cm³ per hour. The volume of the lucite box is about 20,000 cm³; therefore, the concentration change due to oxygen consumption would be only about 0.1% per hour, which is negligible.

The absorbing solution used was ammoniacal cuprous chloride in contact with copper gauze, as recommended by Mullen.³¹ It was found, as pointed out by Badger,³² that the oxygen absorption was satisfactory only when the copper gauze in the absorption buret came into direct contact with the admitted gas sample. Copper gauze which remains submerged completely has almost no absorption effect on the oxygen. With the system used, the absorption was rapid; and in four passes, complete absorption was achieved for a sample containing over 83% oxygen.

CHAPTER IV

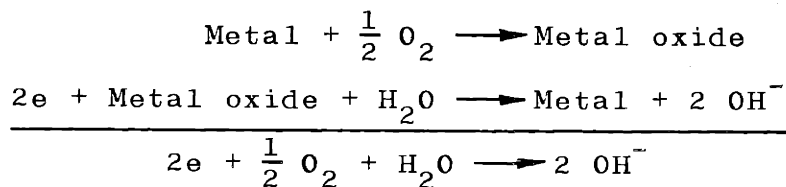
RESULTS AND DISCUSSION OF RESULTS

A. MECHANISM OF OXYGEN TRANSPORT TO AIR-DEPOLARIZED CATHODES

1. Introduction

Metals, like copper, nickel, and silver, exist under normal conditions with a coating of oxide, or physically adsorbed oxygen, which can be used as the oxide source for the cathode of a caustic cell. The surfaces of these metals, when freshly reduced, react rapidly with oxygen; hence, all that is needed to use these metals as oxygen electrodes is a means of transporting oxygen to their surfaces.

Early batteries sometimes used, as did von Rhorer³³ in a fuel cell, partially submerged metals as cathodes. In the von Rhorer cell the metal was copper; but metals, like nickel, silver, platinum, etc., could also have been used. The partially submerged metal reacts with oxygen from the air, and the "oxide" is reduced by the electrochemical action of the electrolyte. Ideally, nothing else occurs; and the metal electrode may be considered to operate according to the following simplified equations.*



If the metal electrode is to function as an air-depolarized cathode, oxygen in some form must be present at the electrode-electrolyte interface. It is the mechanism of transport of oxygen from the air to the electrode-electrolyte interface which is of interest to us; and, as shown diagrammatically in Fig. 11, this mass transfer can occur by one or by a combination of three mechanisms.

*Berl³⁴ has shown that the actual reactions involve the formation and destruction of peroxide ions.

The first possibility is that the oxygen is adsorbed at the electrode-electrolyte oxygen intersection, so that the rate of adsorption would depend on the length of the three-phase intersection.

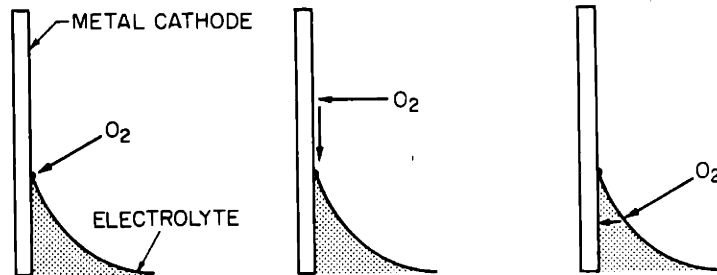


Fig. 11 Possible Oxygen Transport Mechanisms

A second possible mechanism is that the oxygen is first adsorbed on the electrode surface, and then migrates along the surface until it enters the electrolyte. In this case the mass-transfer rate would be dependent on the electrode area exposed to the oxygen, the rate of oxygen migration along the electrode surface, and the length of the three-phase intersection.

The final possibility is that the oxygen must first dissolve in the electrolyte, and then be carried to the electrode by diffusion and convection. In this case the mass-transfer rate of oxygen would be proportional to the area of the electrolyte exposed to the oxygen, and inversely proportional to some function of the thickness of the electrolyte film.

In order to determine the mechanism of oxygen transport to air-depolarized metal electrodes, experiments were performed using copper, nickel, and silver electrodes in a caustic cell, as shown in Fig. 2. The area of the steel-wool anode was much larger than the area of the cathode, so that the maximum current of the cell was dependent only on the rate of the reactions occurring at the air-depolarized cathode.

2. Results

a. Mechanism. When the metal cathode is completely submerged, the current is very small. If some electrolyte is

removed from the U-tube, the current goes up sharply when part of the electrode projects above the level of the electrolyte. Table 1 contains data obtained using a copper electrode, and the current is seen to rise from 0.04 to 0.32 milliamperes when the copper projects out only about 1/64 of an inch. Thus, it is seen that the contribution of the exposed portion to the current is much greater than the submerged portion, even though the area of the former is very small.

Table 1
Partially Submerged Copper Electrode

Exposed Height (inches)	i, ma	Time from Start (hours)
0	0.04	0
1/64	0.32	-
3/64	0.48	-
7/64*	0.74	-
10/64	0.92	-
12/64	0.85	-
16/64	0.9	-
20/64	0.89	1/2
30/64	0.7	48
31/64	0.75	-
33/64	0.75	74

*Top edge of copper began darkening.

Anode: steel wool
Copper Electrode: 1-1/4" x 1-1/4"
Electrolyte: 20 per cent KOH

The exposed height listed in the above table is taken as the difference in height between the top of the copper electrode and the main body of the electrolyte, as is shown in Fig. 4, and was measured with a depth gauge. A needlepoint on the end of the depth gauge enabled accurate location of the electrolyte surface. When the exposed height was only 1/64 of an inch, the cathode was completely wet by the electrolyte; and the only difference between the "exposed" and the submerged portion is the thickness of the electrolyte layer on the electrode. It is quite significant, however, that this difference results in such a marked change in the current.

As more electrolyte is removed from the U-tube so that the wetted-exposed area increases, the current also increases. As seen from the data in Table 1, however, the current reaches a maximum; and further removal of the electrolyte does not affect the current.

When the exposed height is large, the upper part of the cathode is not completely wetted; thus, the cathode can be divided into three parts: the submerged, the wetted-exposed, and the unwetted-exposed areas. The contribution of each of these areas to the total current allows one to determine the mechanism of oxygen transport.

The explanation of these results is aided by the fact that the unwetted-exposed portion of the copper electrode becomes dark, while the wetted-exposed and completely submerged areas retain their shiny copper color. Copper was chosen as a metal to study precisely because it affords this visual evidence which is not present with nickel or silver. It is found experimentally that, after the maximum current is obtained, further lowering of the electrolyte results only in an increase in the unwetted-exposed area, and does not change the wetted-exposed area (after steady state is reached).

The results of these data for a partially submerged copper cathode can be summarized as follows:

- (1) The current is essentially independent of the submerged area.
- (2) The current is essentially independent of the unwetted-exposed area.
- (3) The current is not directly proportional to the length of the electrode-electrolyte-oxygen intersection.
- (4) The current is a function of the wetted-exposed area.

These results lead to the conclusion that the mechanism of oxygen transport to the copper cathode is solution in the electrolyte followed by diffusion to the electrode.

It is also important to note from Table 1 that the partially submerged electrode is fairly stable with time. After 2-1/2

days the current was 0.75 ma, and the wetted-exposed height was found to be about 3/16 inches.

It is of interest to compare the current obtained from the partially submerged electrode with that calculated from oxygen solubility and diffusivity data. It was calculated previously, using oxygen solubility and diffusivity data in 20 per cent NaOH, that a diffusion thickness of 0.001 cm would limit mass transfer of oxygen to a rate corresponding to a current density of about 0.01 ma/cm².

In Table 1 it is seen that the current at 7/64 inches exposure height was 0.74 ma. At this point the top edge of the copper electrode began to darken, indicating the onset of incomplete wetting of the exposed portion. Neglecting edge effects, the wetted-exposed area is approximately $7/64 \times 1-1/4 \times (2.54)^2 \times 2 = 1.76 \text{ cm}^2$. Assuming that the current due to the submerged portion is still 0.04 ma, the current due to the wetted-exposed area is $0.74 - 0.04 = 0.7 \text{ ma}$, which corresponds to a current density of almost 0.4 ma/cm². This is much larger than the mass-transport rate calculated above; however, the calculation is based on an assumed diffusion thickness of 0.001 cm. If the diffusion thickness were less than this, the calculated rate would come more in line with the experimental rate. On the other hand, other investigators have found, for similar systems, that the actual mass-transfer rate of oxygen through a very thin electrolyte film is greater than that predicted by solubility and diffusivity relations.³⁵

Support of the conclusions arrived at in the above experiment was obtained in experiments in which the geometry, the angle of inclination, and the metal used were varied. For example, when a 1" x 2" copper electrode is placed in a partially submerged horizontal position, the current is almost exactly twice that when placed in a vertical position (see Fig. 12).

In the horizontal position the submerged area is identical, while the wetted-exposed area is twice as large as in the vertical position. Thus, the finding that the current doubles when the wetted-exposed area doubles is in agreement with the

conclusion that the current is mainly dependent on the wetted-exposed area. However, it must be noted that the length of the three-phase intersection also doubles in going from the vertical to the horizontal position.

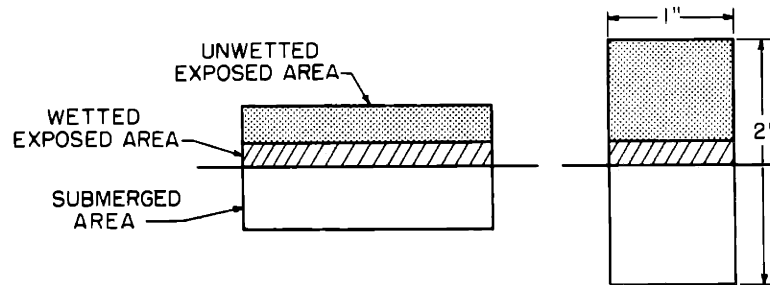


Fig. 12 Horizontal and Vertical Cathodes

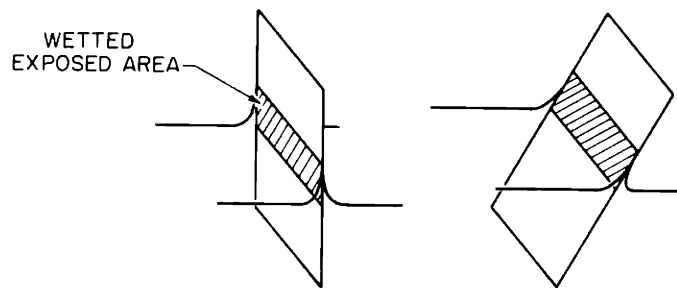


Fig. 13 Vertical and Inclined Cathodes

In order to change the wetted-exposed area without changing the three-phase perimeter, an inclined electrode was used as is shown in Fig. 13. Assuming that the electrolyte rises to the same vertical height in both positions, the wetted-exposed area will be greater when the electrode is inclined. At the same time the three-phase perimeter is the same for both positions.

The results obtained, using an inclined copper electrode, are presented in Table 2 and clearly show a rise in current with constant perimeter, but increasing wetted-exposed area. The readings were taken over a long period of time to ensure steady-state conditions.

Table 2

Inclined Partially Submerged Copper Electrode

Position	Wetted-Exposed Height (inches)	i, ma	Time from Start (hours)
Inclined	1/2	0.434	20
Vertical	5/16	0.280	22
Vertical	5/16	0.250	28
Inclined	1/2	0.415	34
Inclined	1/2	0.515	44
Inclined	1/2	0.412	49

Anode: steel wool
 Copper Electrode: 1-1/8" x 1/2"
 Electrolyte: 20 per cent KOH

These experiments clearly establish the conclusion that the mechanism of oxygen transport to a partially submerged, air-depolarized, copper cathode is solution in the electrolyte followed by diffusion to the electrode.

b. Rate Determining Step. The results of the previous section establish the mechanism of oxygen transport to partially submerged, air-depolarized electrodes, but do not establish whether the rate-determining step is mass-transfer rate or chemical-reaction rate. If mass-transfer rate is controlling, the current should depend only on the geometry of the electrolyte-electrode wetted-exposed region, and not on the chemical nature of the electrode. If, on the other hand, chemical-reaction rate is controlling, then the current should be different for different metal surfaces.

In order to determine whether mass-transport or chemical-reaction rates were limiting, an experiment was set up using cathodes of copper, nickel, and silver.

The electrodes of copper, nickel, and silver were all mounted in one leg of a U-tube; while their corresponding steel-wool anodes were in the other leg. The cathodes were carefully placed so that their tops were all at the same level. In this manner the exposed heights are the same for each electrode, and

the currents obtained are directly comparable. In addition, an extra steel-wool anode was present so that the effect of doubling the anode area could be observed. The steel-wool electrodes were placed so that they would always be completely submerged when electrolyte was removed. The data are shown in Table 3.

Table 3

Partially Submerged Copper, Nickel, and Silver Electrodes

Exposed Height (inches)	Current, ma			Number of Steel-Wool Anodes	Time
	Cu	Ni	Ag		
0	0.010	0.010	0.026	1	11:25 A.M.
	0.010	0.010	0.026	2	
Edge at Electrolyte Surface	0.067	0.060	0.065	1	11:30 A.M.
	0.067	0.060	0.065	2	
1/64 ~ 1/32	0.250	0.255	0.258	1	11:34 A.M.
	0.255	0.260	0.260	2	
~ 1/16	0.585	0.517	0.595	1	11:40 A.M.
	0.590	0.527	0.600	2	
~ 3/32	0.865	0.731	0.855	1	11:45 A.M.
	0.875	0.743	0.86	2	
~ 1/8	0.97	0.77	1.01	1	11:51 A.M.
	0.98	0.79	1.02	2	
~ 3/16 *	1.00	0.75	1.03	1	11:56 A.M.
	1.02	0.77	1.04	2	
~ 1/4	1.00	0.79	1.10	1	12:00 noon
	1.02	0.81	1.12	2	
~ 1/4 **	0.75	0.55	0.8	1	1:10 P.M.

*Top edge of copper began darkening.

**About 3/32 ~ 1/8" of top of copper cathode is dark.

Cathode size: 1" x 1/2"
Electrolyte: 20 per cent KOH

When the cathodes were completely submerged, the currents were small, with that of silver being the largest. The

submerged current is made up of two parts: that due to diffusion of dissolved oxygen to the electrode, and that due to other electrochemical reactions. The current due to the latter will be called, for purposes of differentiation, the "galvanic" current. Galvanic currents are discussed in detail in Appendix B. The difference in current between the submerged silver and the other electrodes could have been due to differences in surface roughness, differences in galvanic current, or the possibility that steady-state had not yet been achieved at the silver electrode. The latter is a possibility since, when the electrodes are first connected, there is first a rapid drop in current followed by a slow tapering decline. There is an effect when the anode area is doubled; however, even for nickel which shows the largest change, the rise is small and can be neglected.

The important fact observable from the data is that, when electrolyte was removed so that the top edges of the cathodes were right at the surface of the electrolyte, the current was, within experimental error, the same for the three metals. As more electrolyte was removed, the currents rose about the same amount so that they remained about the same for the three metals. Differences in current did not begin to be significant until the exposed height was about $3/32$ " , with the current for nickel being less than that for copper or silver. This difference increased as the exposed height increased.

The use of different metals introduces, besides a change in chemical nature, a change in wetting characteristics; and both of these must be taken into account in the interpretation of the results.

The differences in the wettability of the three metals can be characterized by the maximum height to which electrolyte will rise at the surface of a vertical electrode. The higher the electrolyte rises, the smaller the contact angle and the thinner the average film thickness become. Thus, differences in wettability, in general, result in a different electrolyte-electrode geometry. However, when the electrodes are raised

to a height above the electrolyte surface, which is less than the smallest maximum wetted height, the electrolyte will rise to the top of each electrode; and the geometry of the electrolyte-electrode area will be the same for each of the metals.

The results show that, for exposed heights of less than $3/32$ ", the currents are the same for all the metals; and the conclusion is that it is the electrolyte-electrode geometry, and not the chemical nature of the metal, which determines the rate of reaction (i.e., the mass-transport rate is limiting).

When the exposed height increases beyond $3/32$ ", there are differences in the currents at the electrodes. This can be explained by differences in the wetted-exposed height at the different electrodes. The lower current obtained at the nickel electrode indicates that the maximum wetted-exposed height of the nickel is less than that of copper or silver. No applicable wetting data were found in the literature to permit comparison with this result.

The final notable characteristic of the data presented in Table 3 is the drop in current at all the electrodes when allowed to stand for one hour. This is easily explained by noting the growth of the dark area on the upper portion of the copper electrode. When electrolyte is removed from the U-tube, the electrolyte film on the electrode is stretched; and wetted-exposed height is larger than at equilibrium. With time the equilibrium height is restored, the wetted-exposed area is decreased; and the current goes down.

The above results are in agreement with the conclusion that the mechanism of oxygen adsorption at an air-depolarized metal cathode is solution of oxygen in the electrolyte followed by diffusion to the electrode, and establish that mass transport is the rate-determining step.

The latter finding was confirmed by observing the effect of a change in temperature on the current obtainable from a cell. If the current is chemical-reaction rate controlled, it should increase significantly with an increase in temperature. On the other hand, if the current is limited by the solubility

and diffusivity of oxygen in the thin electrolyte film, an increase in temperature should result in little increase, and possibly a decrease, in the current.

Using a cell with an air-depolarized, partially submerged copper electrode, the current was found to decrease on increasing the temperature; and it supports the finding that the mass transport of oxygen through the electrolyte film is the rate-determining step in the depolarization of a partially submerged metal electrode.

It must be pointed out that, in this experiment, the excess dissolved oxygen in the bulk electrolyte must be removed; otherwise, on heating it would come out of solution and accumulate at the submerged portion of the electrode. This would interfere with the interpretation of the results; and, in order to avoid this, the cell was first heated to remove the dissolved oxygen, cooled, and then reheated again to determine the temperature effect.

c. Drowning of Electrodes. It is a well-known fact that, if porous fuel cell electrodes are completely permeated by electrolyte, they do not function properly; i.e., the current densities obtainable drop off sharply. This is called "drowning" of the electrode. Knowledge of the mechanism of oxygen-transport to air-depolarized metal cathodes is important because it gives an insight into the causes of the drowning of fuel-cell electrodes.

In fuel cell electrodes drowning is prevented in a number of different ways. In the Schmid electrode, the permeation of electrolyte into the electrode is prevented by maintaining a positive pressure on the gas side of the electrode. Bacon has refined this method by using electrodes whose electrolyte-electrode surfaces have a smaller pore size than the bulk of the electrode.

The other principal method of preventing drowning is to add a water-proofing agent, as in the National Carbon fuel cell. This is done by adding a dilute solution of paraffin or rubber in a volatile solvent, and then evaporating the solvent.

In this study only flat-plate electrodes were used, and it is difficult to compare the results obtained here with porous electrodes; however, a porous electrode may be thought of as an almost infinite number of cylindrical pores, and a thin longitudinal section of the wall of such a pore may be considered to be a flat plate. Though the specific action of the water-proofing agent in porous electrodes is somewhat uncertain, its effect is to keep the electrolyte from completely filling up the pore. Thus, the pore, as the electrodes studied in this thesis, is partially submerged in the electrolyte. For these reasons it is felt that a study of partially submerged flat electrodes is a very important step in the understanding of the porous electrodes which are found in fuel cells.

The drowning of the oxygen electrode in a fuel cell can be due to one of two things: deactivation of the electrode by the adsorbed electrolyte, or a decrease in the rate of mass transfer of oxygen to the electrode. Since the current rose sharply when, in the experiments and systems described herein, the submerged electrode was partially exposed to air, and since the current here depended mainly on the area of the electrode which was covered by a thin film of electrolyte, it follows that the drowning of oxygen electrodes is due, not to a decrease in catalytic activity, or poisoning of the electrode, but rather to a decrease in the oxygen mass-transfer rate.

The current obtainable from a drowned fuel cell electrode is very small. The analogous situation is the completely submerged electrode. In both cases the current is small because the oxygen transport rate is small.

When the fuel cell electrode is treated or constructed to prevent drowning, the current rises sharply. When the completely submerged electrode is lifted partially out of the electrolyte, the current also rises sharply. We have found, in the case of the partially submerged electrode, that the rate of oxygen transport through the electrolyte film was controlling. If the analogy holds true, then we would conclude that the

current at a treated fuel-cell electrode is also limited by the mass-transfer rate of oxygen through the electrolyte.

These comparisons indicate that mass transfer of oxygen through the electrolyte may limit the output of a fuel-cell oxygen electrode; and that the sharp rise in current in going from the drowned to the undrowned electrode is not due to a difference in mechanism, but rather due to a sharp increase in the oxygen transport rate.

Of course, it must be kept in mind that these conclusions have been obtained with smooth air-depolarized metal electrodes and may not be directly applicable to porous carbon or other fuel cell electrodes; but, since the latter are active due to the presence of metals and metal oxides, it seems reasonable that the conclusions regarding the mechanism of oxygen transport and drowning might also apply to them. In order to test these theories, an oxygen electrode which is not limited by mass transport of oxygen through the electrolyte was built. The results obtained with this electrode (the wiped, rotating, partially submerged oxygen electrode) are discussed in the following sections.

B. RATE OF OXIDATION OF ELECTRODE SURFACES

1. Characteristics of Wiped, Rotating, Partially Submerged Oxygen Electrodes

a. Discussion. The discussion, presented in the introduction, of mass-transfer processes as applied to a generalized caustic fuel cell electrode suggests that mass-transport rates of oxygen through the electrolyte may control the current obtainable from an oxygen electrode. This theory was experimentally confirmed for flat, partially submerged metal electrodes. The question then arises, "How large a current density can be obtained from an oxygen electrode if mass transport of oxygen through the electrolyte were not controlling?" The wiped, rotating, partially submerged oxygen electrode was built to try to arrive at some sort of an answer to this question.

The rotating electrode is described in detail in Section III, but it essentially consists of a metal ring embedded in the rim of a lucite disc. The surface of the ring is smooth and flush with the lucite rim. The metal surface is wiped clean of electrolyte film by means of a gum-rubber wiper.

The principle of operation of the rotating electrode is simple. The metal surface, after it leaves the electrolyte, is wiped, thus allowing oxygen to have free access to the electrode surface. The metal adsorbs, or is oxidized by the oxygen; and the metal "oxide" thus formed re-enters the electrolyte where it is electrochemically reduced, regenerating the metal.

Since the metal surface is not consumed, but acts only as a media for adsorbing and ionizing oxygen, it is in one sense a catalyst. On the other hand, if the adsorbed oxygen forms a true oxide, there is a free energy loss due to the oxidation step; and in this sense the rotating electrode is not exactly a catalyst for the ionization of oxygen. The effect, however, of the rotating electrode is to remove oxygen from the gas phase and pump oxygen-containing ions into the electrolyte.

In the experiments with the stationary electrode, the oxygen electrode was "isolated" from the anode by the artifact of making the area of the former relatively very small. This principle was also employed with the rotating electrode; however, the rotating electrode also permits the separation of the oxidation step, which occurs in the gas phase, from the electrochemical reduction step, which occurs in the liquid phase. By proper choice of submerged and exposed areas of the rotating electrode, one can make either the oxidation or the electrochemical reduction controlling so that the rate of either step limits the output of the cell. In order to study the oxidation rate, which is what we are primarily interested in, it is necessary to make the oxidation the limiting step.

It is important to note, however, that the very device which permits us to "isolate" and study the oxidation rate (i.e., the separation of the oxidation and electrochemical reduction steps by the rotating electrode) also causes problems

of interpretation of results. Since in an ordinary oxygen electrode the oxidation and reduction steps presumably occur simultaneously, the chemical reactions may be different from those of the rotating electrode. Though it is difficult to evaluate the effect of this difference, it must be kept in mind.

b. Results. With different metal surfaces the properties of the rotating electrode will vary somewhat. These differences are discussed in the following sections; but first, it is important to describe the properties and capabilities of the rotating electrode in general. This can best be done by limiting the discussion to one metal only. This section will deal only with the properties of the rotating electrode when the surface is copper.

The most significant characteristic of the rotating electrode is the effect of wiping on the current obtainable from the electrode. In general, the current of the unwiped electrode is low and relatively insensitive to R.P.M.; while, that of the wiped electrode is markedly higher and varies somewhat more with R.P.M. Results obtained with copper are shown in Fig. 14.

The current of the unwiped electrode was found to be due to electrochemical processes other than those associated with the ionization of oxygen. These diverse electrochemical processes have been termed "galvanic" and are discussed in detail in the Appendix. It was found experimentally that the unwiped current was essentially independent of the oxygen partial pressure, as would be expected if the unwiped current were not due to reaction with oxygen.

The other important characteristics of the oxygen electrode are those which confirm that the oxidation step is the limiting one in the cell.

When the zinc-anode area was doubled, there was no significant change in the maximum current obtainable from the cell. This shows that the limiting step is at the oxygen electrode. It now remains to be shown that the limiting step at the oxygen electrode is the oxidation, and not the reduction step.

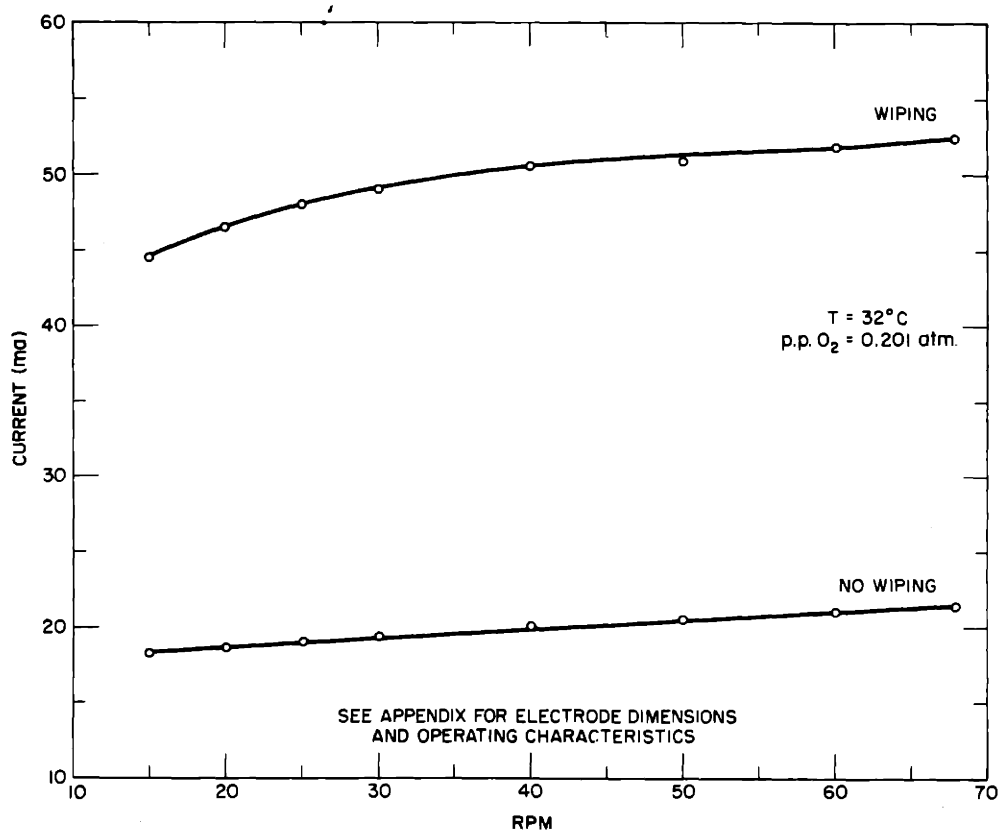


Fig. 14 Effect of Wiping on Current of Rotating Copper Electrode

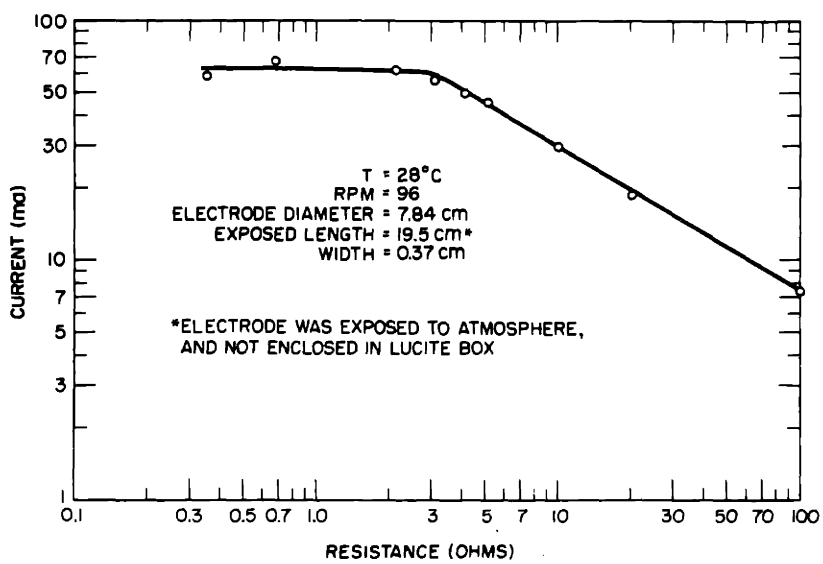


Fig. 15 Effect of Resistance on Current of Rotating Copper Electrode

The oxidation step is not electrochemical and, therefore, should be independent of the external resistance of the cell. On the other hand, the rate of reduction is directly dependent on the external resistance and should increase as the external resistance is lowered. Figure 15 is a plot of current versus resistance for a rotating copper surface.

It is seen that, for resistances above 3 ohms, the current decreases as the resistance increases. In this range, therefore, the rate of reduction is the limiting step at the oxygen electrode. Below 3 ohms, however, it is seen that the current is independent of the resistance. In this range, it is the oxidation step which is limiting; and the cell is a constant-current variable-voltage device in which the current is determined by the rate at which oxygen reacts with the copper surface.

Another method of determining if the oxidation step is limiting is by varying the ratio of the exposed to submerged areas of the rotating electrode. This was done, as described in Chapter III, by adding electrolyte to a portion of the wiped electrode surface, thus "masking" this portion from further reaction with oxygen. For the copper electrode, the maximum current was found to increase when the electrolyte mask was removed. Since the current increased when the exposed area increased, this supports the conclusion that, for external resistances of less than 3 ohms, the oxidation step is the limiting step in the cell.

2. Oxidation of Metals

a. Introduction. The purpose of the work with the rotating electrode was to try to measure the rate of oxidation of metal surfaces, and to compare these rates with the rate deemed satisfactory for the oxygen electrode of a fuel cell. In order to be in a position to interpret the results, a brief review of the field of oxidation or tarnishing of metals will be presented.

Broadly, the oxidation of a metal can be separated into two parts: the formation of the initial mono-molecular oxide layer, and the growth of the oxide layer. The first of these is known to be extremely rapid, and it was found by Schlier and Farnsworth³⁶ that, on a nickel crystal at room temperature, the oxygen monolayer was complete after a pressure times time exposure of 2×10^{-6} mm Hg-min. Thus, at an oxygen partial pressure of 0.21 atm, the oxygen monolayer should take about a microsecond to form.

In order to investigate the growth of the oxide layer, we assume the model given in Fig. 16. The growth of the oxide can

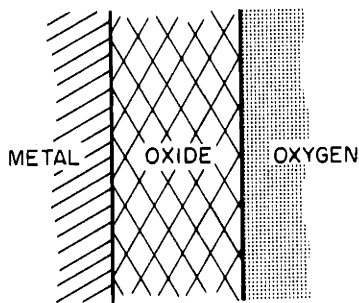


Fig. 16 Metal Oxidation Model

be divided into three separate parts: the reactions at the metal-oxide interface, the transport of material through the oxide layer, and the reactions at the oxide-oxygen interface. If any one of these steps is slow compared to the others, it will be rate determining. As the growth

proceeds, or as the conditions change, the rate-determining step may change. For example, when the oxide layer is thick, the rate-determining step may be mass transfer through the oxide layer. When the oxide layer is very thin, the material transport rate is high; and the reactions at the interfaces become limiting. At low-oxygen partial pressures the reaction rate at the oxide-oxygen interface is limiting, while at high-oxygen partial pressure the reaction rate at the metal-oxide interface is rate determining.

The above model can be treated analytically in a straightforward manner if we assume that the two interfaces and the oxide layer represent three resistances in series. The resistances at the interfaces are assumed to be independent of the oxide thickness, while the resistance of the oxide film is taken

to be directly proportional to its thickness. If r_m is the resistance at the metal-oxide interface, r_o the resistance of the oxygen-oxide interface, and $r_f y$ the resistance of the oxide film, the total resistance of the system is

$$R_T = (r_m + r_o + r_f y) \quad (6)$$

and the rate of growth of the film is

$$\frac{dy}{dt} = \frac{c_1}{R_T} = \frac{c_1}{(r_m + r_o + r_f y)} \quad (7)$$

which upon integration becomes

$$(r_m + r_o + r_f y/2)y = c_1 t + c_2 \quad (8)$$

When the resistance of the film is small compared to the resistances at the interfaces, we get

$$(r_m + r_o)y = c_1 t + c_2 \quad (9)$$

which, when noting that r_m and r_o are constants, can be written more simply as

$$y = k_1 t + k_2 \quad (10)$$

This is the familiar linear-rate law which was proposed by Pilling and Bedworth³⁷ for metals whose oxide films were non-protective. This equation was predicted for metals whose oxides were more dense than the parent metal. The oxide film of such metals should crack, peel, and be non-protective so that the oxygen would have "free access" to the metal surface. This equation holds surprisingly well for most of the light metals of groups I_A and II_A of the periodic table, where the oxides are normally denser than the metals.

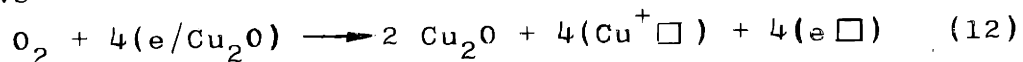
When the oxide layer is protective and material transport through the oxide film is controlling, the interface resistances can be neglected and Eq. 8 becomes

$$y^2 = k_1 t + k_2 \quad (11)$$

the well-known parabolic equation. This equation has been derived theoretically by a number of workers,³⁸⁻⁴¹ but it is usually associated with the name of Carl Wagner. The equation is often found to hold at high temperatures and for thick oxide

films, where one might expect the resistances at the interfaces to be negligible in comparison with that of the oxide film.

The importance of the Wagner theory of oxidation is that it permits the calculation of the rate constant in the parabolic equation from fundamental properties of the metal oxide. According to Wagner the oxidation of copper to cuprous oxide proceeds as follows



Where (e/Cu_2O) is an electron from a cuprous oxide molecule, $(Cu^+\square)$ is a deficiency or vacancy of a cuprous ion and $(e\square)$ is an electron deficiency or a positive hole.

The equation may be interpreted in the following way. An oxygen molecule adsorbed on the oxide surface removes four electrons, (e/Cu_2O) , from the outermost layer of cuprous oxide. This results in a deficiency of four electrons, $(e\square)$ in the cuprous-oxide layer so that the copper is in the cupric state. The adsorbed oxygen is in the requisite lattice positions for cuprous oxide; however, there are no cuprous ions in this layer. Hence, there are four cuprous ion vacancies, $(Cu^+\square)$. The cupric ions formed in the above reaction then remove electrons from the underlying cuprous oxide layer. This continues from layer to layer down to the metal-oxide interface where the electrons are finally removed from the metallic copper. The cuprous ions formed from the metal then migrate from the metal-oxide interface to the oxide-oxygen interface, where they fill in the vacant lattice positions, "destroy" the cation vacancies, and complete the growth of the oxide layer.

Wagner postulates that the growth of the oxide film depends on the ionic conductivity of the oxide film, and is limited by the mobility of the cation vacancies and electron holes. The oxidation rate of copper to cuprous oxide at $1000^\circ C$ was found to agree, within the experimental error, to the calculated one and is a good confirmation of Wagner's theory.⁴²

A further justification of Wagner's theory is the effect of the oxygen partial pressure on the rate of oxidation.

Applying the law of mass action to Eq. 7, we obtain

$$\frac{[\text{Cu}^+\square]^4 [\text{e}\square]^4}{[\text{O}_2]} = k \quad (13)$$

but, since $[\text{Cu}^+\square] = [\text{e}\square]$, we get

$$[\text{e}\square]^8 = k[\text{O}_2] \quad (14)$$

The concentration of electron holes is proportional to the eighth root of the oxygen partial pressure. Thus, the electrical conductivity and, if Wagner's theory is correct, the rate of oxidation of copper should also be proportional to the eighth root of the oxygen partial pressure. Experimentally, Wagner found that at 1000°C the electrical conductivity⁴³ of the oxide and the rate of oxidation⁴⁴ were both approximately proportional to the seventh root of the oxygen partial pressure, which is satisfactory agreement.

There are many other "laws" which describe the oxidation of metals, and they can be found in the many reviews in the literature.^{42,45-51} However, at room temperatures the oxidation of metals often follows the logarithmic law; therefore, the logarithmic law will also be discussed in detail.

At room temperatures the movement of electrons across an oxide film may be relatively slow and may be the rate-determining step. At these temperatures oxide films tend to be very thin and electron transfer can occur by the so-called "tunnel effect", a phenomenon dependent on the fact that electrons can behave as waves. Holm⁵² describes the tunnel effect as, "... a wave-mechanical analogy to the transmission of light through a thin metal foil, if the thickness of the foil is comparable to the wave length." Assuming that electron tunnel transfer is similar to the transmission of light through thin films, Evans⁴⁹ obtains the logarithmic law in the following way.

The probability of an electron penetrating a film of thickness y is

$$p = e^{-c_1 y} \quad (15)$$

Thus, if electron penetration controls the rate of growth, we

get

$$\frac{dy}{dt} = c_2 e^{-c_1 y} \quad (16)$$

or on integration

$$e^{c_1 y} = c_3 t + c_4 \quad (17)$$

which, after taking the logarithm of both sides leads to the familiar logarithmic equation

$$y = k_1 \ln(k_2 t + k_3) \quad (18)$$

A second derivation of the logarithmic equation is also due to Evans.⁴⁹ In a growing film, material transport can occur by diffusion through the oxide lattice or along grain boundaries, dislocations, and pores. At low temperatures diffusion through the lattice is very slow and probably does not contribute much to the growth of the oxide. Evans' derivation assumes that the rate of oxidation is limited by the rate of mass transport of oxygen, gaseous or adsorbed, along discontinuities in the oxide film; and that the number of these "leaky" points decreases with growth since the oxide is less dense than the metal.

Evans assumes that, for a differential increase in the weight of the oxide film, dw , the disappearance of the discontinuities, dD , is proportional to the number of discontinuities present so that

$$dD = -c_1 D dw \quad (19)$$

which on integration becomes

$$D = c_2 e^{-c_1 w} \quad (20)$$

Since the rate of growth depends on the number of discontinuities, we get

$$\frac{dw}{dt} = c_3 e^{-c_1 w} \quad (21)$$

which, as before, leads to the logarithmic growth law

$$w = k_1 \ln(k_2 t + k_3) \quad (18a)$$

Uhlig⁵³ assumed that the rate-determining step was the rate of electron transfer from metal to oxide at the metal-

oxide interface, and was also able to derive a logarithmic equation.

A number of other equations which have been found experimentally have also been justified theoretically; however, one must always remain aware of the simplifications and assumptions made in the derivation. For example, the effect of varying surface temperature has not yet been taken into account; and the temperature of the surface certainly changes as growth occurs. Also, the oxide layer is usually not of uniform thickness; has cracks, pores, and cavities in it; and, in addition, the surface area may change as oxidation proceeds.

Before the oxidation results can be discussed, the effect of impurities at the metal surfaces must be mentioned. Though the wiper removes the electrolyte film which lowers the mass transport of oxygen to the metal surface, the wiper cannot remove the last traces of KOH. Thus, when a piece of moist red-litmus paper is placed on the wiped, rotating metal surface, the litmus immediately turns blue. The oxidation measurements, therefore, are of metal surfaces which are "contaminated" by KOH. Though the presence of KOH should certainly change the magnitude of the rate, it should not affect the oxidation law which is followed.

b. Results. In this section are presented the oxidation data obtained for the three metal surfaces (copper, silver plated on copper, and nickel plated on copper), which were used in the rotating electrodes. These data are discussed in terms of oxidation theory and show that the rotating electrode can, when properly designed, be used for studying the rates and mechanisms of metal oxidation. To permit more clarity in the discussion, details of the electrode dimensions and operating characteristics are reserved for the Appendix.

(i.) Copper. The data obtained from the rotating, wiped copper electrode are presented in Fig. 17, which is a plot of current versus R.P.M. for various oxygen partial pressures, at a temperature of about 32°C. The external resistance was 0.352 ohms.

In order to be certain that the current was, in fact, limited by the rate of oxidation of the copper, an extra zinc anode and an electrolyte mask were used. When one of the two

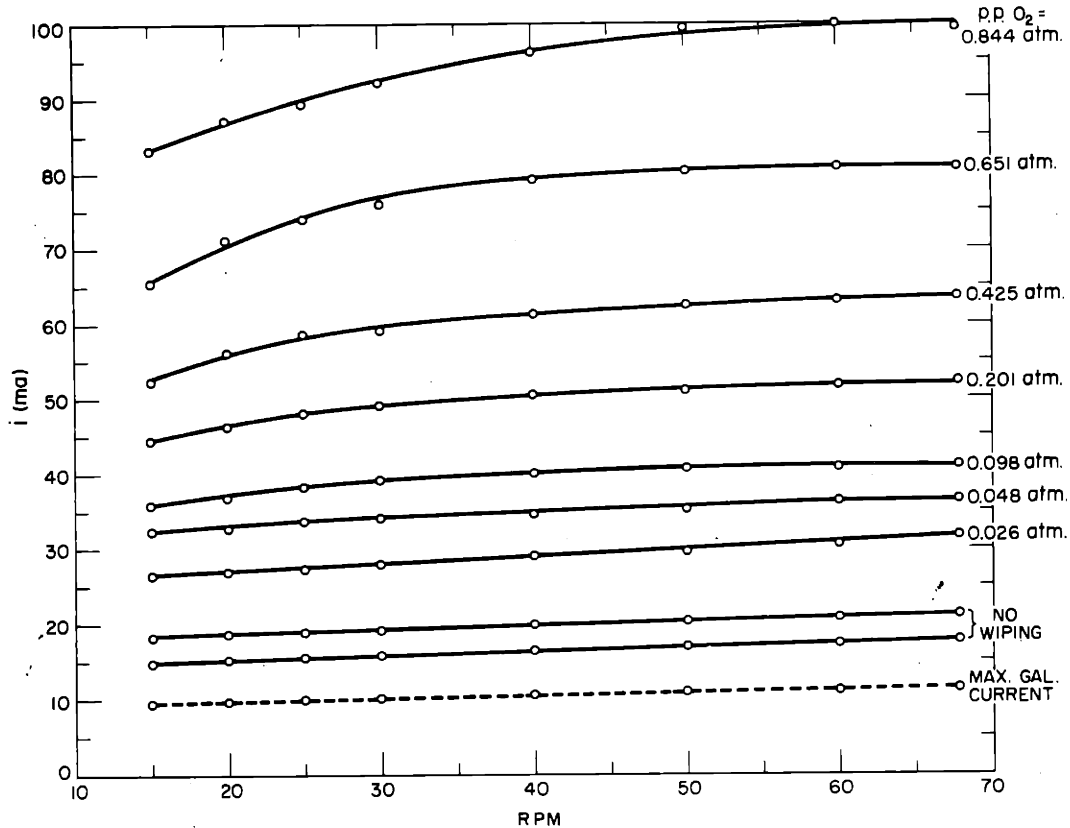


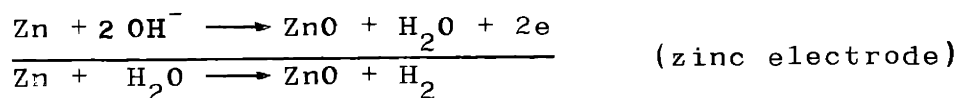
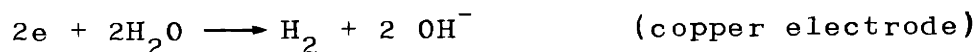
Fig. 17 Data for Rotating Copper Electrode

zinc electrodes, which were of about the same surface area, was switched out of the circuit, the current essentially remained constant. This indicated that the current of the cell was limited by the rate of reactions occurring at the copper electrode. It was found that, when the electrolyte mask was removed, the current went up. Removing the mask serves to increase the area of electrode available for oxidation, while decreasing or keeping constant (if one assumes negligible electrochemical reduction in the masked area) the area available for reduction of the oxide. The fact that the current goes up when the electrolyte mask is removed indicates that, when the mask is used, the rate-determining step is the oxidation

of the exposed copper area.

All the data were taken with both zinc anodes in the circuit, and with the electrolyte mask present, thus, ensuring that the oxidation of the copper was the rate-determining step in the operation of the cell.

When the electrode is not wiped and has, as a result, a continuous film of electrolyte, the amount of oxygen reaching the copper is exceedingly small. The two lower solid curves on Fig. 17 were obtained with an unwiped electrode, and the current is much higher than one would expect if oxygen alone were involved. This current was shown to be primarily due to evolution of hydrogen at the copper electrode. This presumably occurs in the following manner:



As the ZnO forms, it dissolves in the electrolyte, leaving fresh zinc surface available for reaction.

The current due to reactions other than the ionization of oxygen at the copper electrode has been termed the "galvanic" current. The currents plotted in Fig. 17 are really the sums of the currents due to oxygen depolarization and galvanic currents. At high-oxygen partial pressures the galvanic current is only a small fraction of the total current, but at low partial pressures it may be a considerable portion. It is impossible to obtain exact values for the galvanic currents in the data, but limits may be established.

It was found that the current of a completely submerged rotating electrode was essentially the same as a partially submerged unwiped rotating electrode. This means that the galvanic current is determined by the area of copper which is wet by electrolyte, irrespective of whether the electrolyte is a thin film. Assuming that, when the copper surface is wiped free of electrolyte there is no galvanic action in the wiped

portion, the maximum galvanic current is equal to the galvanic current with no wiping times the fraction of the copper area which is covered by electrolyte.

The fraction of the area covered by electrolyte in the runs plotted in Fig. 17 was about 0.58, so that the maximum galvanic current at a wiped electrode is significantly less than the unwiped current. The maximum galvanic current based on the average of the two wiped currents is plotted as a dashed line on Fig. 17.

The galvanic current is proportional to the area of copper covered by electrolyte. However, in the wiped and rotating electrode, a portion of the submerged copper electrode is covered by oxide; and copper oxide would not contribute to the galvanic current since it should be electrochemically reduced before hydrogen evolution occurred. Thus, the actual galvanic current is less than the plotted current in Fig. 17.

As the partial pressure of oxygen increases, the thickness of the oxide entering the electrolyte increases; therefore, the time required to reduce the copper oxide increases. As the "residence" time of the copper oxide increases, the fraction of the submerged portion of the electrode that is copper decreases; and, therefore, the galvanic current decreases.

We can thus conclude that, as the oxygen partial pressure approaches zero, the galvanic current approaches the maximum shown in Fig. 17; and that, as the oxygen partial pressure increases, the galvanic current approaches zero.

From the current, the width of the copper and the R.P.M., the amount of oxygen adsorbed per centimeter squared of copper can be calculated. This quantity will be called n . At a given partial pressure, as the R.P.M. increases, the time of exposure of the copper to the oxygen decreases; and, hence, n decreases. A plot of n versus the time of exposure of the copper is, in effect, a plot of the amount of oxygen adsorbed on a centimeter squared of copper as a function of time.

Figure 18, n versus t , is the plot obtained when the galvanic current is assumed to be zero; and Figure 19, n' versus t ,

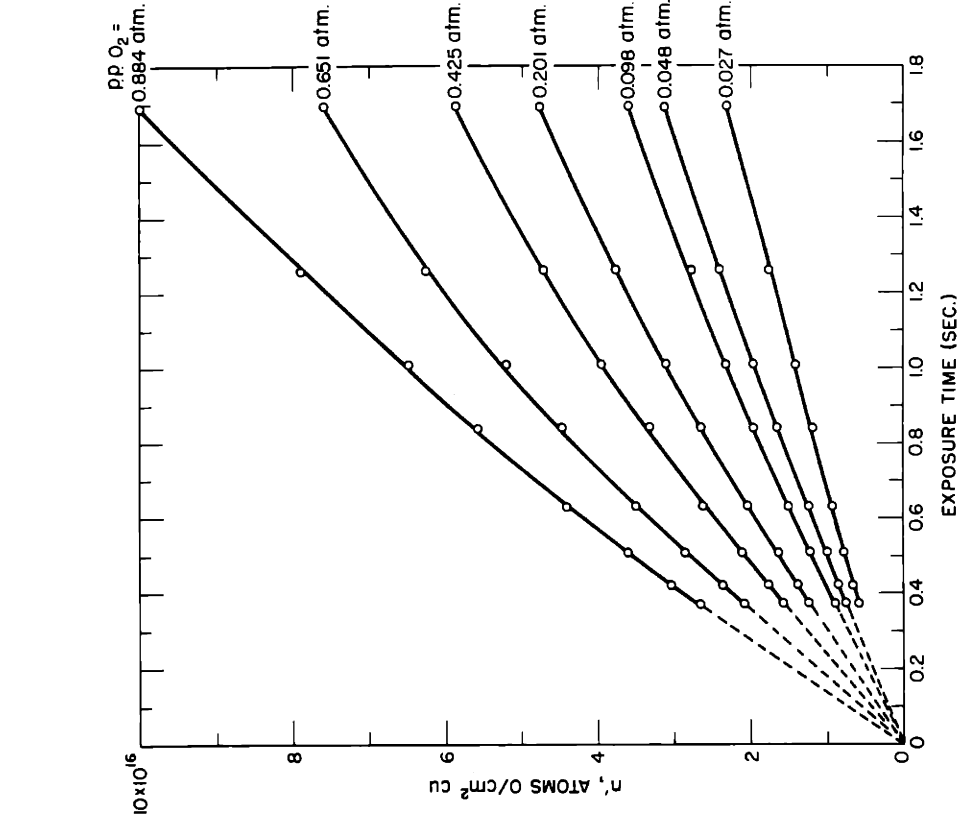


Fig. 19 Copper Oxide Thickness versus Exposure Time

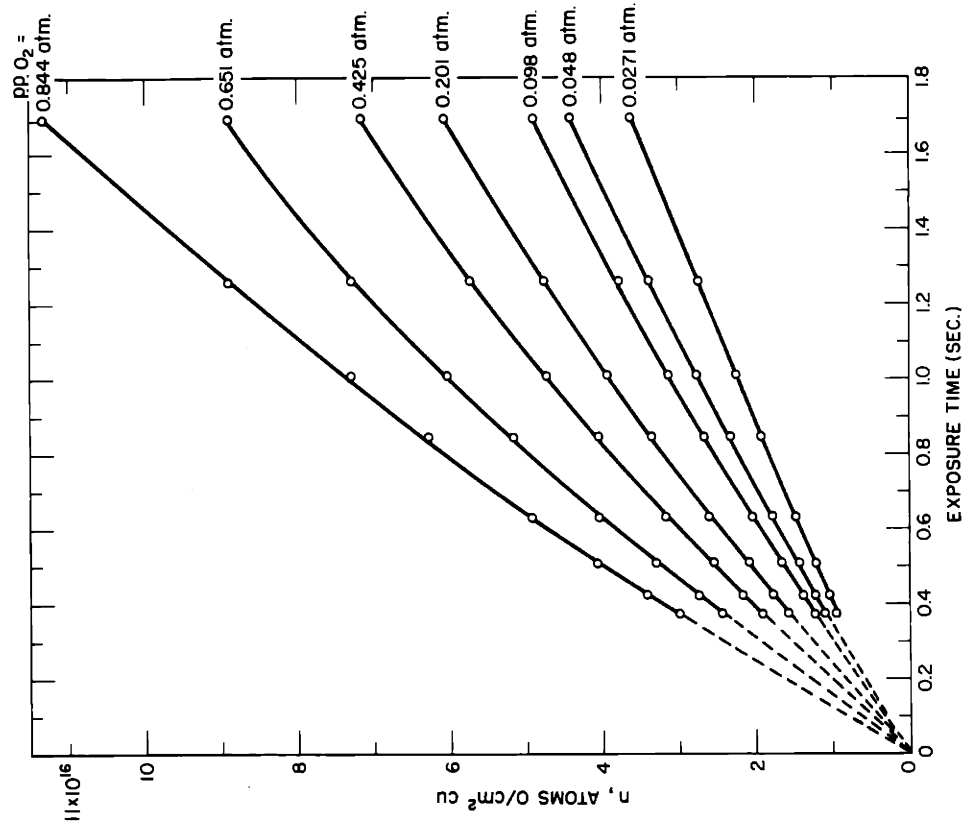


Fig. 18 Copper Oxide Thickness versus Exposure Time

is the plot obtained when the maximum galvanic current is subtracted from the observed current. The use of the primes in this sense will be continued from here on.

The plots of n and n' versus t are quite similar in shape, and the difference is only one of magnitude. The first point to note is that they extrapolate to zero when the exposure time goes to zero. This is what one would expect if the currents were really dependent on the oxidation of the exposed copper. The second important fact is that the plots are not straight lines.

If the mass-transfer rate of oxygen to the exposed surface were limiting, then the rate of reaction with oxygen should be constant; and n versus t would be a straight line. This indicates that the wiping is effective in removing the electrolyte film; and that the data is, in fact, a measure of the oxidation of copper. Of course, it is possible that the wiping characteristics change with R.P.M., in which case the rate of reaction would not be constant; however, in view of the characteristics of the wiping system, it is felt that this is not probable. Also, as will be pointed out later, the effect of the partial pressure of oxygen on the current supports the contention that the wiper is effective.

The question then becomes, if the current is a measure of the oxidation of copper, "How do the data compare with what one might expect from oxidation theory?"

If the oxidation followed the linear law, n versus t should again be a straight line. Since this is not the case, we can conclude that the oxidation of copper under the conditions of the experiment does not follow the linear law.

A second possibility is that the oxidation proceed according to the parabolic law

$$y^2 = k_1 t + k_2 \quad (11)$$

In this case a plot of n^2 versus t would be a straight line. Figures 20 and 21 are such plots, and the lines are not straight. Thus, the conclusion is that in this case the oxidation of copper does not follow the parabolic law.

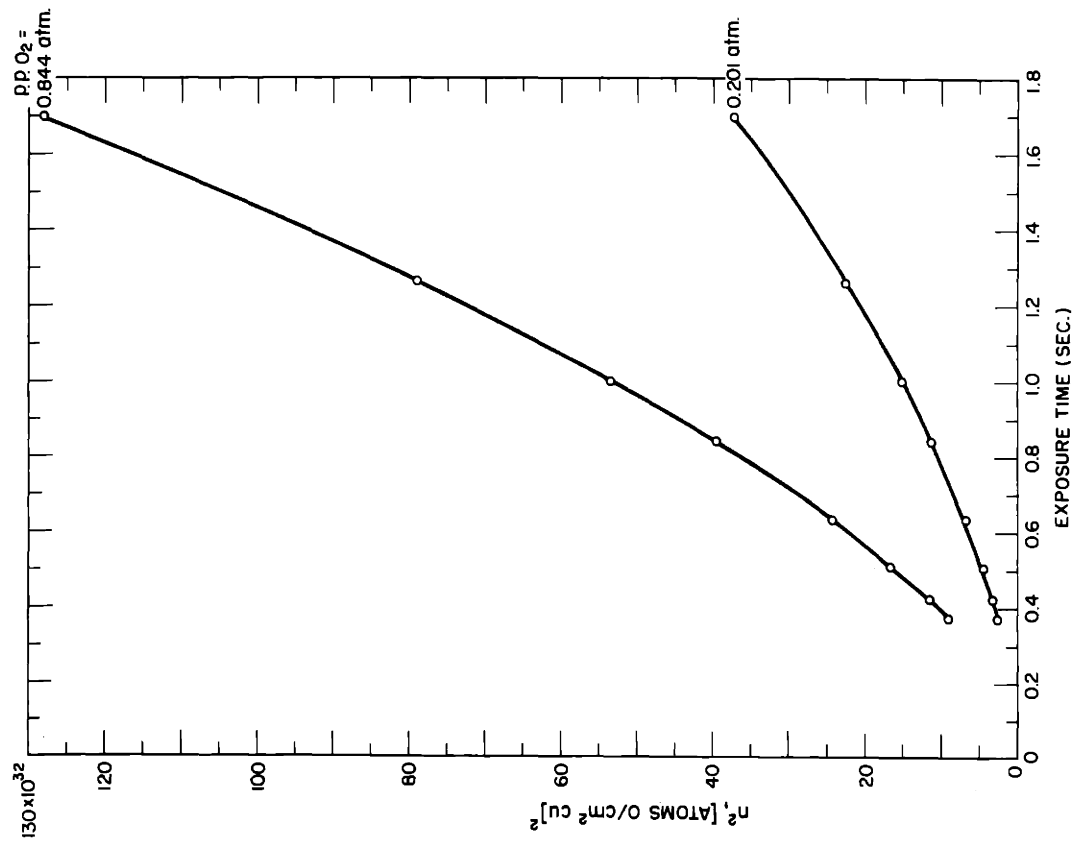


Fig. 20 Test of Parabolic Equation, Copper

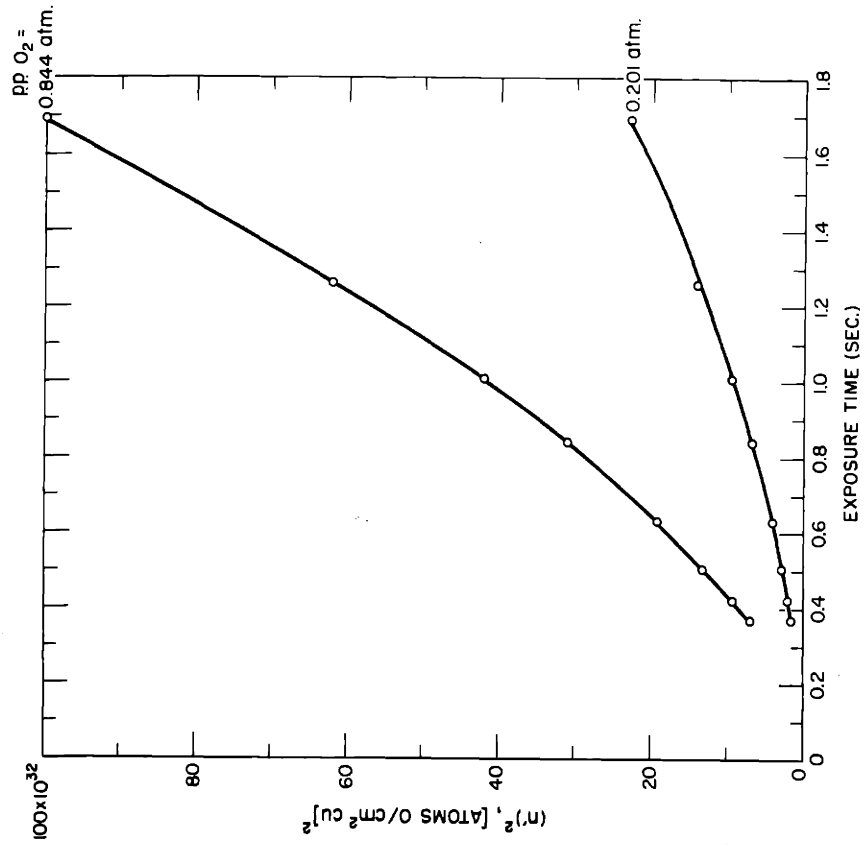


Fig. 21 Test of Parabolic Equation, Copper

It is not too surprising that the data do not correspond to a linear or parabolic law, since the former equation usually applies to metals whose oxides are more dense than the metal and the latter mainly to the growth of thick films. At low temperatures (in oxidation of metals, room temperature is considered low) one often finds that the oxidation follows the logarithmic law

$$y = k_1 \log (k_2 t + k_3) \quad (18b)$$

Since from Fig. 4 we see that, as $t \rightarrow 0$, $n \rightarrow 0$ (note that n and y are equivalent), k_3 must be 1; and the logarithmic equation becomes

$$n = k_1 \log (k_2 t + 1) \quad (18c)$$

From the values of n at two different times, the values of k_1 and k_2 can be calculated by a trial-and-error process for each of the oxygen partial pressures. Using these constants, it was found that the data did follow the logarithmic equation.

Figure 22 is a plot of n versus t , in which the correlated and the experimental data are compared.

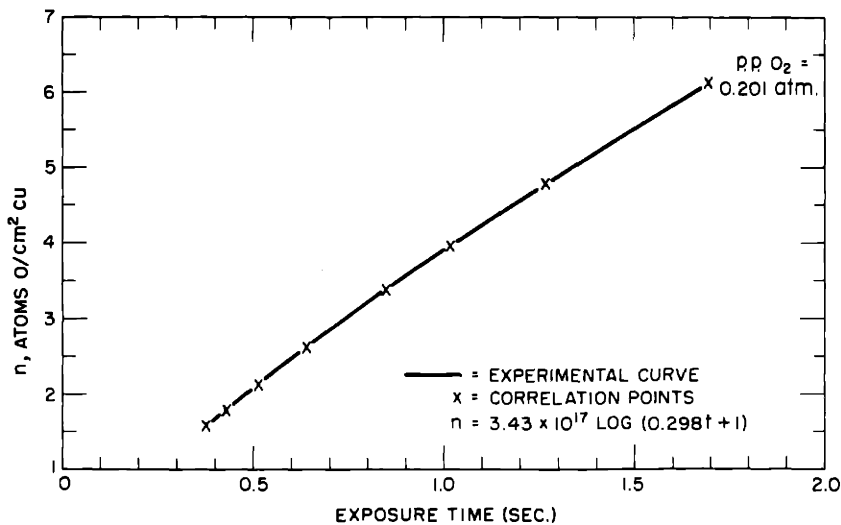


Fig. 22 Test of Logarithmic Equation, Copper

Table 4 is a compilation of values of k_1 and k_2 obtained, using the values of n at $t = 0.5$ and 1.3 secs for each partial pressure. The first thing to note in Table 4 is that the values

Table 4

Calculated Constants of Logarithmic Equation

pp O ₂ , atm	k ₁	k ₂	k ₁ '	k ₂ '
0.844	4.98 x 10 ¹⁷	0.402	4.00 x 10 ¹⁷	0.455
0.651	4.20 x 10 ¹⁷	0.386	3.24 x 10 ¹⁷	0.438
0.425	3.41 x 10 ¹⁷	0.374	2.80 x 10 ¹⁷	0.377
0.201	3.43 x 10 ¹⁷	0.298	3.17 x 10 ¹⁷	0.250
0.098	3.61 x 10 ¹⁷	0.219	2.75 x 10 ¹⁷	0.211
0.048	3.77 x 10 ¹⁷	0.184	4.02 x 10 ¹⁷	0.118
0.027	1.83 x 10 ¹⁷	0.328	1.24 x 10 ¹⁷	0.302

of the constants at the lowest partial pressure are quite different from the others. This may be explained by the fact that at this partial pressure the current is very small and errors are apt to be more pronounced. Evidence of this is that the extrapolation at 0.027 atm of oxygen does not quite go to zero. Neglecting the values at 0.027 atm, one finds a definite trend in the value of k₂ as the partial pressure varies; but the value of k₁ seems to oscillate about an average value.

It thus seems plausible that k₁ and k₁' might, in fact, be constants; and that the variation of the data with partial pressure could be represented by a variation of the second constant in the equation. Using an average value of k₁ and k₁' of 3.90 x 10¹⁷ and 3.33 x 10¹⁷, values of k₂ and k₂' were calculated for three different times: t = 1/2, t = 1, and t = 1.5 secs for each partial pressure. These results are given in Tables 5 and 6.

Table 5

Calculated Values of k₂ Based on Average Value of k₁

pp O ₂ , atm	0.844	0.651	0.425	0.201	0.098	0.048	0.027
t = 1/2 sec	0.518	0.418	0.324	0.260	0.202	0.178	0.148
t = 1 sec	0.540	0.428	0.320	0.258	0.202	0.176	0.141
t = 1.5 sec	0.553	0.418	0.315	0.256	0.197	0.176	0.141
ave k ₂	0.537	0.421	0.320	0.258	0.200	0.177	0.143
	+ 13	+ 14	+ 1	+ 1	+ 2	+ 1	+ 3

Table 6

Calculated Values of k_2' Based on Average Value of k_1'

pp O_2 , atm	0.844	0.651	0.425	0.201	0.098	0.048	0.027
t = 1/2 sec	0.552	0.426	0.312	0.238	0.174	0.144	0.108
t = 1 sec	0.558	0.433	0.311	0.239	0.172	0.144	0.102
t = 1.5 sec	0.581	0.417	0.302	0.233	0.170	0.143	0.101
ave k_2'	0.564	0.425	0.308	0.237	0.172	0.144	0.104
	+ 12 - 12	+ 6 - 6	+ 4 - 4	+ 2 - 2	+ 1 - 1		+ 3 - 3

It is seen from Tables 5 and 6 that, at a given oxygen partial pressure, the values of k_2 and k_2' are fairly constant. Therefore, the data may be expressed by the following equation:

$$n = 3.90 \times 10^{17} \log(k_2 t + 1), \text{ or} \quad (18d)$$

$$n' = 3.33 \times 10^{17} \log(k_2' t + 1) \quad (18e)$$

If these equations are accurate, a plot of n versus $\log(k_2 t + 1)$ should be a straight line.

Using all the data points obtained, the values of the log terms were calculated and are plotted against n and n' in Figs. 23 and 24.

It is clear from the conformity of the data that the logarithmic equation is followed quite closely. The fact that k_1 in the logarithmic equation is independent of oxygen partial pressure is interesting, and leads one to wonder if this is significant or accidental. Therefore, more attention must be paid to the constants in the derivation of the logarithmic equation.

The first derivation of the logarithmic equation in the introduction is developed assuming that the rate of transfer of electrons by tunnel effect through the thin oxide film is rate determining.

The transfer of electrons by tunnel effect should be independent of the oxygen partial pressure, but experimentally the oxidation rate was found to be a strong function of the partial

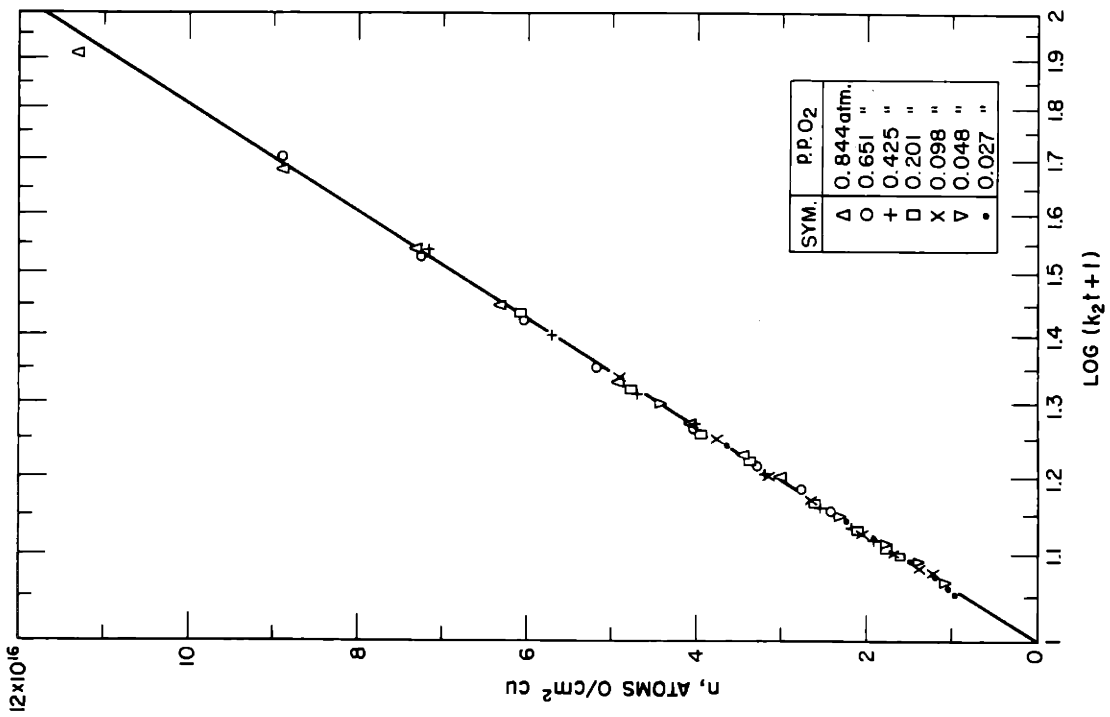


Fig. 23 Test of Logarithmic Equation, Copper

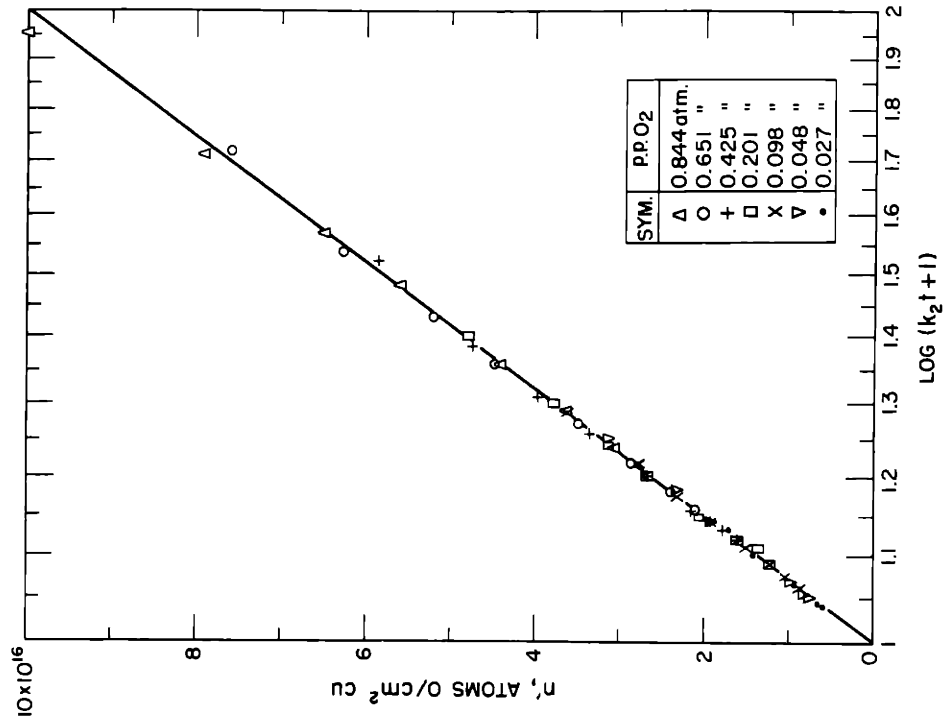


Fig. 24 Test of Logarithmic Equation, Copper

pressure; therefore, the mechanism assumed in this derivation is not the correct one.

The second derivation of the logarithmic equation assumes that the growth of the oxide is limited by the rate of mass transfer of oxygen through "leaky" points in the oxide film, the number of leaky points decreasing as oxidation progresses. This mechanism is compatible with the finding that the rate of oxidation is a function of the partial pressure of oxygen.

The number of weak points at a given weight of oxide is not dependent on the partial pressure of oxygen; therefore, the constants c_1 and c_2 in Eq. 20

$$D = c_2 e^{-c_1 w} \quad (20)$$

are not functions of the partial pressure. However, c_3 in the rate expression, Eq. 21,

$$\frac{dw}{dt} = c_3 e^{-c_1 w} \quad (21)$$

is clearly a function of the oxygen partial pressure. Performing the integration of this equation stepwise, we get

$$e^{c_1 w} dw = c_3 dt \quad (21a)$$

$$\frac{e^{c_1 w}}{c_1} = c_3 t + c_4 \quad (22)$$

$$e^{c_1 w} = c_1 c_3 t + c_1 c_4 \quad (22a)$$

Taking logarithms of both sides, this becomes

$$c_1 w = c_3 c_4 \ln(c_1 c_3 t + c_1 c_4) \quad (23)$$

or

$$w = \frac{1}{c_1} \ln(c_1 c_3 t + c_1 c_4) \quad (23a)$$

Comparison of this equation with Eq. 18b shows that

$$k_1 = \frac{1}{c_1}, \quad k_2 = c_1 c_3$$

Since c_1 is independent of the partial pressure of oxygen, k_1 must also be independent of it; and, since c_3 is a function of the oxygen partial pressure, so is k_2 . Therefore, the finding

that k_1 was a constant; and that k_2 varied with the partial pressure of oxygen is justified.

In the derivation of the logarithmic equation, Evans⁴⁹ proposes that oxygen in the ionic, atomic, or molecular form is transported through the leaky points in the oxide film to the metal surface. The effect of the partial pressure of oxygen on the constant k_2 should clarify somewhat the form that the oxygen is in. For example, if it is molecular oxygen or diatomic ions which are transported, the constant c_3 in the rate of growth equation would be directly proportional to the partial pressure of oxygen.

Figures 25 and 26 are plots of k_2 and k_2' versus partial pressure of oxygen. Since k_2 must be zero when the partial pressure of oxygen is zero, the origin has been taken as a point in the curve. The plots show that the constant is not directly proportional to the partial pressure of oxygen; hence, the oxygen is not transported in the diatomic form.

If the wiping action were not satisfactory and electrolyte resistance to oxygen transport still limited the oxidation, the oxidation rate would be directly proportional to the oxygen partial pressure. The fact that this proportionality does not exist supports the conclusion that the rubber wiper does remove the electrolyte film; and that the current is limited by the rate of oxidation of the metal surface.

If, in the Evans model, the oxygen transported through the leaky points were in the monatomic form (O , O^- or $O^{\bar{}}$), the oxidation rate would be proportional to the square root of the partial pressure of oxygen.

Figures 27 and 28 are plots of k_2 and k_2' versus the square root of the partial pressure of oxygen. Although there is some scatter, the correlation is satisfactory. At the same time, however, it should be noticed that in Fig. 27 the line doesn't extrapolate to the origin. This is to be expected since the data in this case are not corrected for galvanic currents. The error introduced as a result of this is most significant at the lower partial pressures, causing the corresponding

WADD TR 60-166

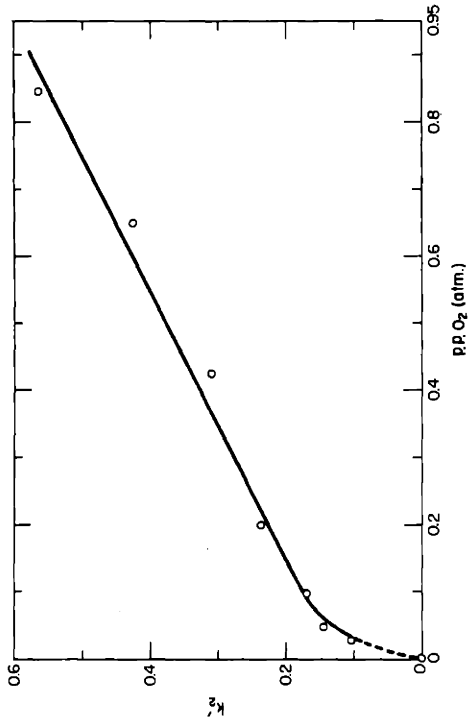


Fig. 25 k_2 versus Partial Pressure O_2

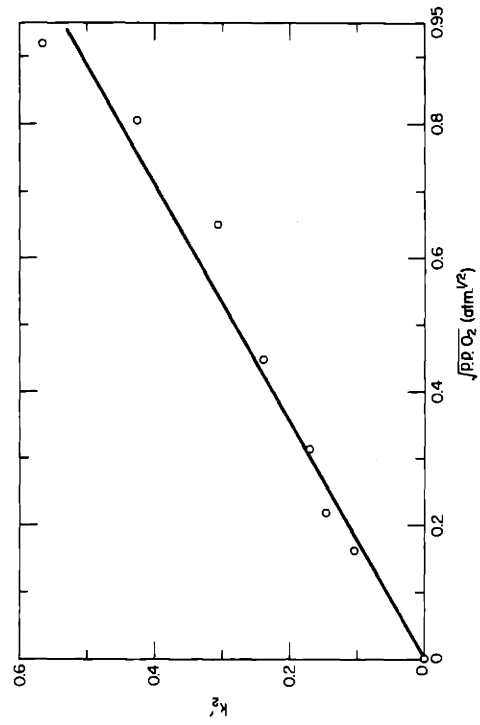


Fig. 27 k_2 versus Square Root of Oxygen Partial Pressure

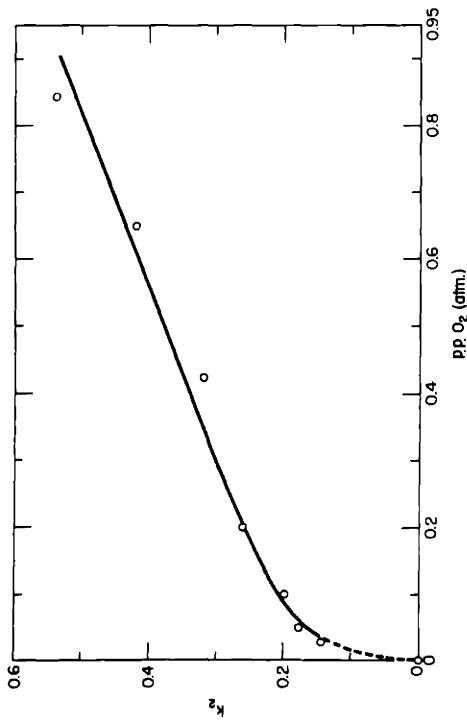


Fig. 26 k_1 versus Partial Pressure O_2

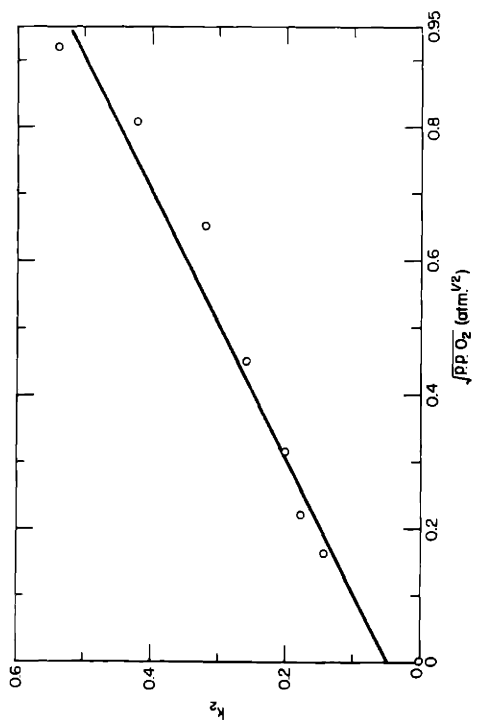


Fig. 28 k_1 versus Square Root of Oxygen Partial Pressure

values of k_2 to be too large and the data to extrapolate to a point above the origin. In Fig. 28 the data were "corrected" by subtracting the maximum possible galvanic currents. At low partial pressures the correction is good; hence, the line does extrapolate to the origin.

The conclusion is that the results agree with the Evans model for logarithmic growth and follow the equation

$$w = k_1 \log (k_2 t + 1) \quad (18f)$$

where k_1 is a constant independent of the oxygen partial pressure and k_2 is proportional to the square root of the oxygen partial pressure. In addition, if the Evans model is correct, the dependency of the oxidation rate on the square root of the partial pressure of oxygen indicates that the rate-determining step in the room-temperature oxidation of copper is the mass-transport rate of oxygen in the monatomic form (O , O^- , or $O^=$) to the metal surface.

Uhlig's⁵³ derivation of the logarithmic equation assumes that the rate of oxidation is controlled by the rate of electron flow from metal to oxide; and that this rate is affected by the space charge distribution in the oxide layer. Presumably, the partial pressure of oxygen should alter the space charge distribution in the oxide layer; however, Uhlig makes no mention of the effect of oxygen partial pressure. Therefore, no comparison with his derivation can be made.

The analysis of the rate of growth of the oxide layer does not show whether the oxide formed is cuprous or cupric. It was noticed that, when the partial pressure of oxygen was increased above 0.20 atm, the appearance of the copper surface became darker, indicating the presence of cupric oxide. At lower partial pressures the surface of the copper was reddish and quite similar to the color of cuprous oxide.

At low temperatures cupric oxide is more stable than cuprous oxide; however, the presence of metallic copper apparently affects this. Most investigators have found that the oxide film on copper is mainly cuprous oxide with a layer of

cupric oxide at the oxygen-oxide interface; and that the cupric oxide layer becomes more pronounced as the partial pressure of oxygen goes up. This would explain the change in the appearance of the copper surface which was encountered in the experiments.

(ii.) Silver. The data obtained for the oxidation of silver at 30°C are presented in Fig. 29, and are seen to be

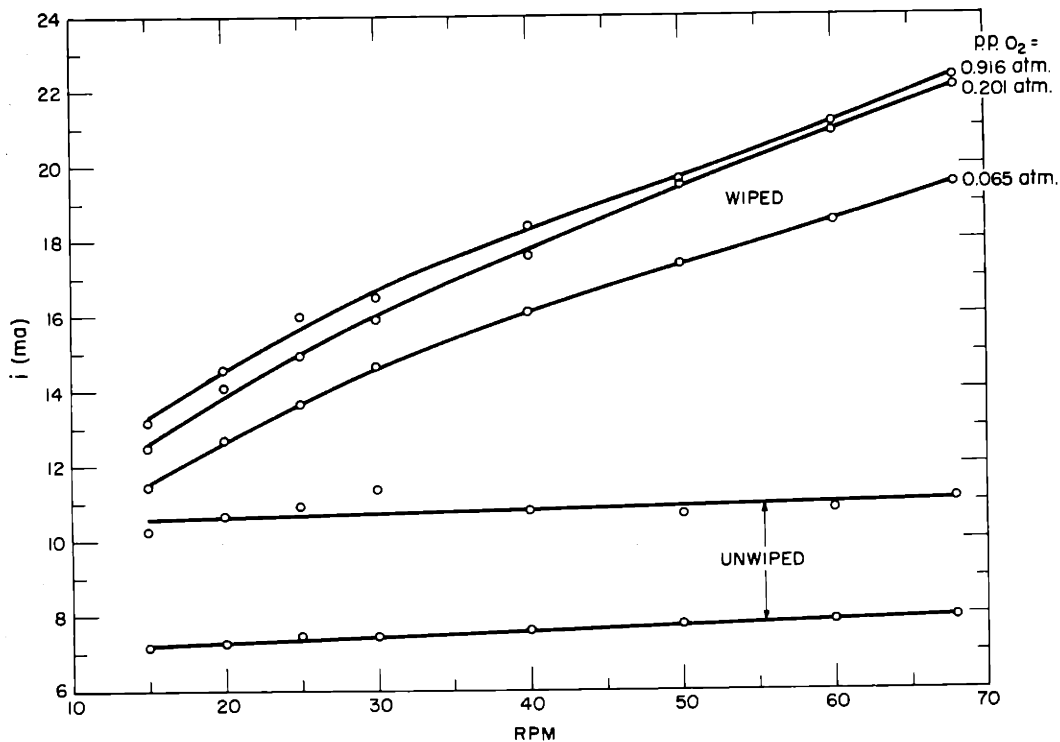


Fig. 29 Data for Rotating Silver Electrode

markedly different from those obtained for the oxidation of copper. The most significant difference is the relatively low value of the wiped currents. This makes quantitative interpretation of the results difficult because of the magnified importance of the galvanic current; however, some important conclusions can be obtained from the data.

First of all, there is a definite trend upward with partial pressure; but, considering the uncertainty in the data, it is impossible to be more quantitative about the partial-pressure dependence. It is significant, however, that the effect of

partial pressure is not as great as with copper. This suggests that the rate-determining step, and hence the oxidation law it follows, is different for silver.

It was seen in the analysis of the copper-oxidation data that the current of the wiped electrode had to be corrected by subtracting the galvanic current. Since the amount of oxygen reacting with the silver is small, one would expect that the oxide is reduced rather quickly on entering the electrolyte so that the submerged portion of the electrode is practically all silver with almost no silver oxide. In this case the galvanic current is very closely approximated by the maximum galvanic current; i.e., the unwiped current times the electrode fraction covered by electrolyte. In the following analysis the average value of the unwiped current multiplied by the fraction submerged was subtracted from the currents obtained.

Figure 30 is a plot of n' , the number of atoms of oxygen reacted per centimeter squared of silver, versus exposure time. It is clear from this plot that the oxidation is not linear with exposure time; and, hence, silver does not oxidize according to the linear law.

The parabolic law is tested in Fig. 31, which is a plot of $(n')^2$ versus the exposure time. The data do seem to lie on straight lines, and it appears that the silver oxidizes according to the parabolic law

$$y^2 = k_1 t + k_2 \quad (11)$$

Since the lines extrapolate to some point close to the origin, the constant k_2 in the parabolic equation appears to be zero; and the data can be represented by the equation

$$y^2 = k_1 t \quad (11a)$$

where k_1 varies with the partial pressure of oxygen. This finding indicates that all the oxygen that reacted with the metal is electrochemically reduced when the electrode surface passes through the electrolyte. Additional support of this, and of the conclusion that the oxidation step was limiting, is the fact that the current went up when the electrolyte mask was removed.

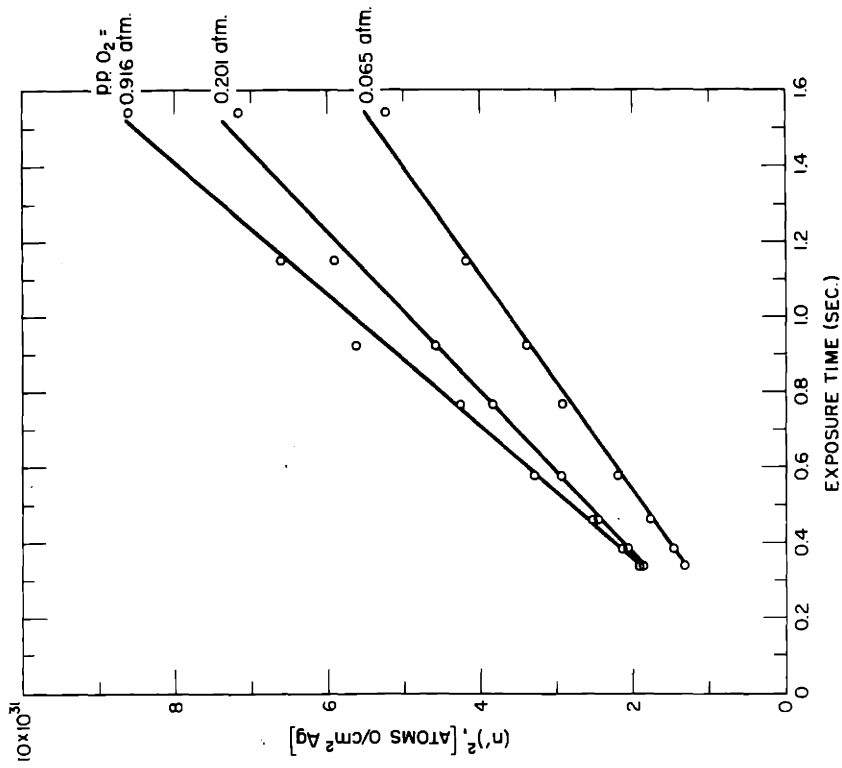


Fig. 31 Test of Parabolic Equation, Silver

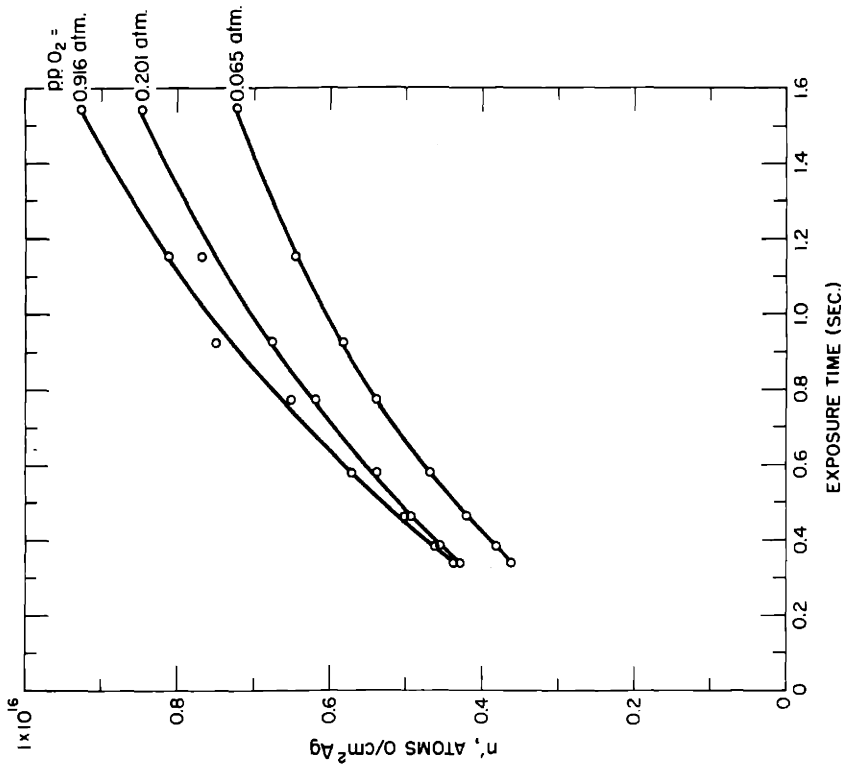


Fig. 30 Silver Oxide Thickness versus Exposure Time

The data can also be represented by the logarithmic equation; but, considering the uncertainties present and the arbitrary constants in the logarithmic equation, no significance can be attached to this correspondence.

Previous investigators have found that at room temperature the adsorption of oxygen on silver is chemical.^{54,55} However, no oxidation-rate data were found in the literature which could be compared with the results obtained with the wiped, rotating, partially submerged silver electrode.

In order to increase the reliability of silver-oxidation data obtained from a rotating electrode, such as was used here, it is necessary to either increase the oxygen uptake or decrease the galvanic current. A rotating electrode with a larger exposed perimeter and a smaller submerged perimeter would allow more oxygen to react and, at the same time, lower the galvanic current. Thus, though the electrode geometry used in this work was such that it did not allow a clear-cut interpretation of silver-oxidation rates, it should be possible using a different electrode geometry to obtain more reliable silver-oxidation data.

(iii.) Nickel. The current obtained from the rotating electrode is the sum of two currents: a current due to oxygen depolarization, and a "galvanic" current due to other electrochemical processes. With a copper electrode, the former was large compared to the galvanic current; and this allowed a detailed analysis of the copper oxidation. In the case of silver, though the galvanic current was less than for copper, the amount of oxygen which reacted was also less; and the difference between the total current and the galvanic current was not large enough to permit as reliable an analysis as might be desired. Nickel, the final metal studied, gave entirely different results. The oxygen reaction appeared to be large; however, the galvanic current was found to be high, and so uncertain that an analysis of the rate data was impossible.

With copper and silver the use or removal of the wiper gave instantaneous and reversible changes in the current.

Nickel, on the other hand, possessed a kind of hysteresis effect. When the wiper was removed, the current did not decrease stepwise, as was true for the other metals, but decreased more gradually with time. Since oxygen transport to the nickel surface is essentially cut off when the wiper is removed, the continued high current must be due to either a removal of oxide not previously reduced or an exceptionally high galvanic current. Again, since no further oxygen is reaching the nickel surface, any previously unreduced oxide should be consumed in a relatively small number of additional passes through the electrolyte. The duration of the high current was too long to be due to unreduced oxide; hence, it must have been due to a high galvanic current.

When a nickel electrode is connected to a zinc electrode in 20% KOH, there is, as explained in more detail in the Appendix, a considerable amount of hydrogen evolution at the nickel. This hydrogen evolution, and as a result the current of the cell, decreased rapidly at first, and then more slowly with time. Thus, the current at an unwiped, rotating nickel electrode will decrease with time to a value which is fairly low compared to its initial current. The finding that the current doesn't change stepwise, or reversibly in going from an unwiped to a wiped and then back to an unwiped electrode, indicates that oxidation of the nickel surface results in a change in the hydrogen-evolution rate at the nickel. In particular, the oxidation of a previously not-too-active, hydrogen evolution-wise, nickel surface results in a large increase in the hydrogen evolution rate. Of course, with continued hydrogen evolution, this rate will again go down. The cause of the change in hydrogen-evolution activity may be due to changes in the arrangement of atoms in the nickel surface; however, regardless of what the cause is, the effect is to make it impossible to estimate the galvanic current of a rotating nickel electrode, which is continuously being oxidized and reduced. This, in turn, makes it impossible to interpret the currents obtained from the rotating nickel electrode in terms of oxidation theory.

The data obtained using the rotating nickel electrode at 29°C are presented in Fig. 32. It is important to note that

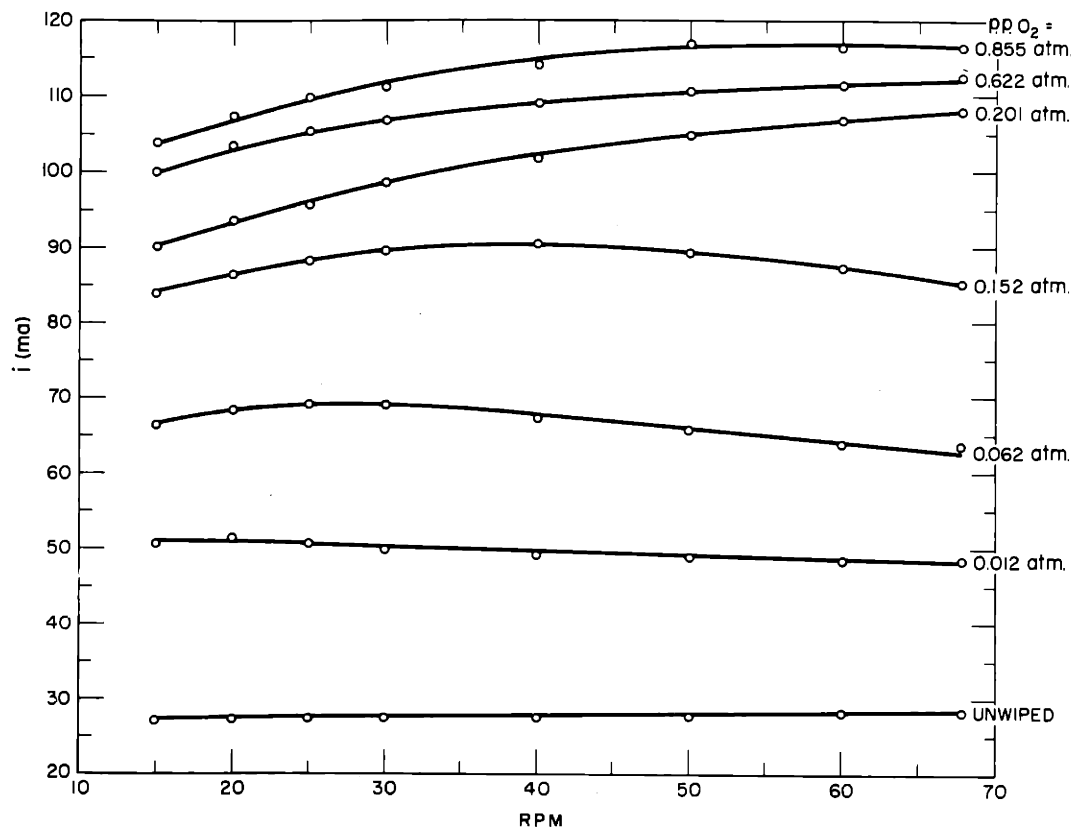


Fig. 32 Data for Rotating Nickel Electrode

the unwiped current is for an electrode which had been operating without interruption for over an hour; and, as a result, its magnitude is small compared to a freshly reduced nickel-oxide surface.

Though no analytical interpretation is possible, the data do have some interesting aspects. For example, the current is a strong function of the partial pressure of oxygen. It seems reasonable to conclude that much of this increase is due to oxygen adsorption. Since the oxidation of copper was also found to be a strong function of the partial pressure of oxygen, this is an indication that possibly copper and nickel oxidize in a similar manner.

If the current were due solely to oxidation, then there should be no maximums in the curves. The presence of such maximums indicates a high galvanic current which varies with exposure time and oxygen partial pressure.

It was also found that, for oxygen partial pressures above 0.201 atm, the removal of the electrolyte mask resulted in a decrease in the current, which is the opposite of what was found for copper and silver. This can be explained if the decrease in galvanic current, resulting from the decrease in submerged area, is greater than the increase in oxidation current, resulting from the increase in the exposed area. At a partial pressure of 0.012 atm, the masking effect was found to have been reversed; and the current went up when the electrolyte mask was removed.

The galvanic current, the magnitude and uncertainty of which made the analytical interpretation of the data impossible, is strongly dependent on the anode used. With a steel-wool anode the galvanic current is very small; but, when zinc is used as the anode, the galvanic current is considerably higher. Since a lower galvanic current results in more reliable data, it would at first seem that steel wool should be used as the anode; however, during the operation of the cell, the surface of the steel wool becomes oxidized and inactive. Thus, the steel-wool electrode can only be used when the current is small, as for example with the stationary electrodes. The rotating electrodes operate at a much higher current and require anodes which do not become deactivated. A zinc electrode does not become deactivated because zinc oxide, the product of the electrochemical action at the zinc anode, dissolves in the 20% KOH electrolyte, thus exposing a fresh zinc surface for further electrochemical reaction.

A second reason for not using steel-wool anodes with the rotating electrode is the requirement of a high electrochemical-reduction rate. In order to make the oxidation step the limiting one, it is necessary to reduce all the oxide which enters the electrolyte in the relatively short time it remains in the

electrolyte. All other things being equal, the reduction rate will be directly dependent on the open-circuit voltage of the cell. The cell voltage, and hence the reduction rate, is much higher with the zinc than with the steel-wool anode.

Zinc was selected as the anode because it provides a stable anode and a high cell voltage; however, the results show that it cannot be used to obtain oxidation data for nickel. In order to obtain reliable nickel oxidation data, it is necessary to use an anode which does not cause such a high and uncertain galvanic current.

c. Comparison of Oxidation Rates with Oxygen Electrode Requirements. The purpose of the wiped, rotating, partially submerged oxygen electrode was to try to measure the oxidation rates of copper, nickel, and silver and to compare them with the rate requirements of an oxygen electrode. Though it was not possible to determine the oxidation rate of nickel, values were obtained for copper and silver; and they can be compared with fuel cell requirements.

The oxidation rate of copper was found to increase with the square root of the oxygen partial pressure; and, at a partial pressure of 0.844 atm, a current of as high as 100 ma was obtained. The exposed perimeter of the copper disc was 10.4 cm, and its width was 0.37 cm; therefore, the exposed area was 3.85 cm^2 . The average oxidation rate of the exposed copper surface was thus about 26 ma/cm^2 . If the surface roughness of the copper surface could be increased by a factor of four, the current density based on the apparent area would be greater than the 100 ma/cm^2 rate requirement. It is difficult to determine the difference in surface roughness between the smooth metal surface used here and the porous-carbon or porous-metal surfaces used in fuel cell electrodes, but it certainly should be much greater than four. Also, the oxidation rate could be increased by increasing the oxygen partial pressure. Thus, it is seen that the copper oxidation rate is more than adequate for fuel cell requirements.

In addition, the above oxidation rate is an average rate for a copper surface having a considerable oxide thickness; and it is a fact that the oxidation rate decreases as the oxide-film thickness increases. In a fuel cell electrode, the oxidation and reduction steps occur simultaneously; and presumably there should be no oxide film. Therefore, the rate of oxidation of a copper surface used in a fuel cell electrode should be even higher than that obtained here.

The thickness of the oxide layer can be estimated from the values of n or n' in the following way:

The density of cuprous oxide is 6.0 g/cm^3 . Since the molecular weight is 143.1, one cm^3 of cuprous oxide contains

$$\frac{6.0}{143.1} \times 6.02 \times 10^{23} = 2.52 \times 10^{22} \text{ atoms of oxygen}$$

Assuming uniform spacing in each direction, the number of oxygen atoms in a cm of length is

$$(2.52 \times 10^{22})^{1/3} = 2.93 \times 10^7$$

The thickness of an oxide layer is, therefore,

$$\frac{1 \text{ cm}}{2.93 \times 10^7} = 3.4 \times 10^{-8} \text{ cm} = 3.4 \text{ angstroms}$$

The number of oxygen atoms in a cm^2 of area is

$$(2.93 \times 10^7)^2 = 8.58 \times 10^{14}$$

At an oxygen partial pressure of 0.844 atm and a rotational speed of 67.8 R.P.M., we find from Fig. 18 a value of n of 3×10^{16} atoms O/cm^2 of copper. Therefore, the oxide thickness is about

$$\frac{3 \times 10^{16}}{8.58 \times 10^{14}} = 35 \text{ layers}$$

It is difficult to establish a surface roughness for the copper; but, assuming a roughness of, say, three, then the oxide thickness is about 11.7 layers, or approximately 40 angstroms.

This is the oxide thickness on the copper as it re-enters the electrolyte. The copper, as it leaves the electrolyte, has no oxide on it; so, the average oxide thickness is less than this value.

The thickest oxide layer obtained with the copper electrode, again referring to Fig. 18 and assuming a roughness of three, is

$$\frac{11.3 \times 10^{16}}{(3)(8.58 \times 10^{14})} = 43.9 \text{ layers}$$

or approximately 150 angstroms.

The highest current obtained with the rotating silver electrode, when correction is made for the galvanic current, was 16.4 ma. Since the exposed length was 9.5 cm and the width 0.42 cm, the exposed area was 3.99 cm². The maximum current density was, thus, about 4.1 ma/cm². This is much lower than the 100 ma/cm² required; but, when one takes into account the increased rate due to decreased oxide-film thickness and the increase in surface roughness resulting from a porous construction, it may be possible to achieve such a current density in a porous fuel cell electrode, made or coated with silver. The issue unfortunately is not as clear cut as was with copper.

It is interesting to compare the thickness of the silver oxide formed on the rotating electrode with that obtained for copper. Using a density of 7.14 g/cm³, and a molecular weight of 231.8, the number of oxygen atoms in a Ag₂O monolayer is calculated to be 7.0 x 10¹⁴ atoms O/cm². The maximum oxygen adsorption was found to be 9.26 x 10¹⁵ atoms O/cm² Ag (see Fig. 30). Again assuming a surface roughness of three, this amounts to an oxide film about 4.4 layers thick, which is about 1/10 the number of layers obtained for copper under approximately comparable conditions.

In the case of nickel, though no oxidation rates were determined, the high currents and the marked partial pressure effect indicate that nickel's oxidation rate might be enough to obtain a current density of 100 ma/cm² in a properly designed electrode; however, further work is required to establish this definitely.

The results of the experiments with the rotating electrode definitely show that, as far as oxidation rate is concerned, an oxygen electrode operating at 100 ma/cm² can be constructed

using copper as the active electrode surface; and they indicate that such a current density might be possible with nickel or silver surfaces.

CHAPTER V

CONCLUSIONS AND RECOMMENDATIONS

The investigation of partially submerged, air-depolarized cathodes of copper, nickel, and silver in a caustic cell showed that the mechanism of oxygen transport to these flat metal cathodes was solution of oxygen in the electrolyte, followed by transport through the electrolyte to the electrode surface. It was also found that the limiting step in the operation of these partially submerged cathodes was the rate of oxygen transport to the electrode surface.

These results lead to the conclusion that, in the porous electrodes commonly used in fuel cells, drowning is caused by a large increase in the resistance to mass transport of oxygen. In addition, they indicate that, in operating porous electrodes which are not drowned, the limiting step may still be the rate of oxygen transport through the electrolyte to the electrode surface.

The wiped, rotating, partially submerged oxygen electrode was designed to eliminate this resistance to oxygen transport and, thereby, to measure the oxidation rates of the electrode surfaces. With a smooth copper surface at 32°C and an oxygen partial pressure of 0.844 atm, current densities of 26 ma/cm² exposed area were obtained. When differences in surface roughness and oxide thickness are considered, this shows that the oxidation rate of a porous electrode, containing or made of copper, is more than sufficient to provide a current density of 100 ma/cm², which has been established as a criterion for an economical fuel cell. The results with silver and nickel, though not conclusive, indicate that this may be true for these metals too.

These findings show the importance of designing fuel cell electrodes with a view towards decreasing the mass transfer resistance posed by the electrolyte. Moreover, they point to the necessity of learning more about the physical and chemical

processes occurring in fuel cells. The knowledge of these processes is invaluable for the development of economical fuel cells.

The oxidation results obtained with a rotating copper electrode were found to obey the logarithmic law

$$w = k_1 \log(k_2 t + 1) \quad (18f)$$

It was also found that k_1 was constant and that k_2 was proportional to the square root of the partial pressure of oxygen. These findings are compatible with a derivation of the logarithmic law by Evans,⁴⁹ which assumes that the limiting step is the transport of oxygen in some form to the metal-metal oxide interface. The finding that k_2 is proportional to the square root of the oxygen partial pressure, when interpreted in the light of the Evans theory, indicates that the oxygen is transported in the monatomic, O , O^- , or $O^=$, form.

The oxidation rate obtained with silver was much less than for copper, and the maximum current density obtained was about 4.1 ma/cm^2 exposed area. The effect of partial pressure of oxygen on the oxidation rate was also less than for copper and suggests a different oxidation mechanism. The data appeared to fit the parabolic equation

$$y^2 = k_1 t \quad (11a)$$

however, more-accurate data is needed to definitely establish this.

It was impossible to obtain accurate rates for the oxidation of nickel; however, the oxidation rate did appear to be a strong function of the oxygen partial pressure.

The use of the rotating electrode, despite its disadvantage of contaminating the metal surface with electrolyte, appears to be a very useful tool for studying the low-temperature oxidation of metals. It is recommended that further work be done with silver and nickel, as well as with other metals, and activated carbon surfaces.

APPENDIX A

DETAILS OF ROTATING ELECTRODES AND OPERATING CHARACTERISTICS

In this section are presented the electrode dimensions and operating characteristics of the copper, silver, and nickel electrodes used to obtain the data discussed in the section, Oxidation of Metals.

1. Copper

Electrode Diameter = 7.84 cm
Exposed Length = 10.4 cm
Electrode Width = 0.37 cm
Temperature = 32° C
External Resistance = 0.352 ohms

2. Silver

Electrode Diameter = 7.84 cm
Exposed Length = 9.5 cm
Electrode Width = 0.42 cm
Temperature = 30° C
External Resistance = 0.352 ohms

3. Nickel

Electrode Diameter = 7.84 cm
Exposed Length = 9.8 cm
Electrode Width = 0.36 cm
Temperature = 29° C
External Resistance = 0.352 ohms

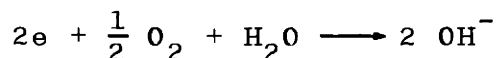
APPENDIX B

DISCUSSION OF GALVANIC CURRENTS

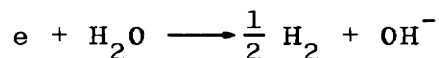
The current obtained from a partly or completely submerged air-depolarized electrode may be divided into two parts: that due to depolarization by oxygen and that due to other electrochemical reactions. This latter contribution to the total current has been arbitrarily termed the "galvanic" current.

It can be seen from the data listed in the section Mechanism of Oxygen Transport to Air-Depolarized Cathodes, that the current with a completely submerged copper, nickel, or silver electrode in a metal--20% KOH--steel-wool cell is much less than with a partially submerged electrode. This means that, for the partially submerged electrode in the above cell, the current due to air-depolarization is much greater than the galvanic current; and, for all practical purposes, the latter may be neglected. However, this may not be true for other electrode systems, or for the completely submerged case.

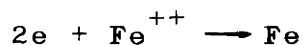
In order for the submerged electrode to behave as a cathode, the electrochemical reactions occurring there must lead either to the formation of anions or the destruction of cations. Depolarization by oxygen results in the formation of anions, the net reaction for which is



Anions can also be produced by evolution of hydrogen, according to the following equation:



The alternate cause of current, the removal of cations, can occur by the plating out of the anode material. For example,



In this case the plated iron must exist in a state which has a lower free energy than at the anode. The last two reactions make up what has been termed the galvanic current.

In itself the galvanic current is not of interest to us, and we would rather like to neglect it; however, if it is of large magnitude relative to the oxygen-depolarization current, this cannot be done. Also, the alteration of the cathode surface by plating may effect the rate of oxygen depolarization. In order to study the galvanic current, copper, nickel, and silver cathodes were used with two different anodes, steel wool and zinc, both with and without stirring.

1. Steel-Wool Anode

Data obtained using completely submerged cathodes of copper, nickel, or silver, and a steel-wool anode in 20% KOH electrolyte are listed in Table 7. The current densities,

Table 7

Completely Submerged Cathodes with Steel-Wool Anode

Time	$i_d, \text{ ma/cm}^2$			Remarks
	Cu	Ni	Ag	
5 min	0.0085	0.012	0.0065	
10 min	0.0059	0.0099	0.0065	
15 min	0.0057	0.0088	0.0062	2 steel-wool anodes
	0.0057	0.010	0.0062	
20 min	0.014	0.014	0.013	Stirring (230 R.P.M.) Stirring : 2 s.w. anodes
	0.014	0.016	0.013	
25 min	0.0034	0.0051	0.0043	2 steel-wool anodes
	0.0034	0.0062	0.0043	

which are very small to start with, are seen to decrease with time. This drop in current can be partly attributed to a decrease of oxygen concentration in the vicinity of the cathode, and partly to other polarization effects.

Doubling the anode area does not affect the currents obtained from the copper and silver cathodes, but does raise slightly the current at the nickel cathode. This indicates that the galvanic current for the nickel is greater than for copper or silver; however, since the increase is small, one would expect that the galvanic current, even for nickel, is not a large portion of the total current. Another reason for

suspecting that the galvanic current is not important is the fact that the current is of the same order of magnitude at each metal, which indicates that it is due mainly to the same process at each electrode; i.e., depolarization by oxygen.

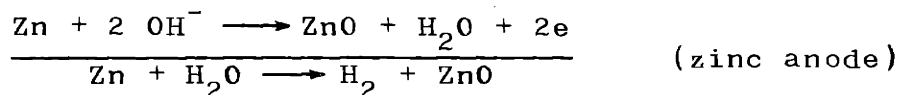
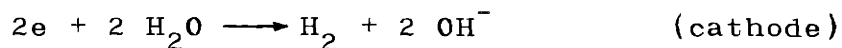
The sensitivity of the current to stirring shows that the current is mass-transfer rate controlled, the controlling step presumably being the mass transport of oxygen to the cathode surface. When nitrogen was bubbled past the cathodes, the current momentarily went up, but then decreased to a value well below that present before the nitrogen bubbling was initiated. The momentary rise is attributed to an increase in the oxygen-transport rate, resulting from the agitation caused by the nitrogen bubbler; and the ensuing decrease, to a lowering of the oxygen concentration in the electrolyte. The presence of a small current, even with continued nitrogen bubbling, indicates that a small part of the submerged current is indeed galvanic. This of course is to be expected, due to the presence of two dissimilar metals in an electrolyte.

The conclusion obtained from these data is, thus, that the galvanic current in a caustic cell with a copper, nickel, or silver cathode and a steel-wool anode is small compared to the oxygen-depolarization current. At the same time, however, even though the galvanic current is small, it must be remembered that it may result in changes of the cathode surface, which may alter its properties considerably.

2. Zinc Anode

The results obtained using a zinc anode are quite different from those obtained with steel-wool anodes. The most obvious difference is the evolution of hydrogen at the cathodes. The evolution of hydrogen at the nickel electrode is quite vigorous, and much greater than at the copper or silver electrodes. Correspondingly, the current of the Ni-20% KOH-Zn cell is much larger than with copper or silver. As was found with steel-wool anodes, the magnitude of the current decreased with time.

It is thought that the hydrogen evolution occurs according to the following equations:



In one test, after the electrodes had been connected for about five minutes, the current densities were 0.053 ma/cm^2 for silver, 0.15 ma/cm^2 for copper, and about 3 ma/cm^2 for nickel. This corresponds to a ratio of approximately 1 to 3 to 60 for silver, copper, and nickel, respectively. These currents, essentially entirely galvanic, are not negligible in comparison with those obtained with partially submerged cathodes.

In addition to the hydrogen evolution, zinc was found to plate on the copper and, to some extent, on the silver cathode. Since it took considerable time for the plate to develop, the contribution of this current to the total current must have been very small. On copper, the plate is very shiny and smooth when new, but has a tendency to become dull and disappear with time. This is presumably due to diffusion of copper outward, or of zinc inward. There was no evidence of any zinc plating out on the rotating electrode surface for any of the runs reported in this thesis.

APPENDIX C

CONCENTRATION CELL EFFECT

It was previously noted that, when a piece of moist red litmus paper is placed on the wiped rotating surface, the paper immediately turns blue. Though the rubber wiper removes the macroscopic electrolyte film that all but eliminates the transport of oxygen to the metal surface, it is clear that a microscopic electrolyte film remains on the surface. The presence of the microscopic electrolyte film was found, under certain conditions, to influence the current of the cell.

When the wiped, rotating, partially submerged oxygen electrode was first built, it was not enclosed in a lucite box; and it was found that blowing air over the rotating metal surface resulted in a lowering of the current. If the air was made more humid, by first bubbling it through a gas washing bottle, its effect on the current was much less. Since the evaporation of the microscopic electrolyte film would also decrease with increasing humidity, it appears that the lowering of the current is due to the evaporation of this film.

The decrease in current due to the evaporation of the microscopic film of electrolyte may be attributed to either of two effects: a decrease in the temperature of the copper surface, or an increase in the KOH concentration of the film.

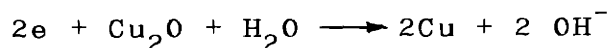
If the current is limited by the chemical rate of oxidation of the copper surface, one would expect that a lowering of the surface temperature would result in a lowering of the current. However, it is difficult to believe that the surface temperature lowering could be sufficient to cause as large a drop in current as was evidenced, which was oftentimes as much as 50%.

It is, therefore, more plausible to attribute the drop in current to an increase in the KOH concentration in the microscopic electrolyte film on the copper surface.

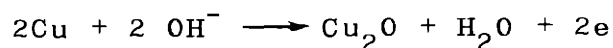
A change in the hydroxyl-ion concentration at either electrode of the cell would, in effect, result in a concentration

cell. This concentration cell would act in conjunction with, or in opposition to, the $\text{Cu}_2\text{O-KOH-Zn}^*$ cell. The following analysis shows that an increase in the electrolyte concentration at the copper electrode would indeed result in a decrease in the current of the cell.

The reaction occurring at the copper cathode is



Following Latimer²⁰ and writing the equation as an oxidation reaction with the electrons on the right-hand side, we get



$$E_{\text{Cu,Cu}_2\text{O}} = E^\circ - (0.05916/n) \text{Lg} \frac{(a_{\text{Cu}_2\text{O}})(a_{\text{H}_2\text{O}})}{(a_{\text{Cu}})^2 (a_{\text{OH}^-})^2} \quad (26)$$

Since the activity of the solids is unity, the oxidation potential becomes

$$E_{\text{Cu,Cu}_2\text{O}} = E^\circ - (0.05916/n) \text{Lg} \frac{(a_{\text{H}_2\text{O}})}{(a_{\text{OH}^-})^2} \quad (26a)$$

When the concentration of hydroxyl ion increases, the right-hand term decreases; hence, the value of $E_{\text{Cu,Cu}_2\text{O}}$ increases. The voltage of the cell is

$$E_{\text{cell}} = E_{\text{Zn,ZnO}_2} - E_{\text{Cu,Cu}_2\text{O}} \quad (27)$$

Therefore, the increase in the oxidation potential $E_{\text{Cu,Cu}_2\text{O}}$ caused by an increase in the electrolyte concentration at the copper electrode would lower the cell voltage and result in a smaller current.

As a result of this finding, it became necessary to have a controlled atmosphere above the rotating electrode; and so, the electrode was placed in an airtight lucite box. In order to prevent evaporation or condensation from taking place on the copper surface, the atmosphere inside the lucite box was kept saturated with respect to the electrolyte by continuously bubbling the enclosed air through an electrolyte bath.

*It is assumed for purposes of discussion that the oxide formed is Cu_2O . The argument and conclusions would not change if other oxides are formed.

The effectiveness of the saturated atmosphere was tested by means of a motorized stirrer placed just above the rotating electrode in the lucite box. When the enclosed air was saturated, the rotation of the stirrer had no effect on the current of the cell.

APPENDIX D

NOMENCLATURE

A	Area, cm^2
c	Constant in oxidation equation
C	Concentration, molecules/ cm^3
($\text{Cu}^+ \square$)	Cuprous ion vacancy
D	Number of discontinuities in an oxide film
D_L	Diffusivity, liquid, cm^2/sec
D_V	Diffusivity, gas, cm^2/sec
($e/\text{Cu}_2\text{O}$)	Electron of a cuprous oxide molecule
($e \square$)	Electron deficiency
E	Reversible cell voltage, volts
f	Faraday constant, 96,500 coul/g equiv
F	Free energy
H	Enthalpy
i	Current
i_d	Current density, ma/cm^2
k	Constant in oxidation equation
M	Molecular weight
n	Oxide thickness, atoms O/cm^2
n_e	Number of electrons transferred per molecule
N	Collisions of gas molecules with wall, collisions/ cm^2
N_A	Rate of diffusion, g moles/ $\text{cm}^2 \text{ sec}$
p	Probability
p_B	Partial pressure of inert gas, atm
P	Total pressure
r	Electrical resistance
r_f	Resistance to oxidation per unit thickness of oxide film
r_m	Resistance to oxidation at metal-metal oxide interface
r_o	Resistance to oxidation at oxygen-metal oxide interface
R	Gas constant

R_T	Total resistance to oxidation
S	Entropy
T	Temperature
w	Weight of oxide film
y	Thickness of oxide film
Z	Stagnant film thickness, cm

Superscripts

' Indicates that correction has been made for galvanic current

APPENDIX E

LITERATURE CITATIONS

1. Grove, W.R. Phil. Mag. (3), 14, (1839), p. 139.
2. Adams, A.M. Chemical and Process Engineering (July 1954) pp. 199-203. Also (August 1954) pp. 238-246.
3. Sherwood, T.S., and Pigford, R.L. Absorption and Extraction. McGraw-Hill Book Company, Inc., New York (1952), p. 6.
4. Reid, R.C., and Sherwood, T.S. The Properties of Gases and Liquids. McGraw-Hill Book Company, Inc., New York (1958), p. 274.
5. Mond, L., and Langer, C. Proc. Roy. Soc. Lond., 46, (1889) pp. 296-308.
6. Schmid, A. Diffusion Gas Electrodes. Stuttgart, F. Enke (1923).
7. Heise, G.W., Schumacher, E.A., and Fisher, C.R. Trans. Electrochemical Soc., 92, (1947), p. 173.
8. Davtyan, O.K. Direct Conversion of Chemical Energy of Fuel into Electrical Energy. Moscow, Academy of Sciences (1947).
9. Kordesch, K., and Marko, A. Ost. Chem. Ztg., 52, (1951), pp. 125-131.
10. Kordesch, K., and Marko, A. U.S. Patent 2,615,932, (October 28, 1952).
11. Kordesch, K., and Marko, A. U.S. Patent 2,669,598, (February 16, 1954).
12. Kordesch, K. M.I.T. Seminar (December 4, 1957).
13. Bacon, F.T. Beama Journal, 61, (1954), pp. 6-12.
14. Bacon, F.T. U.S. Patent 2,716,670 (August 30, 1955).
15. Bacon, F.T., and Forrest, J.S. Trans. Fifth World Power Conf., Vienna, 15, (1956), pp. 5397-5412.
16. Bauer, E., and Preis, H., Z. Elektrochem., 43, (1937), pp. 727-732.

17. Gorin, E. U.S. Patent 2,570,543 (October 9, 1951).
18. Gorin, E. U.S. Patent 2,581,650 (January 8, 1952).
19. Gorin, E. U.S. Patent 2,581,651 (January 8, 1952).
20. Business Week (October 17, 1959) p. 33.
21. Posner, A.M. Fuel, 34, (1955), pp. 330-8.
22. Lowry, H.H., ed. Chemistry of Coal Utilization. John Wiley and Sons, Inc., New York, 2, (1945), pp. 1568-85.
23. McKee, J.H., and Adams, A.M. Fuel, 28 (1949) pp. 1-6.
24. Watson, R.G.H. Direct Current, 1, (1952), pp. 30-4.
25. Watson, R.G.H. Research, 7, (1954), pp. 34-40.
26. Danckwerts, P.V. Industr. Chem., 28, (1952), p. 99.
27. Genin, G. Electricite, 37, (1953), pp. 1-7, 125-132.
28. Adams, A.M. J. Inst. Fuel, 27, (1954), pp. 366-73.
29. Austin, L.G. Scientific American (October 1959) pp. 72-78.
30. Butler, J.A.V., and Randall, J.T. Progress in Biophysics. Academic Press, Inc., New York, 4, (1954), p. 304.
31. Mullen, P.W. Modern Gas Analysis. Interscience Publishers, Inc. (1955), p. 135.
32. Badger, W.L. Ind. Eng. Chem., 12, (1920), p. 161.
33. von Rhorer, L. Zeitsch. Elektrochem., 29, (1923), p. 478.
34. Berl, W.G. Trans. Electrochem. Soc., 83, (1943), p. 253.
35. Baker, W.J., et.al. Ind. Eng. Chem. (June 1959), p. 727.
36. Schlier, R.E., and Farnsworth, H.E., Proc. Int. Cong., Catalysis. Philadelphia (1956) pp. 434-440.
37. Pilling, N.B., and Bedworth, R.E. J. Inst. Met., 29, (1923) p. 529.
38. Wagner, C. Z. Phys. Chem., B21 (1933) p. 25.
39. Jost, W. Diffusion u. Chem. Reaktion in Festen Stoffen. Leipzig (1937).
40. Hoar, T.P., and Price, L.E. Trans. Faraday Soc., 34 (1936) p. 867.

41. Cabreara, N., and Mott, N.F. Rep. Prog. Phys., 12, (1948-49), 163.
42. Garner, W.E. Chemistry of the Solid State. Butterworths Scientific Publications, London (1955), p. 346.
43. Gundermann, J., and Wagner, C. Z. Phys. Chem., B37, (1937), p. 155.
44. Wagner, C., and Grunewald, K. Z. Phys. Chem., B40, (1938), p. 455.
45. Evans, U.R. An Introduction to Metallic Corrosion. Edward Arnold and Company, London (1948).
46. Mott, N.F., and Gurney, R.W. Electronic Processes in Ionic Crystals. Clarendon Press, Oxford, 2, (1948) p. 249.
47. Kubaschewski, O., and Hopkins, B.C. Oxidation of Metals and Alloys. Academic Press, Inc., New York (1953).
48. Rees, A.L.G. Chemistry of the Defect Solid State. John Wiley and Sons, Inc., New York (1954) p. 102.
49. Evans, U.R. The Oxidation of Metals, Review of Pure and Applied Chemistry, 5, (1955), pp. 1-21.
50. Hauffe, K. Oxydation von Metallen und Metallegierungen. Springer-Verlag, Berlin (1956).
51. Gray, T.J., et al. The Defect Solid State. Interscience Publishers, New York (1957). p. 139.
52. Holm, R. Electric Contacts. Gebers, Stockholm (1946) p. 115.
53. Uhlig, H.H. Acta Met., 4, (5), (1956), p. 541.
54. Benton, A.F., and Drake, L.C. J. Am. Chem. Soc., 56, (1934), p. 255.
55. Benton, A.F., and Elgin, J.C. Ibid, 48, (1926), p. 3027.
56. Latimer, W.M. Oxidation Potentials. Prentice-Hall, Inc., 2, (1952), p. 2.

APPENDIX F

BIBLIOGRAPHY ON FUEL CELLS

The following was compiled by Mr. A.M. Adams of the Central Electricity Research Laboratories, Leatherhead, England, and is reproduced through the courtesy of the Director, Dr. J.S. Forrest:

Bibliography on "Fuel Cells"

This bibliography gives a fairly complete list of references for the period 1801 to 1949. An indication of the type of cell described or other contents of the paper can be obtained by referring to the section of the attached appendix indicated in the right-hand column.

<u>Author</u>	<u>Date</u>	<u>Appendix Section</u>
Allemand, A.J. and Ellingham, H.J.T. "Principles of Applied Electrochemistry" London: Longmans, Green and Co. Ltd.	1924	5.3.
Anon. Zeits. Elektrochem. <u>3</u> , p.192 German Patent No. 88, 327	1895	3.3.
Anon. Electrical Engineering <u>21</u> p. 261, p. 497	1896	1.3.2.
Anon. Zeits. Elektrochem. <u>4</u> , pp.129-36, pp.165-7	1897	1.3.2.
Andreas, E. v. Fodor	1895	2.1.2. 2.1.3.
Archereau, H.A. British Patent No. 1,037/A.D. 1883	1883	1.3.2.
Arsonval, A.d' French Patent No. 152,348	1882	2.1.5.
Atkinson, L.B. and Treharne, F.G. British Patent No. 8,906/A.D. 1896	1896	2.1.5.
Auerbach, F. Zeits. Elektrochem. <u>25</u> , p.82	1919	2.1.1.
Bailloé Dissertation, Basle	1927	3.3.
Basset, L.P. British Patent No. 7,375/A.D. 1906 16,905/A.D. 1906	1906	2.1.3.

<u>Author</u>	<u>Date</u>	<u>Appendix Section</u>
Basset, L.P. British Patent No. 21,475/A.D. 1907 22,236/A.D. 1907	1907a	2.1.3.
Basset, L.P. German Patent No. 202,369	1907b	2.1.3.
Baur, E. and Glaessner, A. Zeits. Elektrochem. <u>9</u> , pp.534-539	1903	2.1.1. 2.2.2.
Baur, E. Zeits. Elektrochem. <u>16</u> , pp.300-302	1910	1.2. 1.3.2. 2.1.3. 2.2.2.
Baur, E. and Ehrenburgh Zeits. Elektrochem. <u>18</u> , pp.1002-1011	1912	1.3.3. 2.1.5.
Baur, E., Petersen A., and Füllemann, G. Zeits. Elektrochem. <u>22</u> , pp.409-414	1916a	1.3.3.
Baur, E. and Treadwell, W.D. German Patent Nos. 325,783;325,784 British Patent No. 126,766	1916b 1918	1.3.2. 1.4. 1.3.2.
Baur, E. Zeits. Elektrochem. <u>27</u> , pp.194-199	1921a	2.2.1.
Baur, E., Treadwell, W.D., and Trümpler Zeits. Elektrochem. <u>27</u> , p.199	1921b	1.3.2. 2.1.5.
Baur, E. Helv. Chem. Acta <u>4</u> , pp.325-333	1921c	2.1.5.
Baur, E. German Patent No. 357,290	1921d	2.1.5.
Baur, E. Brennstoff Chem. <u>2</u> , p.147	1921e	5.2.
Baur, E. Zeits. Elektrochem. <u>36</u> , pp.410-414	1930	3.1.
Baur, E. and Tobler, J. Zeits. Elektrochem. <u>39</u> , pp.169-180	1933	2.1.2. 5.1
Baur, E. and Brunner, R. Zeits. Elektrochem. <u>41</u> , p. 794	1935	1.3.2.
Baur, E. and Brunner, R. Zeits. Elektrochem. <u>43</u> , pp. 725-27	1937a	1.3.2. 3.1.
Baur, E. and Preis, H. Zeits. Elektrochem. <u>43</u> , pp. 727-732	1937b	1.4. 2.1.6. 2.2.2.
Baur, E. and Preis, H. Zeits. Elektrochem. <u>44</u> , pp. 695-698	1938	1.4. 2.1.6. 2.2.2.

<u>Author</u>	<u>Date</u>	<u>Appendix Section</u>
Baur, E. Brennstoffchem. <u>20</u> , p.385	1939	2.1.6. 5.2.
Baur, E. German Patent No. 713,570	1941	2.1.6. 2.2.2.
Bechterew, P. Zeits. Elektrochem., <u>17</u> , pp. 851-77 v.a. Sacher and Lorenz	1911	5.1.
Becquerel, A.C. "Treatise on Electricity" (In French) Paris: Firmin Didot Freres Vol. 1	1855	1.3.1.
Bernstein German Patent Nos. 32,822 V 32,988;34,097	1895	2.1.1. 2.1.2.
Bernstein Zeits. Elektrochem. <u>6</u> , p.156	1897	2.1.1. 2.1.2.
Berthier, A. "Electrical Energy of Tomorrow" (In French) Paris: Desforges, Girardot and Cie.	1929	5.1.
Beutner Zeits. Elektrochem. <u>17</u> , pp.91-93	1911	2.1.5. 3.3.
Blanchard, V.W. British Patent No. 5695/A.D. 1882	1882	2.1.2.
Blanke, M. German Patent No. 730,247	1942	2.1.5. 2.2.2. 3.3.
Borchers, W.J. Chemical Industr. (London) <u>17</u> , p.502	1894	2.1.1. 2.2.2.
Boudouard Ann. chem. phys. (VII) <u>24</u> , p.5	1904	5.3.
Bradley v. Anon 1897	1888	1.3.2.
Brandt, R. German Patent No. 408,435	1925	2.2.1.
Brard Compte. rend. Paris. <u>95</u> , pp.890-892 pp.1158-1160	1882	1.3.1.
Braun, G. and Schneider, F. British Patent No. 25,879/A.D. 1910	1910	2.1.1. 6.
British Electrical and Allied Industries Research Association Translation of Davtyan 1947 (q.v.)	1949a	5.1.

<u>Author</u>	<u>Date</u>	<u>Appendix Section</u>
British Electrical and Allied Industries Research Association Technical Report Z/T76	1949b	5.1.
British Electrical and Allied Industries Research Association Annual Report 1949	1950	2.1.2. 4.1.
Britzke, O. German Patent No. 131,893 British Patent No. 23,675/A.D. 1900	1900	2.1.5. 6.
Brooks, E.E. Electrical Review. <u>35</u> p.190	1894a	1.3.1.
Brooks, E.E. Elektrotech. Zeits. <u>15</u> p.550	1894b	1.3.1.
Bucherer, A.H. German Patent No. 88327	1896a	2.1.5.
Bucherer, A.H. Zeits. Elektrochem. <u>3</u> pp.192-6	1896b	2.1.1. 2.1.5.
Bührer, C. Dissertation, Basle.	1929	2.1.4. 3.3.
Bull, H.C. British Patent No. 11,712/A.D. 1891	1891	1.3.2.
Byrnes, E.A. Trans. Amer. Elektrochem. Soc. <u>2</u> pp.113-119	1902	1.3.2.
Cailletet, L. and Collardeau, E. Compt. rend. Paris <u>119</u> pp. 830-834	1894	2.1.2. 3.1. 4.1.
Carbone Soc. Anon. German Patent No. 392,688	1923	3.2.
Case, W.E. v.Berthier 1929	1887	1.1.
Case, W.E. British Patent Nos. 12,171/A.D. 1899 12,172/A.D. 1899	1899	1.1.
Chipman, J. and Murphy, D.W. Ind. Eng. Chem. <u>25</u> pp.319-327	1933	5.3.
Citovich, E. British Patent No. 303,027	1929	4.1. 2.1.2.
Clark, A.M. v. Fodor	1883	1.3.1.
Coehn, A. Zeits. Elektrochem. <u>2</u> p.541	1896	1.1.

<u>Author</u>	<u>Date</u>	<u>Appendix Section</u>
Coehn, A. Zeits. Elektrochem. <u>3</u> p.424	1897	1.1.
Crossley, C.E. British Patent No. 220,422	1923	1.5. 6.
Davies, J.H. v. Fodor	1882	1.3.1.
Davtyan, O.K. Bull. Acad. Soc. U.S.S.R. Dept.Sci.Tech. (No.1) p.107 (No.2) pp.215-218	1946	2.1.2. 2.1.6. 5.1.
Davtyan, O.K. "Direct Conversion of Chemical Energy of Fuel into Electrical Energy", Moscow: Academy of Sciences: E.R.A. Translation 1949.	1947	2.1.2. 2.1.4. 2.1.6. 3.1. 3.2. 3.3. 3.4. 4.2. 5.1.
Davy, H. Ann. Phys. <u>8</u> p.301	1801	2.2.1.
Davy, H. Nicholson's Journal Nat. Phil. p.144	1802	1.1.
Dobell, J.L. J. Soc. Chem. Ind. London <u>14</u> p.974	1895	1.3.1.
Dobell, J.L. British Patent Nos. 2,272/A.D. 1897 4,442/A.D. 1897	1897a	1.3.3. 2.1.5.
Dobell, J.L. British Patent No. 10,484/A.D. 1897	1897b	1.3.3. 2.1.5.
Doyle, J.D. and Doyle, M.K. British Patent No. 428,933	1934	2.1.2.
Ellingham, H.J.T. J. Soc. Chem. Ind. London. <u>63</u> p.125	1944	5.3.
Ellingham, H.J.T. British Association Lecture 5:9:50	1950	5.2.
Eltenberg, A.S. von, and Lach, H. British Patent No. 24,307/A.D. 1907	1907	4.2.
Fabingi and Farkas Compt. rend. Paris. <u>106</u> p.1597	1888	1.3.2.
Faure, C.A. German Patent No. 57,336	1891	2.2.1.

<u>Author</u>	<u>Date</u>	<u>Appendix Section</u>
Fery, C. La Nature. <u>90</u> p.224; v.a. Ind. Engng. Chem. <u>10</u> p.744	1918	3.1.
Fery, C. Comptes rend. Paris, <u>192</u> p.881	1930	3.1.
Fischer, F. and Krönig, W. Ges. Abhandl Kenntis Kohle. <u>7</u> pp.213-30	1922	1.2. 2.1.2. 4.1.
Fischer, F. and Krönig, W. Zeits. anorg.u.allg.Chem. <u>153</u> p.169	1924	1.2. 2.1.2. 4.1.
Fischer, F. and Lepsius, R. Ber.d.Deutch. Chem. Ges. <u>45</u> p.2312	1912	1.3.2. 2.1.5.
Fleischmann and Förster Zeits.anorg.u.allg. Chem. <u>51</u> pp.249-289	1906	2.1.6.
Fodor, E.de "Electricity Direct from Coal" (In German) Vienna. Vol. 46 of Hartleben's "Elektrotechnischer Bibliothek"	1897	5.1. v.a.1.3.1. 2.1.1. 2.1.3.
Förster, F. and Diethelm Zeits. phys. Chem. <u>62</u> p.138	1908	2.1.2. 2.2.2. 3.1.
Förster, F. Zeits. phys. Chem. <u>69</u> p.236	1909	2.1.2. 3.1.
Förster, F. "Electro Chemistry of Acqueous Solutions" (in German)	1915	3.1. 3.3.
Förster, F. Zeits. Elektrochem. <u>29</u> p.64	1923	2.1.2. 2.1.4. 3.3.
Gaiser, C. German Patent No. 346,771	1918	2.1.2.
Gordon, K. J. Inst. Fuel <u>20</u> pp.42-58	1946	5.2.
Gore Phil. Mag. (4) <u>27</u> p.641	1864	1.3.2.
Greger, H.H. Proc. World Engineering Congr. Tokyo 1929 <u>32</u> pp.192-205	1931	2.1.5. 5.1. 5.2.
Greger, H.H. German Patent No. 570,600	1933	2.1.5. 4.2. 5.1.

<u>Author</u>	<u>Date</u>	<u>Appendix Section</u>
Greger, H.H. U.S. Patent No. 1,963,550	1934	2.1.5. 4.2. 5.1.
Greger, H.H. U.S. Patent No. 2,175,523	1939	2.1.5. 4.2.
Greger, H.H. U.S. Patent No. 2,276,188	1942	2.1.5. 4.2.
Gazel v. Tommasi 1889	1886	1.1.
Grove, W.R. Phil. Mag. (3) <u>14</u> p.139	1839	2.1.2. 3.1.
Grube, G. Zeits. Elektrochem. <u>16</u> p.621	1910	2.1.2. 2.2.2.
Grube, G. "Fundamentals of Electrochemistry" (In German)	1932	5.3.
Haber, F. Zeits. anorg.u.allg. Chem. <u>51</u> p.356	1906	2.1.5.
Haber, F. Zeits. anorg.u.allg. Chem. ? pp.91-93	1911?	2.1.6.
Haber, F. and Bruner, L. Zeits. Elektrochem. <u>10</u> p.697	1904	1.3.2.
Haber, F. and Moser, A. Zeits. Elektrochem. <u>11</u> pp.593-609	1905	2.1.6.
Habicht, F.P. British Patent No. 143,532	1919	1.3.2. 2.2.1.
Hamer, W.J. and Schrodtt, J.P. J. Amer. Chem. Soc. <u>71</u> pp.2347-52	1949	2.2.1.
Heise, G.W. and Schumacher, E.A. Trans. Amer. Elektrochem. Soc. <u>62</u> pp.383-391	1932	3.1.
Hering, K. and Dobrowolsky Electr. World. <u>25</u> p.220	1895	2.1.1.
Hoffmann, A.G. German Patent No. 369,829	1920b	2.1.5.
Hoffmann, F. German Patent No. 437,009	1920c	2.1.5.
Hofmann, K.A. Ber. d. Deutsch. chem. Ges. <u>51</u> pp.1526-37	1918a	2.1.1.
Hofmann, K.A. German Patent No. 310,782	1918b	2.1.1.
Hofmann, K.A. Ber. d. Deutsch. chem. Ges. <u>53</u> pp.914-921	1920a	2.1.1.

<u>Author</u>	<u>Date</u>	<u>Appendix Section</u>
Hofmann, K.A. and Ritter, K. Ber. d. Deutsch. chem. Ges <u>47</u> pp.2233-44	1914	1.1.
Hofmann, K.A. and Wurthmann, B. Ber. d. Deutsch. chem. Ges <u>52</u> pp.1185-1194	1919	2.1.1.
Hofmann, K.A. Ber. d. Deutsch. chem. Ges <u>56</u> p.1456	1923	3.1. 3.3.
Howard, H.C. "Chemistry of Coal Utilization" ed. H.H. Lowry, <u>2</u> pp.1568-1585 New York: Wiley, 1945.	1945	5.1.
Hughes, G. British Patent No. 369,920	1930	2.1.5.
Ivanov and Kobezev Zhurn. Fiz. Khim. <u>10</u> p.1	1937	3.1.
Jablochkoff, P. Comp. rend. Paris <u>85</u> p.1052; German Patent No. 6123	1877	1.3.1.
Jacques, W.W. British Patent No. 4,788/A.D. 1896; v.a. Anon 1896	1896	1.3.2.
Jacques, W.W. Harper's Magazine. <u>94</u> pp.144-50	1896-7	1.3.2.
Jacques, W.W. Zeits. Elektrochem. <u>4</u> p.286	1898	1.3.2.
Jedlicka, H. Naturforsch. <u>3a</u> pp.669-70	1948	2.1.4. 2.2.1.
Jedlicka, H. Naturforsch. <u>4a</u> pp.301-302	1949	2.1.4. 2.2.1.
Jone, H. U.S. Patent No. 764,595	1904	2.2.1.
Jungner, E.W. British Patent No. 15,727/A.D. 1906	1906	1.1. 2.1.3.
Jungner, E.W. German Patent No. 199,250 Zeits. Elektrochem. <u>14</u> p.357 British Patent Nos. 5214/A.D. 1908 5223/A.D. 1908	1908a;	1.2. b;c 2.1.3.
Jungner, E.W. German Patent Nos. 206,108 and 206,273 Zeits. Elektrochem. <u>15</u> pp.347-351	1909a;	1.2. b 2.1.3.
Kendall v.Berthier, p.184	1884	3.3.

<u>Author</u>	<u>Date</u>	<u>Appendix Section</u>
Kendall, J.A. and Gore, R.E. British Patent No. 271,581; 273,095	1926	2.1.5.
K"eyser, H.J. British Patent No. 3,913/A.D. 1904	1904	2.1.1. 2.2.2. 3.3.
"Konig, A. Zeits. angew. Chem. <u>44</u> p.461; <u>45</u> p.436	1931	2.1.5. 3.3.
K"onig, A. and Zohner, K. Siebert-Festschr. pp.179-92; Chem.Abs. <u>26</u> 4259 (1932)	1931	2.1.5. 3.3.
Korda, D. Elektrotech. Zeits. <u>16</u> p.273	1895	1.3.2.
Lamb, A.B. and Elder, R.W. J. Amer. Chem. Soc. <u>53</u> pp.137-163	1931	2.2.1. 2.2.2. 3.1.
Langhaus, R. German Patent No. 34,425	1886	1.3.2.
Langhaus, R. British Patent No. 430/A.D. 1901	1901	3.4.
Lavison, H.E. d R. de British Patent No. 9803/A.D.1897	1897	4.2.
Liebenow, C. and Strasser, L. Zeits. Elektrochem. <u>3</u> , p.353	1897	1.3.2.
McKee, J.H. and Adams, A.M. Fuel. <u>28</u> pp.1-6	1949	1.3.3. 1.4. 5.1.
Mond, L. and Langer, C. Proc. Roy. Soc. London <u>46</u> pp.296-308	1889	2.1.1. 3.1.
Mond, L. and Langer, C. Zeits. Elektrochem. <u>4</u> p.131	1897	2.1.2. 3.1.
Mugdan Chem. Ztg. <u>26</u> p.1156	1902	2.1.5.
M"uller, W.A. and Wallmann, J.F. German Patent No. 99,544	1898	2.1.2.
M"uller, W.A. Zeits. phys. Chem. <u>40</u> p.158	1902	2.1.4.
Nasarischwily, A. Zeits. Elektrochem. <u>29</u> pp.320-323	1923	3.1.
Nelson, J.B. and McKee, J.H. Nature, London. <u>158</u> p.753	1946	6.

<u>Author</u>	<u>Date</u>	<u>Appendix Section</u>
Nernst, W.		
German Patent Nos. 259,241	1911a)	
259,500	1911b)	2.1.1.
265,424	1912a)	2.1.4.
264,026	1912b)	2.2.2.
Nernst, W. and Wartenburg, von	1906	5.3.
Zeits. phys. Chem. <u>56</u> p.548		
Nobis	1909	2.1.4.
Dissertation, Dresden		
Noble and Anderson	1903	1.1.
U.S. Patent No. 759,740		
Ostwald, W.	1894	5.2.
Zeits. Elektrochem. <u>1</u> p.122		
Polyani, M. and Hevesy, G. von	1916	2.1.4.
German Patent No. 306,153		
Rasch, E.	1900	2.1.6.
German Patent No. 143,423		6.
Rawson, W.S.	1898	2.1.5.
British Patent No. 24,570/A.D. 1898		
Reed, A.	1918	1.3.3.
Trans. Amer. Electrochem. Soc. <u>33</u> p.189		
Reed, C.J.	1898	1.3.
Electrical World. <u>28</u> pp.44-5, 74-5		2.2.1.
98-100, 134-5		
Regensburger	1929	2.1.2.
Dissertation, Karlsruhe		3.3.
Reid, J.H.	1903	2.1.2.
British Patent No. 1670/A.D. 1903		2.1.5.
German Patent No. 181,814		3.3.
U.S. Patent Nos. 730,016 and 730,017		
Swedish Patent No. 16936	1904	
Rhorer, L.von	1923	1.3.1.
Zeits. Elektrochem. <u>29</u> p.478		
German Patent No. 367,151		
Ribbe, P.	1902	3.3.
German Patent No. 142,470		
Rideal, E.K. and Evans, U.R.	1921	2.1.2.
Trans. Faraday Soc. <u>17</u> pp.466-482		2.1.5.
		2.2.1.
		2.2.2.
		3.1.
		5.1.
Rodgers	1888	2.1.5.
U.S. Patent No. 487,644		

<u>Author</u>	<u>Date</u>	<u>Appendix Section</u>
Ruzicka, C. British Patent No. 18,931/A.D. 1905	1905	1.1. 4.1.
Sacher and Lorenz v. Bechterew 1911	?	1.3.2.
Scharf, P. German Patent No. 48,466	1888	2.1.1. 2.1.2. 2.1.4. 3.2. 3.3.
Schmid, A. "Diffusion Gas Electrodes" (In German) Stuttgart: F. Enke.	1923	2.1.4. 3.3.
Schmid, A. Helv. Chem. Acta. <u>7</u> , p.370	1924	2.1.4. 3.3.
Schmitz, G. Elektrotech. Zeit. <u>16</u> p.145	1895	1.3.1.
Schoop, P. "Primary Elements" (In German) Halle	1895	1.3.3.
Sconzo, A. Ann. chim. applicata. <u>22</u> pp.794-802	1932	1.3.1.
Seton, A.D. and Dobell, J. British Patent No. 15,903/A.D. 1897	1897	1.3.3. 2.1.5.
Short, R. U.S. Patent No. 569,591	1896	1.3.1.
Shrewsbury, C.P.; Marshall, F.L.; Cooper, J. and Dobell, J.L. Jour. Soc. Chem. Ind. <u>14</u> p.874; German Patent No. 88,704; British Patent No. 12,483/A.D. 1894	1894	1.3.1.
Shurmovsky, N. and Burns, L. Zhurn, Fiz. Khim. <u>14</u> Nos. 9-10 p.1183	1940	6.
Siegel, K. Elektrotech. Zeits. <u>34</u> p.1317	1913	2.1.2. 3.1.
Siemens Schuckertwerke German Patent No. 284,821	1913	2.1.3.
Sims British Patent No. 315,209	1929	2.1.2.
Spiliotopol British Patent No. 18,115/A.D. 1908	1908	2.2.1.
Spiridonov Nauk. i. zhizn (Acad. Sci. U.S.S.R.) No.6, p.22	1941	2.1.2.
Stärke German Patent No. 421,167	1925	3.2.

<u>Author</u>	<u>Date</u>	<u>Appendix Section</u>
Süssmann, R. and Süssmanns, G. German Patent No. 359,305	1916	2.2.2. 4.1.
Swan, J.W. Electrician <u>33</u> p.127	1894	2.1.4.
Szabo, St. von Naray Zeits. Elektrochem. <u>33</u> p.15	1927	3.1.
Taitelbaum, I. Zeits. Elektrochem. <u>16</u> pp.286-300	1910	1.2. 1.3.2. 2.1.1. 2.1.3. 2.2.2.
Tamaru, S. and Kamada, M. Zeits. Elektrochem. <u>41</u> pp. 93-96	1935a	1.3.2.
Tamaru, S. and Kamada, M. J. Chem. Soc. Japan. <u>56</u> pp.92-103	1935b	1.3.2.
Tatlow, W. Electrician <u>34</u> p.344	1895	2.1.1. 2.2.2.
Thiel, A. Zeits. Elektrochem. <u>21</u> p.325	1915	1.1.
Tobler, J. Zeits. Elektrochem. <u>39</u> pp.148-167	1933	2.1.2. 3.1.
Tommasi "Treatise on Electric Cells" (In French) Paris	1889	1.1. (Grezel 1886)
Tommasi, D. and Radiguet v.Fodor	1884	1.1.
Tourneur, H. French Patent No. 332,982	1903	2.1.3. 2.2.2.
Treeby Electrician. <u>28</u> p.206	1889	2.1.2.
Union Electrilitäts Gesellschaft German Patent No. 42,227	1902	2.1.1.
Waldburger, E. Dissertation, Basle	1930	2.1.2. 2.1.4. 3.1.
Welsbach, A.von Chem. Ztschr. <u>1</u> p.690	1903	2.2.2.
Westphal, C. German Patent	1880	2.1.2. 3.1. 3.3. 4.2.
Winand, P. and Coullery Elektrotech. Zeits. <u>16</u> p.35-36	1895	2.1.1. 2.2.2.

<u>Author</u>	<u>Date</u>	<u>Appendix Section</u>
Wright, A. and Thomson, C. Proc. Royal Soc. (London) <u>46</u> p.372-6	1889	2.1.2. 3.1.
Zettel, T. Zeits. Elektrochem. <u>2</u> p.543	1896	2.1.2.
Zöpke, O. German Patent No. 131,596	1902	2.1.2.

Classification of cells referred to in Bibliography

1. Direct cells operating on solid carbonaceous fuels.
 - 1.1. Aqueous electrolytes at temperatures below 100°C
 - 1.2. Aqueous electrolytes above 100°C
 - 1.3. Molten electrolytes (high temperature)
 - 1.3.1. Nitrate
 - 1.3.2. Carbonate or hydroxide
 - 1.3.3. Borax, etc.
 - 1.4. Solid electrolytes (high temperature)
 - 1.5. Ionised gas electrolytes (high temperature)
2. Indirect Cells.
 - 2.1. Cells operating on gaseous reaction products of carbon
 - 2.1.1. Low-temperature carbon monoxide cells
 - 2.1.2. Low-temperature hydrogen cells
 - 2.1.3. Low-temperature cells using other gases; e.g. SO₂
 - 2.1.4. Cells using halogens
 - 2.1.5. High-temperature hydrogen and carbon monoxide cells with molten electrolytes
 - 2.1.6. High-temperature hydrogen and carbon monoxide cells with solid electrolytes
 - 2.2. Cells operating on solid or liquid reaction products of carbon
 - 2.2.1. Cells using metals as fuel
 - 2.2.2. Oxidation-reduction cells
3. Electrodes.
 - 3.1. Activation of electrodes
 - 3.2. Liquid proofing
 - 3.3. Diffusion electrodes
 - 3.4. Methods of preparation of electrodes
4. Cell Construction.
 - 4.1. High-pressure cells
 - 4.2. Mechanical arrangements

5. Reviews and General Principles.

5.1. Literature reviews

5.2. General articles, economics, and applications

5.3. Theoretical

6. Miscellaneous.

N.B.: When the electrolyte is shown enclosed by a broken line, it is retained in a porous material. The symbol \parallel is used to indicate the presence of a diaphragm.

1. Direct Solid Fuel Cells

1.1. Using aqueous electrolytes below 100°C.

Davy	1802	$C/H_2O \parallel HNO_3 / (C)O_2$
Tommasi and Radiguet	1884	$C/NaCl \parallel Pb/O_2 / (C)O_2$
Grezel 1886 (v. Tommasi 1889)		$C/Acid \parallel (NH_4)_2CO_3 / (C)O_2$
Case 1887 (v. Berthier 1929)		$C/H_2SO_4 \parallel KClO_3 / (Pt)O_2$
Case	1889	$C(Pt) \left \begin{array}{c} FeCl_3 \\ H_2O \end{array} \right \parallel \begin{array}{c} FeCl_3 \\ HCl \end{array} \left (Pt)O_2 \right.$
Coehn	1896, 1897	$C/H_2SO_4 / (PbO_2)O_2$
Nobel and Anderson	1903	$C/HNO_3 / (Al)O_2$
Ruzicka	1905 (v.a. 4.1)	$C/KOH / (NiO)O_2$ and (non aqueous) $C/liquid Cl_2 / Al$
Jungner 1906; 1908a, b; 1909a, b (v.a. 2.1.3)		$C, SO_2 \left \begin{array}{c} H_2SO_4 \\ H_2SO_4 \end{array} \right \parallel \begin{array}{c} Nitrosyl \\ H_2SO_4 \end{array} \left (C)O_2 \right.$
Hofmann and Ritter (v.a. Thiel 1915)	1914	$C/NaOHaq \parallel NaClO_3 / (Pt)O_2$
Thiel	1915	theory of Case's cell

1.2. Using aqueous electrolytes above 100°C.

Taitelbaum 1910)	C	$H_2SO_4 + V, Tl, \text{ sulphates}$	$\left \begin{array}{c} (Au) O_2 \\ (C) \\ (Pt) \end{array} \right.$
Baur 1910)			
Fischer and Krönig 1922, 1924	$C(Fe)$	$Aq. \text{ alkali}$ $200^\circ C \text{ } 30 \text{ } \text{Atm.}$	$(Fe) O_2$

1.3. Direct cells operating at high temperature with molten electrolyte.

1.3.1. Nitrate Electrolytes e.g. C/molten sodium nitrate/ (metal) O_2

Becquerel	1855	Platinum cathode
Jablochkoff	1877	Iron cathode
Brard	1882	
Davies	1882 (v. Fodor 1897)	
Clark	1882 (" " ")	
Brooks	1894a;b	KHSO ₄ added to electrolyte, CuS cathode
Shrewsbury	1894	
<u>et.al.</u>		
Dobell	1895	Iron cathode
Schmitz	1895	
Sconzo	1930	C/Ag NO ₃ / (Ag, Pt, Pd, etc.) O ₂

1.3.2. Carbonate or hydroxide electrolytes.

Gore	1864	C Na ₂ CO ₃ , CaO glass (Fe)O ₂
Archereau	1883	C Alkali carbonate or hydroxide (metal)O ₂
Langhaus	1886	"
Fabinghi and Farkas	1888	"
Bradley	1888	"
	(v. Anon. 1897)	
Bull	1891	"
Korda	1895	C K ₂ CO ₃ (CuO) O ₂
Anon.	1896; 1897)	
Jacques	1896; 1897)	C/NaOH/(Fe) O ₂
	1898 (v. a. Haber and Bruner 1904)	
Liebenow & Strasser	1897	Modifications of Jacques cell
Reed	1898	" " " "
Sacher and Lorenz		
	(v. Bechterew 1911)	" " " "
Byrnes	1902	" " " "
Haber and Bruner	1904	Addition of sodium manganate to NaOH
	(v. a. 2.1.2.)	
Baur	1910)	C + carbonaceous material NaOH + MnO ₂ (Fe)O ₂
Taitelbaum	1910)	
Bechterew	1911	C NaOH + selenates, tellurates, etc. (FeO)O ₂
Fischer and Lepsius	1912	C NaOH (Fe ₂ O ₄)O ₂
	(v. a. 2.1.5.)	
Baur and Treadwell	1916b; 1918	C [salt] (Fe ₃ O ₄)O ₂
Baur <u>et.al.</u>	1921b	C [carbonates in porous MgO] (Fe ₃ O ₄)O ₂

Habicht	1919	$C, CO, Na \begin{matrix} (Pb, Sn) \\ \text{molten} \end{matrix} \left NaOH \right (Ag) \right. \left. \begin{matrix} \\ O_2 \end{matrix} \right.$
Rhorer, von	1923	Alkali + Barium carbonates and alumina, etc. Pt or Ag cathodes.
Tamaru and Kamada	1935a;b	Carbonates; Pt, Au, Ag cathodes
Baur and Brunner	1935	$C / \text{carbonate} / (Ag \ Pt) O_2$
" 2 "	1937a	$C / \text{carbonates} // (Fe_3O_4) O_2$

1.3.3. Borax and other electrolytes.

Schoop	1895	$C / \text{lead oxides} / (Fe) O_2$
Short	1896	$C / \text{lead oxides} / (Pt) O_2$
Dobell	1897a	$C (\text{molten Pb}) // \text{lead oxides} / (Fe) O_2$
	1897b	$C \text{ or } CO (\text{molten Pb}) \left \begin{matrix} \text{chromates \& } \\ \text{hydroxides} \end{matrix} \right (Fe) O_2$
Seton and Dobell	1897	$C \text{ or } CO (\text{molten Pb, Bi, etc.}) \left \begin{matrix} \text{arsenates} \\ \text{chromates} \\ \text{vanadates} \\ \text{etc.} \end{matrix} \right (Fe) O_2$
Baur and Ehrenberg	1912	$C / \text{borax} / (\text{molten Ag}) O_2$
Baur <u>et.al.</u>	1916a	$C / \text{borax} / (CuO) O_2$
Reed	1918	$C / \text{borax} + MnO_2 / (Au) O_2$
McKee and Adams	1949	$C \left[\begin{matrix} \text{CeO}_2 + \text{WO}_3 \text{ in} \\ \text{porous Al}_2\text{O}_3 \end{matrix} \right] \left(\begin{matrix} Pt \\ (Fe_3O_4) \end{matrix} \right) O_2$

1.4. Direct cells operating at high temperatures with solid electrolyte.

Baur and Treadwell	1916b)	"Nernst mass" or
Baur and Preis	1937b;1938)	$CeO_2 + WO_3 + \text{clay}$
McKee and Adams	1949	$CeO_2 + WO_3 + \text{clay}$

1.5. Direct cells operating at high temperatures and using ionised gas as electrolyte.

Crossley	1923 (v.a. 4.2.)	$C (Fe) / \text{heated ionised gas} / (\text{metal}) O_2$
----------	------------------	---

2. Indirect cells.

2.1. Gas cells.

2.1.1. Low temperature carbon monoxide cells.

Winand and Coullery	1887 (v. 1895)	$CO (Cu?) \left \begin{matrix} Cu_2Cl_2 \\ \\ CuCl_2 \end{matrix} \right O_2$
Scharf	1888 (v.a. 2.1.2.) 2.1.4. 3.3.	$CO / \text{electrolyte} / \text{air}$

Borchers (v.a. Fodor 1897)	1894	$\text{CO}(\text{Cu}) \mid \text{Cu}_2\text{Cl}_2 \parallel \text{CuCl}_2\text{HCL} \mid (\text{Cu})\text{O}_2$
Hering & Dobrowolsky	1895	$\text{CO}(\text{C-Pt}) \mid \text{H}_2\text{SO}_4 \mid (\text{Pt})\text{O}_2$
Bernstein	1895;1897	$\text{CO} + \text{H}_2 \mid \text{H}_2\text{SO}_4 \text{ aq} \mid (\text{C})\text{O}_2$ (water gas)
Tatlow	1895	$(\text{coal gas}) \mid (\text{C})\text{Cu}_2\text{Cl}_2 \parallel \text{CuCl}_2 \mid (\text{C})\text{O}_2$ (water gas)
Bucherer	1896b	Discussion of Borchers cell
Union Elektr.Gesell	1902	Use of acetylene instead of CO
Baur and Glaessner	1903	$\text{CO}, \text{H}_2 \text{ etc } \left(\begin{array}{c} \text{Ni} \\ \text{Pt} \end{array} \right) \mid \text{Ce}^{3+} : \text{NaOH aq} : \text{Ce}^{4+} \left(\begin{array}{c} \text{Pt} \\ \text{C} \end{array} \right) \text{O}_2$
Keyser	1904	$\text{CO}, \text{ etc } \mid \text{KOH}, \text{K}_2\text{CO}_3, \text{FeCl}_2 \mid (\text{Fe})\text{O}_2$ Boiling
Braun and Schneider (v.a. 6)	1910	$\text{CO}(\text{metal}) \mid \text{H}_2\text{SO}_4 \mid (\text{metal})\text{O}_2$
Baur (v.a. 2.2.2)	1910)	$\text{CO}, \text{ etc } (\text{C}) \mid \begin{array}{c} \text{Ti}^{3+} \\ \text{V}^{4+} \end{array} \mid \text{H}_2\text{SO}_4 \mid \begin{array}{c} \text{Ti}^{3+} \\ \text{V}^{5+} \end{array} \mid \left(\begin{array}{c} \text{Pt} \\ \text{Au} \\ \text{C} \end{array} \right) \text{O}_2$
Taitelbaum	1910)	
Nernst (v.a. 2.2.2.)	1911;1912	Use of Ti and Ce instead of Ti, V
Hofmann Hofmann Wurthmann Auerbach	1918a;b;1920a) 1919) 1919)	$\text{CO}(\text{Cu}) \mid \text{NaOH aq.}, \text{ lye soln, etc.} \mid (\text{Cu}) \text{O}_2$ $(\text{CuO}) \text{O}_2$

2.1.2. Low temperature hydrogen cells.

Grove	1839	$\text{H}_2(\text{Pt})/\text{H}_2\text{SO}_4/(\text{Pt})\text{O}_2$
Westphal	1880	$\text{H}_2(\text{Pt})/\text{Acid}/(\text{Pt})\text{O}_2$
Blanchard	1882	$\text{H}_2(\text{Pb})/\text{H}_2\text{SO}_4/(\text{PbO})\text{O}_2$
Scharf (v.a. 2.1.1.;2.1.4.)	1888	$\text{H}_2/\text{electrolyte}/\text{air}$
Treeby Mond and Langer Wright and Thompson	1889) 1889;1897) 1889)	$\text{H}_2(\text{Pt.blk}) \mid \left[\begin{array}{c} \text{H}_2\text{SO}_4 \\ \text{porous} \\ \text{material} \end{array} \right] \mid (\text{Pt.blk})\text{O}_2$
Cailletet (v.a. 4.1.)	Collardeau 1894	$\text{H}_2(\text{Pt})/\text{H}_2\text{SO}_4/(\text{Pt})\text{O}_2$ high pressure
Andreas	1895	
Bernstein	1895;1897	v. 2.1.1.
Zettel	1896	$\text{H}_2(\text{Ag}) \mid \text{H}_2\text{SO}_4 \mid (\text{Ag})\text{O}_2$
Müller and Wallmann Zöpke	1898) 1902)	Hydrogen/oxygen cell

Reid	1903;1904	H_2, CO_2 (porous C) / NaOHaq / $(Fe)O_2$
Förster and Dithelm	1908	H_2 (Pt) / Ti sulphates / $(Pt)O_2$
Förster	1909	$H_2 / H_2SO_4 / O_2$
Grube	1910;1932	$H_2 / H_2SO_4 : Fe^{3+}$ or NO / O_2
Siegel	1913	Platinised C anodes in $H_2 - O_2$ cell
Gaiser	1918	H_2 (Pt) $H_2SO_4 + \text{colloidal}$ $(Pt)O_2$ Pt or Ag
Rideal and Evans	1921	H_2 (Ni, Pt, blk) NaOHaq NaOH + MnO_2 $(C)O_2$
Fischer & Krönig	1922;1924	H_2 (Pt) H_2SO_4, NO $(Pt)O_2$
Hofmann (v.a. 3.1.)	1923	H_2 (Pt) lye soln $(Pt)O_2$
Förster	1923	v. 2.1.4.
Regensburger	1929	H_2 (Pd) / H_2SO_4 NaOH / $(Pt, C)O_2$
Sims	1929	H_2 (C) / ? / $(C)O_2$
Citovich	1929	$H_2 - O_2$ cell with Cu anode (v.a. 4.1.)
Waldburger	1930	H_2 (C-Pt) HCl $(C)Br_2$
Baur and Tobler	1933	H_2 (C-Pt) NaOH (Ag) $(C)O_2$ (Cu)
Tobler	1933	v. 3.1.
Doyle and Doyle	1934	H_2 acid or alk. $(PbO)O_2$
Spiridinov	1941	H_2 (C, Ni) electrolyte $(Active C)O_2$
Davtyan	1946;1947	H_2 (C, Ag) / KOHq / $(C, Ni)O_2$
Brit. E.R.A.	1950	H_2 (Ni) KOHq $(Ni)O_2$ (high pressure)

2.1.3. Low temperature gas cells other than H_2 , CO, and halogen cells.

Andreas (v. Fodor 1897)	1895	SO_2 (C) Cu_2Cl_2 $CuCl_2$ $(C)Cl_2$
----------------------------	------	---

Tourneur	1903	$\text{SO}_2(\text{C}) \mid \text{HNO}_3 \mid (\text{C})\text{O}_2$
Basset	1906;1907a;b	$\text{SO}_2, \text{H}_2\text{S}, \text{HI}, \text{etc (Porous C)} \mid \text{H}_2\text{SO}_4 \text{ aq} + \text{Br}_2, \text{NO} \mid \text{O}_2$ (Graphite)
Jungner	1906;1908;1909	$\text{SO}_2(\text{Coke}) \mid \text{H}_2\text{SO}_4 \parallel \text{Nitrosyl} \parallel \text{H}_2\text{SO}_4 \mid (\text{C})\text{O}_2$
Taitelbaum	1910)	$\text{SO}_2(\text{C}) \mid \text{H}_2\text{SO}_4 + \text{Tl, V, sulphates} \mid \begin{matrix} (\text{Pt}) \\ (\text{Au}) \\ (\text{C}) \end{matrix} \text{O}_2$
Baur	1910) (v.a. 1.2.)	
Siemens Schuckertwerke	1913	$\text{HI}(\text{C}) \mid \text{H}_2\text{SO}_4 \parallel \text{HNO}_3 \mid (\text{C})\text{O}_2$
2.1.4. Halogen Cells.		
Scharf	1888	$\text{H}_2, \text{CO}/\text{electrolyte}/\text{Cl}_2, \text{F}_2$
	(v.a. 2.1.1;2.1.2;3.3)	
Swan	1894	$? \mid \text{KCl, NaCl or PbCl}_2 \mid \text{Cl}_2$
Müller	1902	$\text{H}_2 - \text{Cl}_2$ cell
Nobis	1909	$\text{H}_2 \mid \text{HCl aq } 60^\circ \mid \text{Cl}_2$
Nernst	1911	$\text{H}_2 - \text{Cl}_2$ cell with regeneration of Cl_2
Polyani & v.Hevesy	1916	$? \mid \text{alkaline electrolyte} \mid \begin{matrix} \text{NO,} \\ \text{Cl}_2 \\ \text{(metal oxide)} \end{matrix}$
Förster	1923	$\text{H}_2(\text{Pt})/\text{HCl}/(\text{C}) \text{Cl}_2$
Schmid	1923;1924)	$\text{H}_2(\text{Pt, C})/\text{HCl}/(\text{C}) \text{Cl}_2$
	(v.a. 3.3.)	
Bührer	1929)	
Waldburger	1930	$\text{H}_2(\text{Pt, C})/\text{HCl}/(\text{C}) \text{Br}_2$
Davtyan	1947	$\text{H}_2(\text{Fe, Si})/\text{HCl}/(\text{C})\text{Cl}_2$
Jedlicka	1948;1949	$\text{Na(Hg)}/\text{NaCl aq}/(\text{C})\text{Cl}_2$
2.1.5. High Temperature gas cells with molten electrolyte.		
Arsonval, d'	1888	$\text{H}_2 \text{ etc (Sb, Pb, etc)} \mid \text{Sb}_2\text{O}_3 \parallel \text{Sb}_2\text{O}_5 \mid (\text{Sb}) \text{O}_2$
Rodgers	1888	$\text{H}_2/\text{metal oxide}/\text{O}_2$
Atkinson & Treharn	1896	$\text{H}_2/\text{molten Pb})/\text{PbO}/(\text{Ag})\text{O}_2$
Bucherer	1896a;b	$\text{CO, H}_2(\text{Fe})/\text{carbonate}/(\text{Pt})\text{O}_2$

Jacques	1896	v. 1.3.2. (Haber and Bruner 1904)
Dobell	1897a;b)	
Seton and Dobell	1897)	v. 1.3.3.
Rawson	1898	CO(molten Pb)/metal salts/ (?)O ₂
Britzke	1900	CO(Cu) [PbO] (Cu)O ₂
Mugdan	1902	H ₂ (Pb) Na ₂ CO ₃ NaOH ferrite (Fe) CO O ₂
Reid	1903	CO(C)/NaOH/(metal)O ₂
Haber and Bruner	1904	H ₂ (C)/NaOH, Na ₂ MnO ₄ /(Fe)O ₂
	(v.a. 1.3.2.)	
Haber	1906	CO, H ₂ /carbonates/(metal)O ₂
Beutner	1911	CO, H ₂ (Ni, Pt)/halides/(metal)O ₂
	(v.a. 3.3.)	
Baur and Ehrenburg	1912	CO, H ₂ (Pt, Fe, Ni, Cu) Borax (molten Ag) O ₂
	(v.a. 1.3.3.)	
Fischer and Lepsius	1912	H ₂ (C)/NaOH/(Pt)O ₂
	(v.a. 1.3.2.)	
Hoffmann, A.G.	1920b	CO(C)/molten Cu/(CuO)O ₂
Hoffmann, F.	1920c	CO(Cu)/ - / (CuO)O ₂
Baur <u>et.al.</u>	1921b	H ₂ (Fe) [NaKCO ₃] (Fe ₃ O ₄)O ₂ in MgO
Baur	1921c)	
	1921d)	H ₂ , CO(Fe) NaOH (Fe)O ₂
Rideal and Evans	1921	CO, H ₂ (Pt) UO ₂ phosphate glass Na ₂ MnO ₄ (Fe) O ₂
		Sn may replace Pt and a carbon- bonate the UO ₂ - glass mixture.
Kendall and Gore	1926)	
Hughes	1930)	H ₂ , CO (Ag) [carbonates] (Ag, etc)O ₂ (Ni) borates (Cu)
Greger	1931;1933; 1934;1939; 1942.	CO, H ₂ (metal) [carbonates] (Ni, Fe) + halides (ferrite)O ₂ (etc.)
König and Zohner	1931	H ₂ (Pd)/KNO ₂ + NaNO ₂ /(Pd)O ₂
Blanke	1942	H ₂ , CO Na, Ba, etc. carbonates (C)O ₂ (C) + halides

2.1.6. High temperature gas cells with solid electrolytes.

Rasch	1900	$\text{CO, H}_2, \text{etc.} / \text{Zircon-Yttria} / \text{Salt flame Glass} / \text{O}_2$
Haber and Moser	1905)	$\text{CO (pt. blk)} / \text{Glass} / (\text{Pt. blk}) \text{O}_2$
Haber	1906; 1911)	
Fleischmann & Förster	1906	$\text{H}_2, \text{CO} / \text{glass, porcelain} / (?) \text{O}_2$
Baur and Preis	1937b, 1938)	$\text{H}_2, \text{CO (Fe)} \left \begin{array}{l} \text{"Nernst mass"} \\ \text{CeO}_2, \text{WO}_3, \text{etc.} \end{array} \right (\text{Fe}_3\text{O}_4) \text{O}_2$
Baur	(v.a. 1.4.) 1939)	
Baur	1941	Additions to electrolyte to reduce resistance, etc.

2.2. Indirect solid or liquid fuel cells.

2.2.1. Metal fuel.

Davy	1801	$\text{Zn} / \text{FeCl}_3 / (\text{C}) \text{O}_2$
Faure	1891	$\text{Fe} / \text{NaCl aq} / (\text{C}) \text{O}_2$
Reed	1898	Discussion of metal fuels
Jone	1904	$\text{Pb, Sn, Cd, Sb, etc} / \text{NaCl aq} / \text{O}_2$
Spiliotopol	1908	$\text{Sn, Al} \left \begin{array}{l} \text{Cr}_2\text{Cl}_6; \text{PbCl}_2 \\ \text{MnCl}_2 \text{ (fused)} \end{array} \right (\text{C}) \text{O}_2$
Hahicht	1919	$\text{Na (molten Pb, Sn)} \left \begin{array}{l} \text{molten} \\ \text{Na OH} \end{array} \right (\text{Ag}) \text{O}_2$
Rideal and Evans	1921	$\text{Pb} \left \begin{array}{l} \text{NaOH aq} \\ \text{Na}_2\text{CO}_3 \text{ aq} \end{array} \right \begin{array}{l} \text{Mn O}_2 \\ \text{O}_2 \end{array} \left (\text{C}) \text{O}_2$ $\text{Sn} \left \begin{array}{l} \text{HCl} \\ \text{HCl} \end{array} \right \begin{array}{l} \text{FeCl}_3 \\ \text{HCl} \end{array} \left (\text{C}) \text{O}_2$ $\text{Sn} \left \begin{array}{l} \text{reduced} \\ \text{melt.} \end{array} \right \begin{array}{l} \text{oxidised} \\ \text{melt.} \end{array} \left (\text{Fe}) \text{O}_2$
Baur	1921a	$\text{Na} / \text{NaOH} / (\text{Ag, Fe}_2\text{O}_3, \text{Fe}_3\text{O}_4) \text{O}_2$
Brandt	1925	$\text{Na} / \text{NaOH} / (\text{Passive metal}) \text{O}_2$
Lamb and Elder	1931	$\text{Zn} / \text{H}_2\text{SO}_4 \left \begin{array}{l} \text{FeCl}_3 \\ \text{O}_2 \end{array} \right (\text{Active C, Pt}) \text{O}_2$
Hamer and Schrodt	1949	$\text{Mg} / \text{molten or solid} / (\text{C}) \text{MnO}_2 \text{NaOH}$
Jedlicka	1948; 1949 (v.a. 2.1.4.)	$\text{Na (Hg)} / \text{NaCl aq} / (\text{C}) \text{Cl}_2$

2.2.2. Oxidation-reduction cells using compounds of metals of variable valency, etc.

Tatlow	1894)	
Borchers	1894)	$\text{Cu} + \rightleftharpoons \text{Cu}^{++}$
Windand and Coullery	1895)	(v.a. 2.1.1.)

Welsbach	1903)	$Ce^{3+} \rightleftharpoons Ce^{4+}$
Baur and Glaessner	1903)	(v.a. 2.1.1.)
Tourneur	1904	(a) C + Alkali sulphate - sulphide
		(b) Alkali Sulphide $\left \begin{array}{l} K_2S \\ Soln \end{array} \right \left \begin{array}{l} HNO_3 \\ KClO_3 \end{array} \right \left \begin{array}{l} (C) \\ (Pt) \\ (Fe-Si) \end{array} \right O_2$
K�yser	1904	Fe salts (v. 2.1.1.)
Junger	1906, 1908, 1909.	Mn, Cr, Fe, Cu, Hg salts (v. 1.1.; 2.1.3.)
F�rster and Dithelm	1908	Ti salts (v. 2.1.2.)
Taitelbaum	1910)	
Baur	1910)	V, Tl (v. 1.2.)
Grube	1910	Fe salts (v. 2.1.2.)
Nernst	1911; 1912	Tl, Ti, Ce salts (v. 2.1.2.)
S�ssmann and S�ssmann	1916	Oxidation-reduction cells under pressure
Rideal and Evans	1921	Mn, U, V, Cr, Ce in glass (v. 2.1.5.)
Lamb and Elder	1931	Survey of various systems
Baur and Preis	1937b; 1938)	Addition of Mn, Cr, V, Ti, U, etc.
Baur	1941)	to solid electrolyte (v. 2.1.6.)
Blanke	1942	v. 2.1.5.

3. Gas electrodes for fuel cells.

3.1. Activation.

Grove	1839)	
Westphal	1880)	Platinum for hydrogen
Mond and Langer	1889)	
Wright and Thompson	1889)	Platinum black for H ₂
Caillet and Collardeau	1894)	Pt, Pd, and Au
F�rster and Dithelm	1908)	
F�rster	1909; 1915)	Pt. electrodes for H ₂ and O ₂
Siegel	1913	Platinised carbon for H ₂
Fery	1918; 1930	Porous C electrodes for O ₂
Rideal and Evans	1921	Platinised Ni for H ₂
Hofmann	1923	Platinised clay for H ₂
Nasarischwily	1923	Carbon electrodes for O ₂
Szabo	1927	Platinised carbon electrodes
Baur	1930	"Hopcalite" for O ₂
Waldburger	1930	Poisoning of Pt electrodes

Lamb and Elder	1931	Active carbon for O ₂
Heise and Schumacher	1932	Porous C electrodes
Tobler	1933	Ni, Fe, C, Pt electrodes (plain or platinised) for H ₂ and O ₂
Ivanov and Kobozev	1937)	Fe ₃ O ₄ electrodes
Baur and Brunner	1937a)	
Davtyan	1947	Catalytic activation for H ₂ and O ₂

3.2. Non-wetting electrodes.

Scharf	1888	Wax coating
Carbone, S.A.) Stärke)		Gelatine coating
Davtyan	1947	Wax coating

3.3. Diffusion electrodes.

Westphal	1880	
Kendall	1884	
Scharf	1888	
Anon	1895	
Ribbe	1902	
K ^u yser	1904	
Reid	1903	CO diffusion through C
Beutner	1911	H ₂ diffusion through Pd
F ^o rster	1915	
Schmid	1923;1924	
F ^o rster	1923	
Hofmann	1923	
Baillod	1927	
B ^u hrer	1929	
Regensburger	1929	
K ^o nig	1931;1932)	H ₂ diffusion through Pd
K ^o nig and Zohner	1931)	
Blanke	1942	
Davtyan	1947	

3.4. Methods of preparing active electrodes.

Langhaus	1901	Metallisation of C
Davtyan	1947	Reduction of Ag, Ni, etc, on C

4. Special Construction of Cells

4.1. High Pressure Cells.

Cailleter and Collardeau	1894
Ruzicka	1905
S ^u ssmann and S ^u ssmann	1916
Fischer and Kr ^o nig	1922;1924
Citovich	1929
Brit. E.R.A.	1950

4.2. Mechanical Details.

Westphal	1880	
Lavison	1897	Rotating electrodes
Eltenberg and Lach	1907	" "
Greger	1933;1934; 1939;1942.	
Davtyan	1947	

5. Reviews and General Principles.

5.1. Literature reviews.

Fodor	1897
Bechterew	1911
Rideal and Evans	1921
Berthier	1929
Greger	1931
Baur and Tobler	1933
Howard	1945
Davtyan	1947
Brit. Elec. R.A.	1949a;b
McKee and Adams	1949
Ellingham	1950

5.2. General articles, economics.

Ostwald	1894
Baur	1921e
Greger	1931
Baur	1939
Gordon	1946

5.3. Theoretical.

Boudouard	1904	
Nernst and Wartenburg	1906	
Allemand and Ellingham	1924	
Grube	1932	
Chipman and Murphy	1933	Free energies
Ellingham	1944	" "

6. Miscellaneous

Britzke	1900)	Thermal ionisation of CO
Rasch	1900)	
Braun and Schneider	1910)	Ionisation of fuel gases by U.V. irradiation, etc.
Crossley	1923)	
Shurmovsky and Bruns	1941	Mechanism of CO oxidation by Mn O ₂
Nelson and McKee	1946	Crystal structure of CeO ₂ : WO ₃ compounds

APPENDIX G

BIOGRAPHICAL NOTE

Dominick A. Sama was born in Brooklyn, New York, on January 5, 1933. He attended the public-school system in New York City and graduated from Brooklyn Technical High School in 1950, whereupon he entered Brooklyn College. In 1952 he transferred to M.I.T. where he received the degrees S.B. in Chemical Engineering in 1954 and S.M. in Chemical Engineering Practice in 1955. He was awarded an undergraduate scholarship in 1953, and a Thorp Fellowship and graduate scholarship in 1954. In 1955 he was awarded a Food Machinery and Chemical Corporation-Overseas Summer Fellowship.

Upon returning from Europe he entered the employ of the United States Army for 639 days. During this time he was principally assigned to the Interior Ballistics Laboratory of the Ballistics Research Laboratories at Aberdeen Proving Ground.

In September of 1957 he returned to M.I.T. to resume his doctoral studies, and was awarded a Standard Oil Foundation Fellowship. He was appointed a Research Assistant in the Electrical Engineering Department in 1958, and has continued in this capacity to the present.